92.048B

Prepared by:
Energy Systems Laboratory
Department of Mechanical Engineering
Texas A & M University
College Station, TX

The Effect of Hardware Configuration on the Performance of Residential Air Conditioning Systems at High Outdoor Ambient Temperatures

Prepared for:
Electric Power Research Institute

Final Report
May 1995

Contributors:
Joel A. Bain
Dennis L. O'Neal
Michael A. Davis
Angel G. Rodriguez

92.048B

THE EFFECT OF HARDWARE CONFIGURATION ON THE PERFORMANCE OF RESIDENTIAL AIR CONDITIONING SYSTEMS AT HIGH OUTDOOR AMBIENT TEMPERATURES

Submitted by

Joel A. Bain
Dennis L. O'Neal
Michael A. Davis
Angel G. Rodriguez

Energy Systems Laboratory
Department of Mechanical Engineering
Texas A & M University
College Station, TX

Submitted to

Electric Power Resesarch Institute
3412 Hillview Ave.
Palo Alto, CA 94304

May 1995

92.048B

THE EFFECT OF HARDWARE CONFIGURATION ON THE PERFORMANCE OF RESIDENTIAL AIR CONDITIONING SYSTEMS AT HIGH OUTDOOR AMBIENT TEMPERATURES

Submitted by

Joel A. Bain
Dennis L. O'Neal
Michael A. Davis
Angel G. Rodriguez

Energy Systems Laboratory
Department of Mechanical Engineering
Texas A & M University
College Station, TX

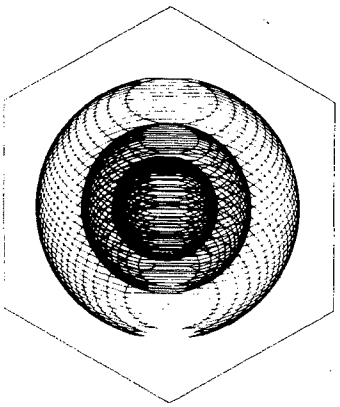

ENERGY SYSTEMS LABORATORY
Department of Mechanical Engineering
Texas Engineering Experiment Station
Texas A&M University System

SUMMARY

A study was performed which investigated the effect of hardware configuration on air conditioning cooling system performance at high outdoor temperatures. The initial phase of the investigation involved the testing of ten residential air conditioning units in psychrometric rooms at Texas A&M University. All units were tested using ARI Standard 210/240 (1989) test procedures. Tests were conducted at indoor conditions of 80°F (26.7°C) db and 67°F (19.4°C) wb, and outdoor db temperatures of 82°F (27.8°C), 95°F (35°C), 100°F (37.8°C), 105°F (40.6°C), 110°F (43.3°C), and 120°F (48.9°C). The second phase of the research involved the analysis of manufacturers' published cooling performance data for various hardware configurations.

For the experimental work, measurements were taken to determine total capacity, system power, EER, and power factor. These results were then compared to manufacturers' predicted values. For the capacity, the experimental results were an average of 2.6% below the manufacturers' published values for outdoor temperatures from 85°F (29.4°C) to 115°F (46.1°C). Experimental power measurements were on average 0.4% above manufacturers' listed results. For the EER, experimental results were an average of 2.9% less than the manufacturers' predicted values. The power factors of all units were above 0.95 for the tested outdoor temperatures.

In the analysis of manufacturers' published data, relationships between steady-state performance, cyclic performance, and hardware configuration were investigated for a variety of air conditioning units. A statistical relationship was found between the SEER of a unit and its corresponding EER. The split-system units possessed greater increases in EER for a given increase in SEER than the package or two-speed units. Averages values of EER/SEER for EER's at 95°F (35°C) were highest for the split-system units, followed by the package and two-speed units, respectively. Normalized capacity, power, and EER curves were investigated at outdoor temperatures from 85°F (29.4°C) to 115°F (46.1°C). On average, the two-speed units showed the smallest decrease in capacity with an increase in outdoor temperature, followed by the split-system and package-system units. The smallest power increase and smallest EER decrease with an increase in outdoor temperature were exhibited by the split-system units, followed by the two-speed and package-system units.

TABLE OF CONTENTS

TABLE OF CONTENTS (CONTINUED)

TABLE OF CONTENTS (CONTINUED)

CHAPTER I

INTRODUCTION

The use of air conditioning in the United States and other industrialized countries has expanded rapidly since 1950 (McQuiston and Parker 1988. Since the mid 1970's, electricity prices in the United States have risen significantly. Between 1978 and 1992, average residential electricity prices went from 4.3 cents/kWh to 8.3 cents/kWh. These increasing costs were the result of several factors. The oil embargo in 1973 and the additional energy crisis in 1979 and 1980 caused an increase in oil prices, affecting utilities relying on oil as the primary fuel (NRC 1986). Also during this time, increasing governmental regulations for power plants caused a rise in the cost per kWh of electricity Inflation and delays affected power plant construction attempts, and prices rose as new plants began their operation (NRC 1986). Due to the increasing costs of expanding power capacity, many electric utilities have used demand-side management (DSM) as an alternative to new construction. Estimated savings of over 90 gigawatts are projected by 2030 due to the DSM programs (Millhone and Pirkey 1991).

In the summer, peak electrical demand usually occurs between 3:00 P.M. and 5:00 P.M. (Talukdar and Gellings 1987). This peak often corresponds to the warmest part of the day (typically between 3:00 P.M. and 4:00 P.M. (Knebel 1983)). Since the efficiency

and capacity of air conditioners decrease as outdoor temperature increases, air conditioners perform worst during these peak times. While residential systems only yield a small portion of utility revenue, they do result in high coincident peak demand (Proctor et al 1994). The cooling performance of modern residential air conditioners has therefore become very important to electric utility companies.

For many years, electric utilities have offered air conditioner rebate programs that provide rebates based on the seasonal energy efficiency ratio (SEER) of the purchased equipment. The SEER is determined from a series of laboratory tests at an outdoor temperature (82°F (27.8°C)) that is lower than the typical high temperature of a summer day when an electric utility's peak demand for electricity may occur (ARI 1989). Because of the 82°F (27.8°C) rating, manufacturers have had an incentive to optimize system performance at 82°F (27.8°C) rather than at high temperatures. Thus, higher SEER's may not necessarily mean performance is optimum at high outdoor temperatures. A recent study indicated that a given percentage increase in SEER did not lead to a similar percentage increase in efficiency (Proctor et al 1994).

Overall hardware configuration of an air conditioning system is an important factor in determining system performance. The combination of the various parts of the system must be optimized to provide the most efficient operation. The majority of the literature available in this area (Farzad 1990; Stoecker, Smith, and Emde 1981; Senshu et al. 1985; etc.) has examined only one aspect of hardware configuration (e.g. expansion devices)

and has not subjected the units to the extreme high outdoor temperatures involved in this study.

This investigation examines the cooling performance of air conditioners and heat pumps at high outdoor ambient temperatures to determine:

(1) The accuracy of published manufacturer cooling performance data at high outdoor temperatures.

(2) The effect of hardware configuration (compressor type, expansion device, etc.) on overall system performance (capacity, power requirements, and energy efficiency ratio) at high outdoor temperatures.

(3) If a statistical relationship exists between the SEER and energy efficiency ratio (EER) of an air conditioning system for various hardware configurations.

Ten air conditioning units were selected by the six electric utilities involved in the project. The units were made by six different manufacturers and included two compressor types (scroll and reciprocating), three expansion devices (capillary tube, short-tube orifice, and thermostatic expansion valve (TXV)), air conditioners and heat pumps, and both split and package systems. Nominal capacities ranged from two tons (7.03 kW) to four tons (14.06 kW). All units were tested in accordance with American Refrigeration Institute (ARI) and Department of Energy (DOE) test procedures (ARI 1989; Federal Register 1995). Measurements of total power, power factor, refrigerant and air flow rate, temperature, pressure, and dew point were made on the systems.

In addition to the tests, data sheets from five manufacturers were examined. The data sheets included air conditioner performance data at high outdoor temperatures as well as hardware configuration. These data were used to develop some simple models to predict air conditioning power requirements based on known characteristics of the system. The establishment of a way to estimate air conditioning power draw provides utilities with a method of determining the value of their rebate programs. Currently, these programs often rely on the SEER of the system alone. The model indicates a relationship between EER and SEER and allows a calculation of the power demand reduction for a particular unit.

Chapter II discusses the relevant literature investigated for this study. Prior research in related areas was reviewed to determine what information was known and what areas should be examined further. In Chapter III, the ten units which were tested are described in terms of their hardware configuration and operating characteristics. Chapter IV and V explain the experimental apparatus and procedure, respectively, to provide a method of repeatability for the tests. Chapter VI compares the results of the testing to available manufacturers' data. Chapter VII discusses the analysis of manufacturers' data sheets. The chapter includes relations between hardware configuration and system performance. Simple models describing these relationships are also listed. Conclusions and future recommendations are stated in Chapter VIII.

CHAPTER II

LITERATURE REVIEW

This chapter examines prior research related to the current project, beginning with individual hardware components of the system and leading to system power requirements and demand. The lack of research in indicated areas provides the basis for the current research, which is explained in more detail at the end of the chapter.

Expansion Devices

The expansion device serves to regulate flow between the condenser and evaporator in an air conditioning system. The most common expansion devices in air conditioning systems include the thermostatic expansion valve (TXV), the capillary tube, and the short-tube orifice. The TXV is the most expensive of the three, but it can more easily adjust to changes in operating conditions, such as an increase in outdoor ambient temperature (Proctor et al 1994). Both the capillary tube and orifices are inexpensive and are fixed area devices. They are sized to produce optimal system operation at a narrow range of operating conditions. In contrast, the TXV can adjust its flow opening to adapt to different conditions in the evaporator. The orifice also eliminates the need for flow direction change check valves when used in heat pump systems (Lennox 1993).

Several researchers have studied the influence of expansion devices on system

performance. Stoecker, Smith, and Emde (1981) investigated the performance of an air conditioner with a capillary tube versus that with a TXV. They found that the system with a TXV experienced between a 2% and 3% higher coefficient of performance (COP), on average, than one with a capillary tube. This work was performed at ambient temperatures ranging from about 70°F (21.1°C) to 100°F (37.8°C). In their study, the COP's of both systems were virtually equal at the high end of the temperature range. The COP of the capillary tube increased at a slower rate than the TXV system as the outdoor temperature was reduced. The capacity of the system with the TXV increased with a decrease in outdoor temperature, whereas the cooling capacity of the capillary tube system showed a small decrease.

Farzad and O'Neal (1993) extended this research with the inclusion of a short-tube orifice expansion device. Their work involved outdoor temperatures ranging from 82°F (27.8°C) to 100°F (37.8°C). Results indicated that the capacities of air conditioners with TXV and capillary tube expansion had a stronger dependence on outdoor temperature than those with short-tube orifices. For example, the TXV and capillary tube systems experienced a 10% drop in capacity for an outdoor temperature increase from 82°F (27.8°C) to 100°F (37.8°C) compared to a 6% drop for the orifice. All three units experienced similar drops in the EER with an increase in outdoor temperature. Over the entire temperature range, EER's of 10.7, 10.4, and 10.3 for the system with the capillary tube, TXV, and orifice, respectively, decreased to around 8.5 for each unit. For both the capacity and EER, the capillary tube unit experienced the highest initial value at 82°F

(27.8°C) with the TXV unit slightly above the orifice. The SEER, however, was highest for the TXV, dropped slightly for the orifice, and dropped more significantly for the capillary tube. The power consumption for each of the units increased with an increase in outdoor temperature by an average of 12% over the temperature range from 82°F (27.8°C) to 100°F (37.8°C).

Farzad and O'Neal (1993) also looked at the importance of refrigerant charge on system performance. The capillary tube system had its highest capacity and EER at full charge at 82°F (27.8°C) and 90°F (32.2°C) outdoor temperatures. For 95°F (35°C) and 100°F (37.8°C), the highest values occurred when the system approached a 5% undercharge. The TXV system performed best when 10% overcharged at 82°F (27.8°C). Its highest capacity and EER occurred closer to full charge as the temperature increased to 100°F (37.8°C). For the orifice, the highest capacity occurred at approximately 10% overcharge for each of the tested temperatures. The optimum EER, however, was measured closer to full charge at each temperature.

Compressor

In air conditioners and heat pumps, compressors consume between 80 and 90 percent of the total electric power required (Senshu et al 1985; Matsubara, Suefuji, and Kuno 1987). Compressor efficiency is therefore important in system performance. Currently, the two most common types of compressors used in residential unitary equipment are the reciprocating and scroll compressors. Scroll compressors were first put

into commercial production for residential unitary air conditioning equipment in 1983 in Japan (Senshu et al 1985). The first scroll systems were introduced in the United States in 1987 (Beseler 1987).

Scroll compressors provide as much as a 5% to 10% efficiency advance over equivalent capacity reciprocating compressors (Beseler 1987). This efficiency improvement at high pressure ratios is particularly important for heat pumps (Matsubara, Suefuji, and Kuno 1987). Furthermore, scroll compressors possess fewer parts than similar reciprocating compressors which should lead to higher reliability. The scroll compressors also require no suction valves and are thus more accepting of liquid refrigerant. With no suction valve, the valve losses are eliminated and the scroll compressor provides inherent efficiency improvements over the reciprocating compressor (Senshu et al 1985). Senshu et al (1985) found that scroll compressors between about 0.65 and 3.5 tons (2.28 and 12.3 kW) should possess between 10% and 13%, respectively, greater adiabatic efficiency ratios than their reciprocating compressor counterparts.

Air Conditioners and Heat Pumps

The main difference between air conditioners and heat pumps is in a reversing valve which allows the heat pump to reverse cycle and provide heating as well as cooling. In an analysis of design optimization for heat pumps, Fischer and Rice (1985) concluded that the higher average SEER values of air conditioners over heat pumps is probably due to the reversing valve losses. David Young also discovered these losses in his analysis of

residential air-source heat pumps (Young 1980). He estimated a heat pump's performance drops by around 10% due to heat and mass leakage caused by a sliding port reversing valve. Refrigerant of approximately 20 lb/h (2.5 g/s) leaked from the discharge to the suction side of the tested system. Damasceno et al (1988) also looked at the effects of the reversing valve on system performance. Using a system with a 9 EER, they found that suction heat gain should lower the heat pump performance by less than 2.5%. Likewise, discharge heat loss should have less than a 3% effect on overall performance.

Many manufacturers use an accumulator on the suction side of the compressor in heat pumps. This protects the compressor during defrost initiation by preventing compressor flooding (ASHRAE 1988). However, much of the refrigerant can be stored in the accumulator during the off cycle. When the unit starts up, the refrigerant must be pulled from the accumulator into the rest of the system. This process takes time, increases cycling losses, and reduces the SEER rating.

Package and Split-System Units

Packaged air conditioners have the evaporator and condenser in a single assembly while the condenser and evaporator are in separate assemblies in a split system. Since 1981, the average seasonal energy efficiency ratios of split-system units has increased at a greater rate than package-system units. In 1981, the average SEER for split-system units was 7.73 (ARI 1985). At this time, 3.2% of these units had SEER's above 9.0. By 1985, the average SEER increased to 8.84, and 40.2% of the units had SEER's above 9.0. For

package systems, the SEER increased from 8.06 to 8.71 between 1981 and 1985. The percentage of units with SEER's above 9.0 went from 8.7% to 24.4% during this time frame.

The vast majority of unitary residential air conditioning equipment sold in the United States are split-system units. In 1992, only 19% of domestic unitary air conditioner shipments were package systems (ARI 1993). For heat pumps, this percentage was only 16%.

Power and Demand

Electric utility companies are interested in the power demand and power factor of the air conditioners during the time of utility system peak demand. The customers are concerned largely with the unit maintaining comfort in their residences and the size of their cooling bills. Lower power demand for new air conditioners could lessen the need for additional power plants and save money for both the utility and the consumer. Some electric utilities have encouraged the purchase of high efficiency air conditioners by subsidizing them with rebates.

Congress passed the National Appliance Energy Conservation Act of 1987 to establish minimum efficiencies for air-conditioners and heat pumps sold in the United States. With the support of the DOE, ARI, and most major manufacturers of unitary air conditioning equipment (Energy Conservation Hearing 1986), a minimum SEER of 10

was established for split systems manufactured after 1991 and a minimum SEER of 9.7 was established for single package systems manufactured after 1992. In addition, a minimum heating seasonal performance factor (HSPF) was established for heat pumps. For split systems, an HSPF of at least 6.8 was required and for package systems, an HSPF of at least 6.6 was mandated (Conservation Act 1987).

In an investigation of the impact of air conditioning charging and sizing on peak electrical demand limited to capillary tube units, Neal and O'Neal (1992) found that proper sizing is a major factor in lowering utility peak demand. For example, the peak demand of a properly sized 10 SEER air conditioner was 23% lower than one which was oversized by 75%. Proper charging was also found to impact peak demand. A 75% oversized and 20% overcharged or undercharged 10 EER air conditioner was found to require 0.65 kW more than a properly charged three ton (10.5 kW) system. Finally, their study indicated a change in SEER from 8 to 10 resulted in an approximate 16% reduction in demand for the system tested.

Another report (Proctor et al 1994) investigated peak electric load as affected by different air conditioning systems. Their results indicated that the SEER of a unit alone does not accurately predict peak kW or kVA. Several reasons were cited for this occurrence. For example, lowering cycling losses does not automatically raise the efficiency under steady state conditions. Also, improvements which increase capacity generally increase power requirements as well, thereby increasing demand. Finally,

different units have different capacities even though their nominal capacities may be identical. Units with design capacities of 34,000 Btu/h (9.96 kW) and 38,000 Btu/h (11.1 kW), for instance, will both likely be listed as three ton units.

For single-speed units of a given rated capacity, Proctor et al (1994) found that higher SEER units usually, but not always, required less power at peak conditions than lower SEER units. One manufacturer's three ton unit had a 10 SEER and a 33,800 Btu/h (9.90 kW) design capacity while another manufacturer's three ton unit had a 11.7 SEER and a 37,000 Btu/h (10.8 kW) rating. At 115°F (46.1°C), the higher SEER unit required almost 7% more power than the lower SEER unit.

Units with two speed compressors generally did not reduce peak demand when compared to their single-speed counterparts as indicated in Figure 2.1 (Proctor et al 1994). Peak conditions normally occur at high outdoor temperatures in the summer when the two speed units are operating at high speed. At high speed, a two-speed units' efficiency is similar to a single-speed unit. Thus a two-speed unit may require as much power at high outdoor temperatures as a single-speed system.

Another result from Proctor et al (1994) related to the performance of scroll compressors at high outdoor temperatures. Performance characteristics were modeled using Oak Ridge National Laboratory's MODCON simulation. Despite the efficiency advantages of scroll compressors, Proctor et al (1994) found that using scroll compressors

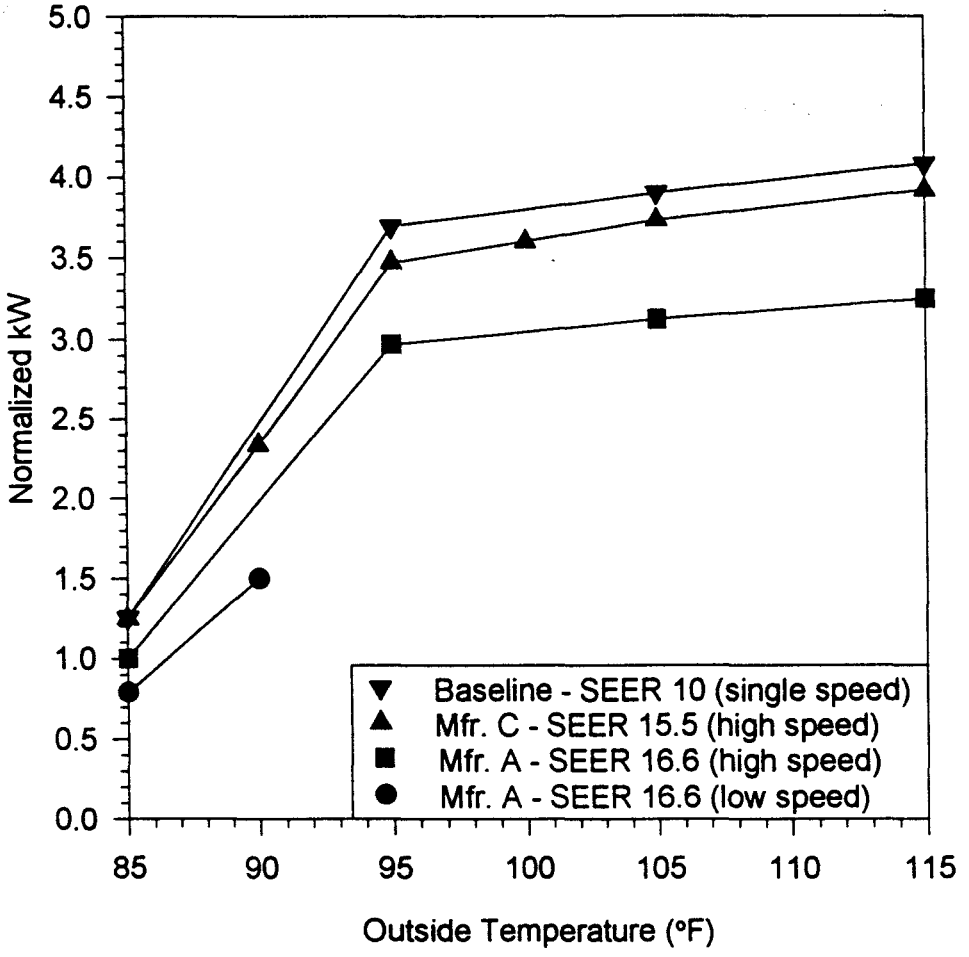

***Figure 2.1** Normalized kW vs. outdoor temperature for two-speed units. (Source: Proctor et al (1994))*

as opposed to reciprocating compressors was ineffective at reducing peak kilowatt demand (Figure 2.2). In the figure, a condensing temperature of 120°F (48.9°C) corresponds to an outdoor temperature of about 95°F (35.0°C) and a condensing temperature of 130°F (54.4°C) corresponds to an outdoor temperature of approximately 105°F (40.6°C). Beyond approximately 100°F (37.8°C), the scroll compressor actually drew more power than a reciprocating compressor of the same nominal capacity. Variable speed compressors were also found to be unproductive in the lowering of demand (Proctor et al 1994).

EER and SEER

The DOE requires a rating system for residential air conditioners and heat pumps based on their seasonal energy efficiency ratios (Federal Register 1995). The SEER is found by dividing the total cooling in Btu's of an air conditioner during its normal cooling period by the total power input in watt-hours during the same time frame. (ARI 1989). This ratio takes into account the cycling of the system. Before 1981, all units were rated based on the EER value. The EER is a ratio determined by dividing net cooling capacity in Btu/h by the total power input in watts. It is a steady state rating which is calculated at a 95°F (35°C) outdoor temperature (ARI 1989). After 1981, the SEER rating was used for all residential air conditioners and heat pumps (Appliance Efficiency Standards Hearing 1981).

A study by Nguyen et al (1982) provided an initial look at a possible relationship between the EER and SEER of an air conditioning unit. This study looked at nearly 200

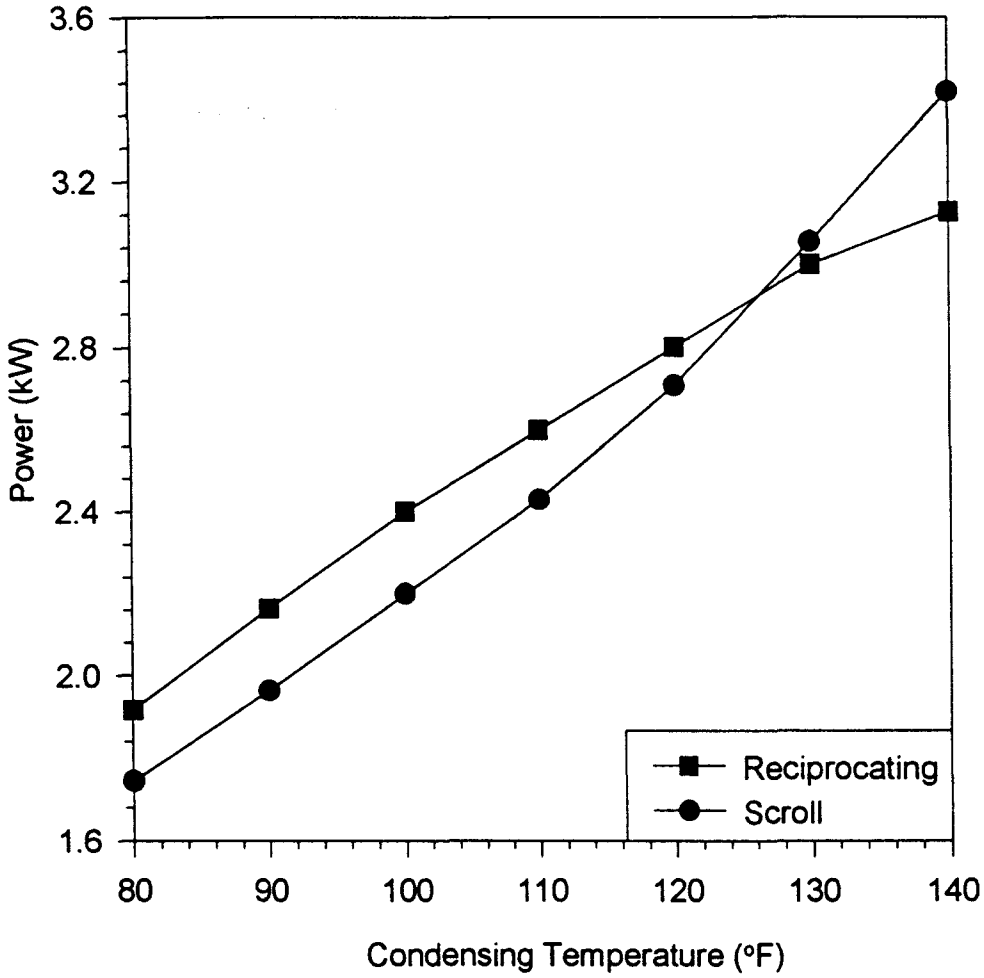

***Figure 2.2** Reciprocating vs. scroll compressor performance at 45°F evaporating temperature. (Source: Proctor et al (1994))*

single-speed units and found a statistical connection between the steady state and cyclic efficiencies. The results of this study are shown in Table 2.1. A fit of the data provided a simple linear relationship of

$$SEER = 1.062 * EER@95 \quad (2.1)$$

with an r^2 of 0.961.

***Table 2.1** Relationship of SEER and EER@95 for various hardware configurations.*

Data Sample	SEER/EER@95	90% Confidence Band
All Data	1.057	± .031
Single-Package	1.063	± .056
Split	1.056	± .036
Thermal Expansion Valve	1.077	± .081
Capillary Tube	1.043	± .055
Orifice	1.063	± .047

Nguyen's work indicated the possibility of predicting the EER of a unit, and thus its approximate power requirements (assuming the nominal capacity is known) using only the rated SEER value. If a simple relationship existed, this would allow the electric utilities to be more confident in their rebate policies by estimating demand requirements for various systems. Since Nguyen's work was completed, a number of technologies such as scroll compressors, variable speed motors, higher efficiency motors, and internally finned tubes have been implemented into the design of air conditioning systems. Thus, the average SEER of residential unitary air conditioning units has improved from 7.78 in 1981 to 10.61 in 1994 (ARI 1995). Likewise, the average SEER for residential heat pumps has risen from 7.70 to 10.94 from 1981 to 1994. As a result, it is not known

whether a statistical relationship still exists between the EER and SEER of a unit, and if so, if the relationship has changed since the initial study was done. The current research examines new manufacturer data to assist in answering this question.

This research extends the work of much of the earlier studies by examining the effect of the overall hardware configuration of an air conditioning system on system performance. The effects of individual components are analyzed to determine common operating characteristics for units containing these components. It is hoped the research will then provide a simple method of predicting performance based primarily on the hardware of the system.

CHAPTER III

UNIT DESCRIPTIONS

The first step in this research was the verification of manufacturers' cooling performance test data for outdoor ambient temperatures between 80°F (26.7°C) and 120°F (48.9°C). A total of ten air conditioners and heat pumps were tested. These units were chosen by the Electric Power Research Institute (EPRI) and six utilities sponsoring the project: Nevada Power, Pacific Gas & Electric Company, Arizona Public Service, Salt River Project, IES Utilities, and Interstate Power Company. The units were representative of those sold in the utilities' service areas and included package and split system units, air conditioners and heat pumps, reciprocating and scroll compressors, and capillary, TXV, and orifice expansion devices. All units tested had single-speed compressors. The major hardware features of each unit are listed in Table 3.1. The explanation of the codes used in Table 3.1 is provided in Table 3.2.

***Table 3.1** Hardware configuration of tested units.*

Unit	Capacity	Package/Split	Expansion	Compressor	AC/HP
1	3.5	S	T	S	C
2	2.5	S	T	S	C
3	3.5	S	O	R	H
4	3.0	S	O	S	C
5	3.5	S	T	S	H
6	4.0	S	O	R	C
7	3.5	P	O	S	C
8	3.5	P	C	S	H
9	3.0	P	T	R	H
10	2.0	S	T	S	C

the suction linewas 1.13" (28.6 mm) and the liquid line was 0.375" (9.53 mm).

The indoor unit consisted of an A-coil evaporator with no air handler. An assist blower was used to obtain the flowrate of 1433 cfm (0.676 m^3/s), and the coil was arranged so the airflow was upward through the evaporator. The rectangular base of the coil was 19.8" (502 mm) by 24.9" (632 mm), with the coil extending vertically 26.8" (680 mm). This provided for a coil face area of 7.58 ft^2 (0.704 m^2). The evaporator consisted of three coil rows containing 12 fins/inch (0.472 fins/mm).

The outdoor unit included a condenser coil and a condenser fan. The base of the unit was 34.1" (865 mm) by 32.1" (816 mm) with a height of 40.9" (1040 mm). There were two coil rows of 20 fins/inch (0.787 fins/mm) providing a face area of 21.6 ft^2 (2.01 m^2) for the outer coil and 20.8 ft^2 (1.93 m^2) for the inner coil. The condenser fan assembly was an 820 rpm, 3230 cfm (1.52 m^3/s) nominally rated fan with a 1/6 hp (124 W) motor. The fan was 24" (610 mm) in diameter and consisted of three blades.

2) E30STS1C

The next unit was a 2.5 ton (8.79 kW) split-system air conditioner with a 13.25 SEER. This unit also included a scroll compressor and TXV expansion. The suction line was 0.75" (19.1 mm) in diameter and the liquid line was 0.375" (9.53 mm).

The evaporator coil was an A-coil of dimensions 14.75" x 19.75" x 19" (375 mm x

502 mm x 483 mm). With three coil rows possessing 12 fins/inch (0.472 fins/mm), the coil face area was 4.44 ft^2 (0.412 m^2). This coil was not equipped with an air handler and was arranged to provide vertical air flow of 999 cfm (0.470 m^3/s) through the evaporator. The outdoor unit was 32.1" x 34.1" x 30.9" (816 mm x 865 mm x 784 mm). On the condenser coil, 20 fins/inch (0.787 fins/mm) were on 1.36 rows of coil tubing, resulting in a coil face area of 15.9 ft^2 (1.48 m^2) for the outer coil and 5.5 ft^2 (0.510 m^2) for the inner coil. The condenser fan was an 820 rpm, 3150 cfm (1.49 m^3/s) rated fan with a 1/6 hp (124 W) motor. It included three blades and was 24" (610 mm) in diameter.

3) B42SOR1H TWR 042 C100 A TWV042B14

This unit was a 3.5 ton (12.3 kW), 10 SEER, split-system air conditioner with a reciprocating compressor and an orifice plate expansion device. The system line sizes were 0.875" (22.2 mm) for the suction line and 0.375" (9.53 mm) for the liquid line.

The indoor unit included an evaporator A-coil and a centrifugal fan, packaged in a single air handler. The air handler was 23.5" x 26" x 46.5" (597 mm x 660 mm x 1180 mm), and was arranged to force air at 1387 cfm (0.652 m^3/s) upward through the coil. The indoor coil had three rows with 14 fins/inch (0.551 fins/mm) on the line. A coil face area of 3.90 ft^2 (0.362 m^2) resulted from this arrangement.

The outdoor assembly consisted of a condenser and a 22" (559 mm) diameter propeller fan. This fan was a direct drive, single-speed, 1/4 hp (186 W), 825 rpm fan rated

nominally at 3070 cfm (1.45 m^3/s). The outdoor coil had one row with 24 spine fins/inch (0.945 fins/mm). This resulted in a face area of 20.32 ft^2 (1.89 m^2). Overall, the outdoor unit was 34.8" x 31.3" x 33.3" (883 mm x 794 mm x 845 mm).

4) D36SOS1C

This unit was a three ton (10.5 kW), split-system air conditioner with a 12 SEER. It had a scroll compressor and utilized orifice expansion. The diameter of the suction line was 0.75" (19.1 mm) and the diameter of the liquid line was 0.375" (9.53 mm).

The indoor system consisted of a rectangular evaporator coil with no air handler. An assist blower helped provide the desired air flowrate of 1202 cfm (0.566 m^3/s), and the air was forced through the coil in a crossflow fashion. With a face area of 3.17 ft^2 (0.295 m^2) the heat exchanger was 25.1" x 28.8" x 9.75" (638 mm x 730 mm x 248 mm). The coil had three rows with 14 fins/inch (0.551 fins/mm).

The outdoor unit had a condenser coil and a propeller, direct-drive fan, which was nominally rated at 3000 cfm (1.42 m^3/s). The condenser had one coil row with 28 fins/inch (1.10 fins/mm), providing a face area of 18.3 ft^2 (1.70 m^2). The entire outdoor system was 30" x 34.3" x 39.8" (762 mm x 871 mm x 1010 mm).

5) D42STS1H

The fifth unit was a 3.5 ton (12.3 kW), 12.7 SEER, split system heat pump with a

scroll compressor and TXV expansion. Copper tubing lines of diameter 0.375" (9.53 mm) suction and 0.875" (22.2 mm) liquid were used on the system.

The indoor unit was an air handler, containing an evaporator coil and fan. The A-coil evaporator consisted of three rows of 14.5 fins/inch (0.571 fins/mm) and had a face area of 5.93 ft^2 (0.551 m^2). Rated at 1300 cfm (0.613 m^3/s), the indoor blower was run by a 1/3 hp (249 W) motor. The entire indoor system was 22.06" x 21.13" x 53.44" (560 mm x 537 mm x 1360 mm). Air was run crossflow through the air handler at a rate of 1326 cfm (0.624 m^3/s).

The outdoor portion of this system was 30" x 34.9" x 33.8" (762 mm x 887 mm x 859 mm). It contained a condenser coil with a face area of 15.15 ft^2 (1.41 m^2). This coil had two rows of 20 fins/inch (0.787 fins/mm). The condenser fan was a propeller, direct-drive fan, rated nominally at 2400 cfm (1.13 m^3/s) and 825 rpm.

6) G48SOR1C

This unit was a four ton (14.1 kW), split-system air conditioner with a 10.2 SEER. It utilized a reciprocating compressor and an orifice expansion device. The diameter of the suction line was 0.875" (22.2 mm) and the liquid line was 0.375" (9.53 mm).

The indoor system consisted of an A-coil evaporator with no air handler. Air was forced upward through the coil at 1610 cfm (0.758 m^3/s) through the use of the assist

blower. The coil had 14 fins/inch (0.551 fins/mm) in three rows, providing a face area of 6 ft^2 (0.557 m^2). The coil was 16" x 13" x 16.5" (406 mm x 330 mm x 419 mm).

The outdoor unit contained a condenser coil and fan. The fan was 24" (610 mm) in diameter and was run at 850 rpm by a 1/4 hp (186 W) motor, providing nominal air flow of 3100 cfm (1.46 m^3/s). With one row containing 13 fins/inch (0.512 fins/mm), the condenser coil had a face area of 20 ft^2 (1.86 m^2). The entire outdoor system was 34.5" x 34.5" x 31.9" (876 mm x 876 mm x 810 mm).

7) D42POS1C

This unit was the first package system tested. It was a 3.5 ton (12.3 kW) air conditioner with a 12 SEER, a scroll compressor, and orifice expansion. The suction line diameter was 0.75" (19.1 mm) and the liquid line was 0.375" (9.53 mm). Since this was a package system, the entire air conditioner was in a single assembly which was placed in the outdoor room. The supply and return openings were then ducted to the indoor room. The overall unit was 45.5" x 52" x 37.4" (1160 mm x 1321 mm x 951 mm).

The rectangular evaporator coil had a face area of 4.4 ft^2 (0.409 m^2) and was comprised of three rows of tubes with 15 fins/inch (0.591 fins/mm). Next to the coil, the evaporator fan was rated at 1100 rpm and provided a nominal airflow of 1400 cfm (0.661 m^3/s). The centrifugal fan was 10" in (254 mm) diameter and 10" (254 mm) wide and was run by a 1/2 hp (373 W) motor. Air was run across the coil at 1420 cfm (0.668 m^3/s) using

the assist blower.

The other section of the package unit included a condenser coil and a condenser fan. The coil had two rows with 17 fins/inch (0.669 fins/mm), providing a face area of 8.7 ft^2 (0.808 m^2). With a nominal airflow of 2400 cfm (1.13 m^3/s), the 1100 rpm condenser fan was 20" (508 mm) in diameter and was run by a 1/4 hp (186 W) motor.

8) A42PCS1H

The next unit was a 3.5 ton (12.3 kW) package heat pump with a 12 SEER. It had a scroll compressor, a capillary tube expansion device, a suction line of 0.375" (9.53 mm) diameter and a liquid line of 0.375" (9.53 mm) diameter. The entire system was 44.4" x 57.8" x 30.3" (1130 mm x 1470 mm x 768 mm).

The evaporator section consisted of an A-coil evaporator and a centrifugal blower. The blower was 9.5" (241 mm) in diameter and 9.62" (244 mm) wide, and was rated at 1620 cfm (0.764 m^3/s) nominally when run by a 1/3 hp (249 W) motor. At the evaporator, two rows of 16 fins/inch (0.630 fins/mm) provided a face area of 4.81 ft^2 (0.447 m^2). Air was forced through the evaporator at 1410 cfm (0.664 m^3/s).

The condenser section was composed of the condenser and a condenser fan. The fan was 22" (559 mm) in diameter, and was rated at 3270 cfm (1.54 m^3/s) and 1100 rpm using a 1/3 hp (249 W) motor. A condenser face area of 11.3 ft^2 (1.05 m^2) resulted from

two rows of tubing with 12 fins/inch (0.472 fins/mm).

9) H36PTR1H

This unit was the last of the three package units tested, and was rated as a three ton (10.5 kW) heat pump with a 12 SEER. It used a reciprocating compressor and TXV expansion. The unit was 32" x 46" x 28" (813 mm x 1170 mm x 711 mm) and used a 0.375" (9.53 mm) diameter suction line and a 0.313" (7.94 mm) liquid line.

The rectangular evaporator coil had three rows with ten fins/inch and a face area of 4.66 ft^2 (0.433 m^2). Air across the coil at 1220 cfm (0.574 m^3/s) was provided by a blower of 10" (254 mm) diameter and 7" (178 mm) width along with the assist blower. The blower in the package system was run by a 1/2 hp (373 W) motor and rated at 1000 rpm and 1200 cfm (0.565 m^3/s).

The outdoor section consisted of the condenser coil and fan. The coil had 10.85 ft^2 (1.01 m^2) of face area. This resulted from two rows of 16 fins/inch (0.630 fins/mm). Run by a 1/4 hp (186 W) motor, the 20" (508 mm) diameter fan was nominally rated at 1100 rpm and 2500 cfm (1.18 m^3/s).

10) D24STS1C

This unit was the last unit tested. It was a two ton (7.03 kW), 13.00 SEER, split-system air conditioner, utilizing TXV expansion and a scroll compressor. On the system,

the diameter of the suction line was 0.625" (15.9 mm) and the liquid line was 0.375" (9.53 mm). This unit consisted of an indoor and outdoor unit from two different manufacturers. The manufacturer code listed is the manufacturer of the condensing unit.

The indoor unit consisted of an A-coil with no air handler. An assist blower was used to cause upflow of the air at 813 cfm (0.383 m^3/s) through the coil. The coil was 14" x 16" x 16.5" (356 mm x 406 mm x 419 mm). It had three rows of coil tubing with 16 fins/inch (0.630 fins/mm) and a face area of 2.92 ft^2 (0.271 m^2).

The outdoor unit was 34.9" x 30" x 27.8" (887 mm x 762 mm x 706 mm) and contained a condenser coil and fan. The coil had a face area of 12.2 ft^2 (1.13 m^2), provided by one tube row containing 25 fins/inch (0.984 fins/mm). The fan was a propeller, direct drive fan rated nominally at 2000 cfm (0.944 m^3/s).

Summary

The number of systems exhibiting each aspect of hardware configuration is listed in Table 3.3. Each of the units was tested under the same conditions as described in the experimental procedure in Chapter V.

Table 3.3 *Summary of the characteristics of the units tested.*

System Characteristic	Number of Units With Characteristic
Split System	7
Package System	3
Air Conditioner	6
Heat Pump	4
Scroll Compressor	7
Reciprocating Compressor	3
TXV Expansion	5
Orifice Expansion	4
Capillary Expansion	1

CHAPTER IV

EXPERIMENTAL SETUP

One of the purposes of the experimentation was to analyze the effects of the hardware configuration of an air conditioning system on its overall cooling performance at high outdoor ambient temperatures. This analysis required the collection of pressure, temperature, and flowrate measurements for the refrigerant; temperature, humidity, dewpoint, wetbulb, and flowrate measurements for the air; and power measurements for the condenser fan, the evaporator blower (when applicable), and the compressor. Chlorodifluoromethane (R-22) was used in each test. The experimental set-up consisted of the psychrometric rooms, an indoor and outdoor unit (connected by appropriate tubing), appropriate instrumentation and a data acquisition system. Each of these are described below.

Psychrometric Rooms

The units were tested in the two psychrometric rooms at the Energy Systems Lab at Texas A&M University Riverside Campus. These rooms provided a method for maintaining an "indoor" and "outdoor" room at a desired temperature and humidity. The psychrometric rooms were built in accordance with ASHRAE specifications (ASHRAE 1983) and were designed for testing units with capacities up to 10 tons (35.2 kW). In each of the psychrometric rooms, heating, cooling, humidification, and dehumidification coils

were mounted near the ceiling.

The control of the room temperatures was accomplished through the use of chilled water coils and electric resistance heaters. The cooling coils were supplied with a water ethylene glycol solution which was cooled using a 150 ton (528 kW) chiller. To provide thermal capacity, a 1000 gallon (3800 L) storage tank was mounted in the chilled water system. Reheat in the rooms was provided to the air using four banks of electric resistance heaters, which were mounted in the supply air ducts. The heating capacity of the heaters was 33,780 Btu/h (9.9 kW) per bank. The temperatures in the rooms could be maintained within ± 0.2°F (±0.11°C) of the desired values.

Humidity in the rooms was controlled with steam humidification and dehumidification coils. Steam from a gas fired boiler was fed into the supply air to raise the humidity. Dehumidification coils in the supply duct received water from the chiller and were used to lower the humidity when necessary.

The indoor room contained an Air Movement and Control Association (AMCA) 210 (1985) air flow chamber and a booster fan which pulled the desired flowrate of air across the evaporator coil. Four ASME nozzles of 8" (203 mm), 8" (203 mm), 5" (127 mm), and 3" (76.2 mm) could be used in any combination to provide air flow between 100 and 5000 cfm (0.0472 and 2.36 m^3/s). A damper in the chamber allowed the adjustment of air flow through the system. In the tests, the flowrate ranged from approximately 800 cfm (0.378 m^3/s) for the two ton (7.03 kW) unit to approximately 1600 cfm (0.755 m^3/s) for the

four ton (14.1 kW) unit. During each set of tests for a particular unit, the flowrate remained approximately constant.

Indoor and Outdoor Test Sections

In each test, units were placed in either the indoor or outdoor room to simulate actual operating conditions. For the split-system units, the indoor test area was comprised of the indoor air flow chamber and the indoor unit (Figure 4.1). The indoor unit contained the expansion device, the evaporator coil, and in some cases an indoor blower in an air handler assembly. Depending on the design and shape of the indoor coil, the unit was arranged to provide air flow either across or up through the evaporator heat exchanger. The arrangement chosen for each unit was described in Chapter III. Ductboard and/or sheet metal were used to duct the air across the evaporator to the air flow assembly.

The outdoor unit consisted of the condenser, the compressor, and an outdoor fan. The fan drew air across the condenser coils on three sides of the unit and exited the warm air through the top. Appropriate copper tubing connected the indoor and outdoor units on both the liquid and suction sides. The sizes of this tubing for the various units were described in Chapter III.

For the package systems, the entire package was set in the outdoor psychrometric room (Figure 4.2). Ductboard was then used to construct ducts and move the air to the desired areas. The supply air duct was run from the package unit, through a hole in the

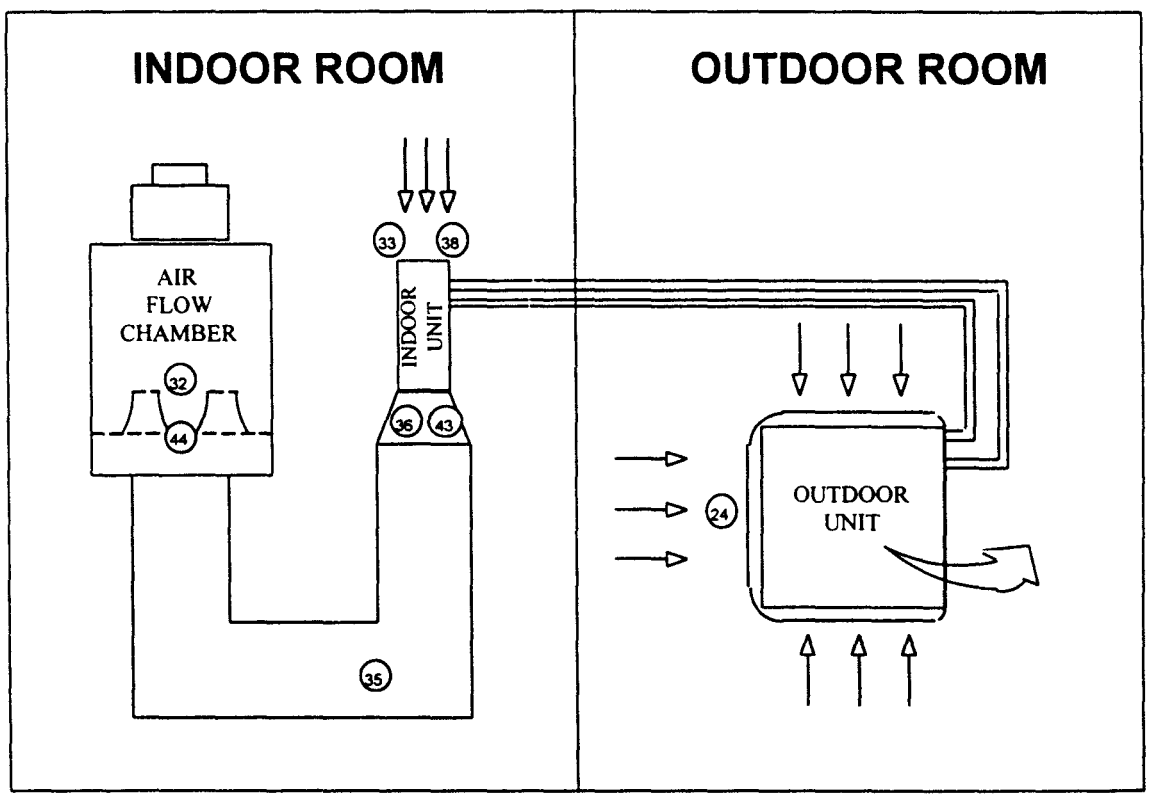

Figure 4.1 *Air-side sensor arrangement -- split-system units (numbers indicate locations of sensors described in Table 4.1)*

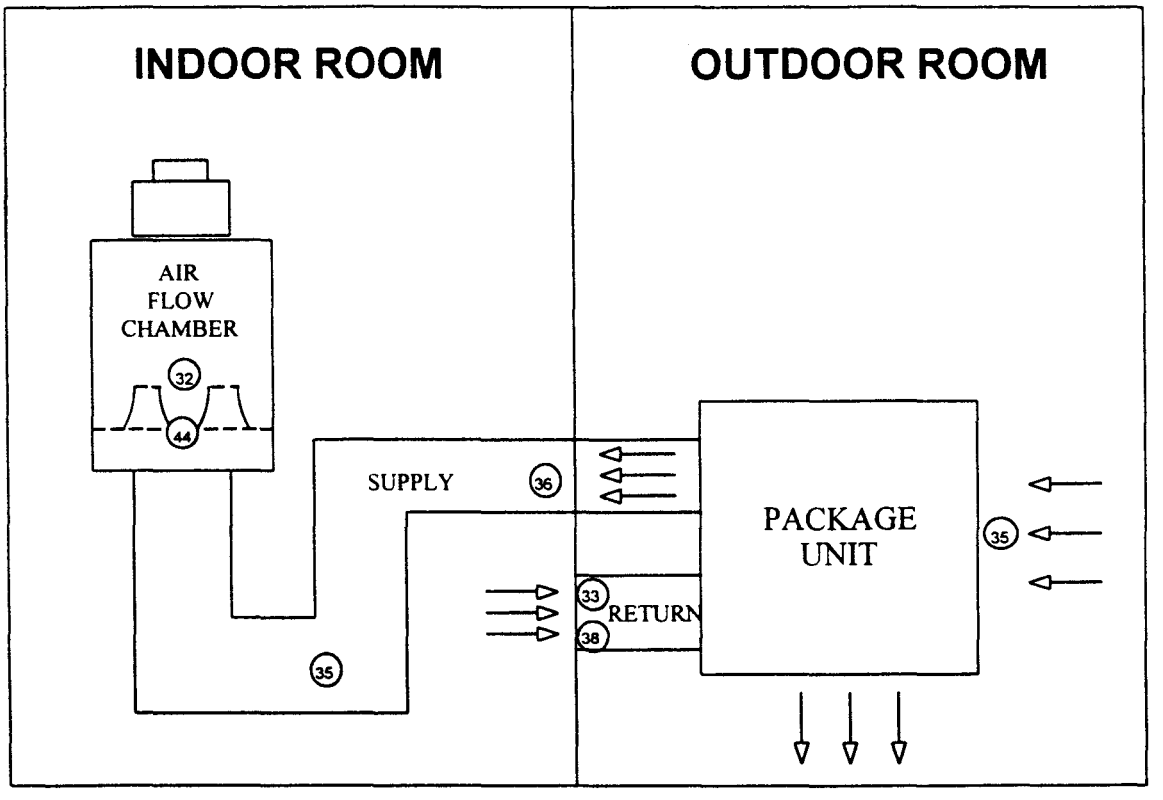

Figure 4.2 *Air-side sensor arrangement -- package units (numbers indicate locations of sensors described in Table 4.1).*

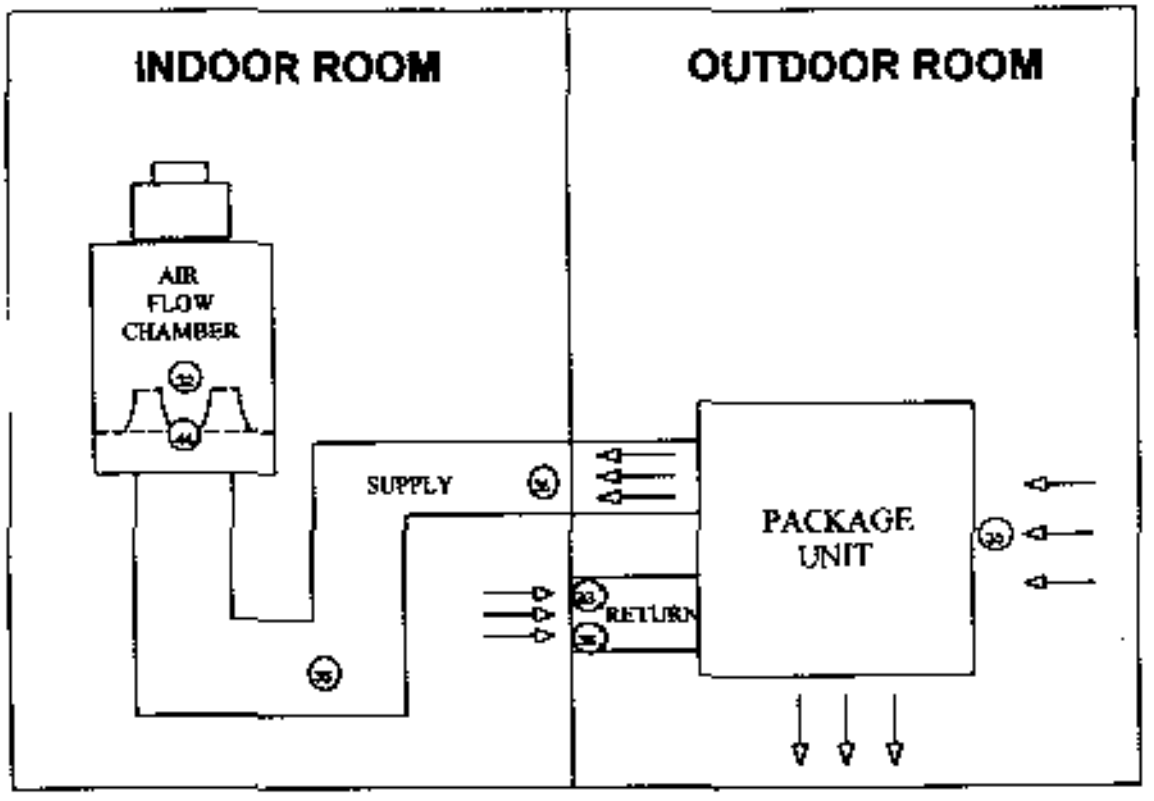

Figure 4.2 Air-side sensor arrangement -- package units (numbers indicate locations of sensors described in Table 4.1).

wall between the indoor and outdoor rooms, to the assist blower in the indoor room. This allowed air to be drawn across the evaporator coil at the desired flowrate. The return air duct extended from the unit to just inside the indoor room, so that the return air was at the temperature and humidity of the room being cooled.

Instrumentation

The test instrumentation consisted of both air-side and refrigerant-side instrumentation. The location of the air-side instrumentation is indicated for the split and package systems in Figures 4.1 and 4.2, respectively. Table 4.1 lists the air-side, refrigerant-side, and power measurement sensors used in the experiment.

For the split systems, an air sampling system was placed in the outdoor room near the unit to measure outdoor ambient temperature. Air was drawn from three sides of the unit to provide an average temperature of air crossing the condenser coils. Type-T thermocouples were used for all temperature measurements. In the indoor room, a wet bulb sensor and a 12 point thermocouple grid upstream of the evaporator provided inlet air conditions. Downstream of the coil, another wet bulb sensor and 12 point thermocouple grid measured exit air conditions. A dew point sensor, also downstream of the evaporator, provided a check of the wet bulb sensor. In the nozzle flow chamber, the differential pressure was measured with a pressure transducer. Entering air temperature was measured with a thermocouple. For the package units, the air-side measurements were identical to those for the split-system units.

Table 4.1 *Data acquisition setup.*

Channel	Sensor Type	Channel Description
0	Mass Flow Meter	Mass Flow Rate
1	Watt Transducer	Condenser Unit Power
2	Pressure Transducer	Mass Flow Meter Exiting Pressure
3	Pressure Transducer	Mass Flow Meter Entering Pressure
4	Pressure Transducer	Condenser Suction Line Pressure
5	Thermocouple	Condenser Liquid Line Pressure
20	Thermocouple	Mass Flow Meter Entering Temp.
21	Thermocouple	Mass Flow Meter Exiting Temp.
22	Thermocouple	Condenser Suction Line Temp.
23	Thermocouple	Condenser Liquid Line Temp.
24	Thermocouple	Outdoor Dry-Bulb Temperature
30	Thermocouple	Evaporator Liquid Line Temp.
31	Thermocouple	Evaporator Suction Line Temp.
32	Thermocouple	Air Flow Chamber Temperature
33	Thermocouple	Evaporator Entering Wet-Bulb Temp.
35	Thermocouple	Evaporator Exiting Wet-Bulb Temp.
36	Thermocouple Grid	Evaporator Exiting Dry-Bulb Temp.
38	Thermocouple Grid	Evaporator Entering Dry-Bulb Temp.
40	Pressure Transducer	Evaporator Liquid Line Pressure
41	Pressure Transducer	Evaporator Suction Line Pressure
43	Dew-point Sensor	Evaporator Exiting Dew-point Temp.
44	Differential Pressure Transducer	Indoor Nozzle Pressure Differential

The refrigerant-side sensor arrangement for the split-system units is shown in Figure 4.3. In the outdoor room, a pressure transducer and thermocouple were placed on the suction line upstream of the compressor, allowing the measurement of refrigerant properties at this point. The pressure transducers were isolated with a ball valve, allowing them to be disconnected, when necessary, without evacuating the system of charge. Another pressure transducer and thermocouple were placed downstream of the condenser on the liquid line. A sight glass was located immediately after these sensors so that any two-phasing of the refrigerant at this point could be observed. A Coriolis type mass flow meter on the liquid line provided direct measuring capability of the refrigerant flow in the system. A pressure transducer , thermocouple, and sight glass were placed on either side of the flow meter to observe the change in refrigerant conditions across the meter.

In the indoor room, a pressure transducer and thermocouple were placed before the expansion device. These sensors were preceded by a sight glass on the liquid line. Another pressure transducer and thermocouple were placed downstream of the evaporator. The indoor refrigerant-side sensors allowed for the calculation of the refrigerant-side capacity. To avoid damaging the package units, their refrigerant lines were not cut. As a result, no refrigerant-side measurements were taken for the package systems.

Power Factor Instrumentation

Power factor measurements were taken on each of the units using a data acquisition system developed at Texas A&M University (Davis 1993). This system was capable of

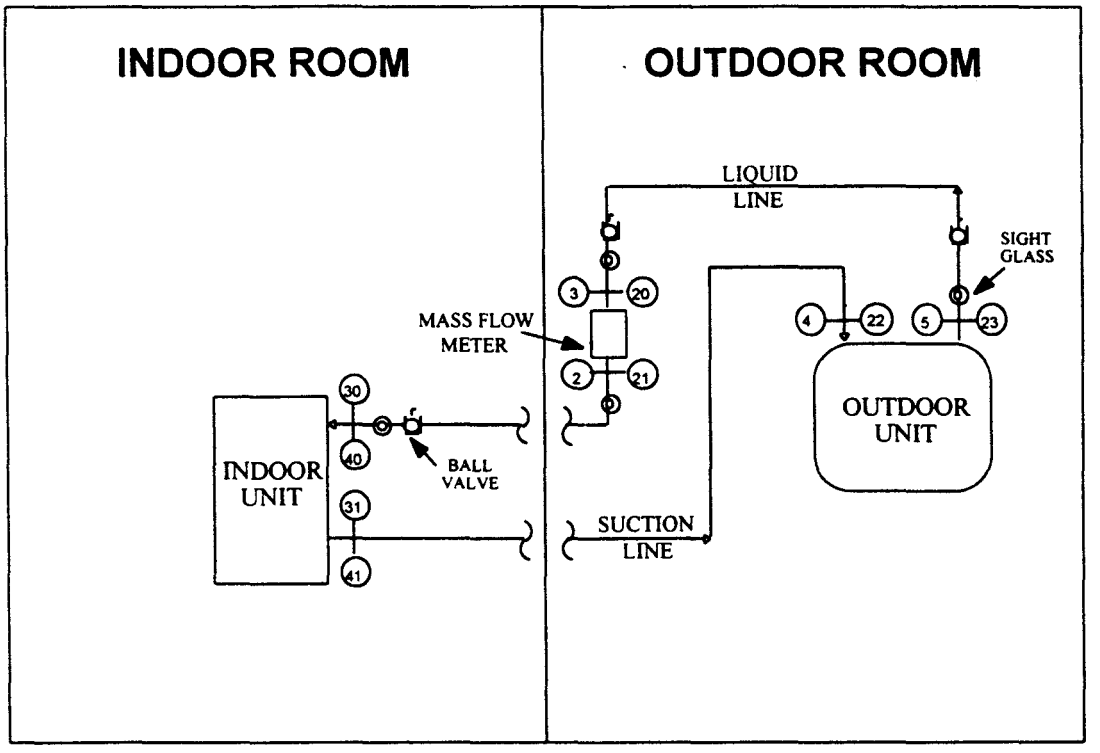

Figure 4.3 Refrigerant-side sensor arrangement -- split-system units.

providing the user with power systems measurements including 10th order harmonics and power factor data. A program was written which produced equally spaced samples of three phase current and voltage waveforms over a single cycle. The system consisted of a master station (MS), a digital data recorder (DDR), and a data acquisition board (DAB). Different parts of the system were able to communicate through serial input/output. The DAB was an embedded controller board which was configured to gather RMS current and voltage on two of the channels. Real-time power systems measurements were possible with the DSP board. Power data were gathered and calculated once every twenty milliseconds. For the experiment, data were averaged over a one second interval and output to a monitor. With the data acquisition system connected to a peak load of 25 kW, a 25 W load could be reliably detected. Amperage loads of as low as 0.2 amp could be measured with sensors calibrated for a 200 amp load.

Data Acquisition

The voltage or current signals from the sensors indicated in Table 4.1 were collected via an Acurex (model Autocalc) data logger. These signals were converted by the logger into engineering units and transferred to a personal computer where the values were displayed real-time on the screen. A controller allowed the values (i.e. desired room temperatures, room humidities, cooling coil valve position, etc.) to be changed on the screen, causing adjustments in the system. The data logger could be programmed to scan at desired intervals and recorded into a file. For each test in this experiment, the scans occurred every 30 seconds for at least 30 minutes, providing in excess of 60 data points for

averaging purposes.

After each test was completed, the data obtained were transferred to a separate computer for the purpose of analysis. The data were averaged over the 30 minute test period. These results were then used in conjunction with Engineering Equation Solver (EES) software to determine air- and refrigerant-side capacity, EER, and energy balances for a given system.

CHAPTER V

EXPERIMENTAL PROCEDURE

The experimental procedure consisted of the testing of the ten units chosen by EPRI and the sponsoring electric utilities. Each of the split-system units was tested in the same manner, and each of the package systems was tested in the same manner. Both procedures are described below.

Refrigerant Charging

Once the system was completely assembled in the psychrometric rooms, the initial process was the charging of the units with the desired amount of refrigerant. This process was only necessary for the split-system units since the package systems were charged with the correct amount of refrigerant at the factory. The charging was accomplished by first evacuating the system of moisture. A vacuum pump was attached to the outdoor unit, and a vacuum was pulled on the system for at least two hours (usually overnight) to ensure the moisture was removed. After the vacuum pump was disconnected, the system was observed for approximately 30 minutes. This was to ensure the system held the vacuum and no leaks were present in the lines.

Once the outdoor psychrometric room reached 95°F (35°C), a refrigerant canister of R-22 was attached to the suction side of the compressor. The canister was placed on a

scale so the exact amount of refrigerant added could be monitored in 0.25 oz (7.09 g) increments. Refrigerant was then released into the system, using the pressure difference between the can and the vacuumed system. This process continued until at least 2 lb (0.907 kg) of R-22 had entered the system and the pressure difference approached zero. At this point, power was applied to the compressor, lowering the pressure on the suction side and allowing the continued flow of refrigerant.

Refrigerant was allowed to flow freely until two-phasing downstream of the condenser almost ceased. The system was allowed to settle for a few minutes and refrigerant was then added slowly until only liquid appeared in the sight glass. Next, R22 saturation tables were read at the given system temperature and pressure to ensure that saturation should be occurring and that no air existed in the refrigerant.

At this point, refrigerant was added to the system again until the desired condition was obtained as indicated by the manufacturer. The desired condition depended on the type of expansion device in the system. For the TXV, refrigerant was added to produce a certain subcooling temperature leaving the condenser. For the short-tube orifice, a recommended superheat temperature leaving the evaporator was obtained. The actual subcooling and superheat values produced were based on the manufacturer recommendation, when available. The only capillary tube device tested was on a package unit, so no charging was done on that system. Once the correct amount of charge was obtained, the refrigerant canister valve was closed and the hoses were disconnected.

Split-System Testing

For each of the seven split-system air conditioning units tested, the same test procedure was used. The indoor psychrometric room was brought to 80°F (26.7°C) dry bulb (db) and 67°F (19.4°C) wet bulb (wb). These conditions remained the same for the entire testing procedure. Once the unit was charged, the outdoor room was initially set to 82°F (27.8°C) db. Since the tests did not involve air-cooled condensers which do not evaporate condensate, the outdoor wet bulb temperature was not controlled (ARI 1989).

The airflow through the evaporator coil was adjusted via a damper on the assist blower to provide an air flowrate of 400 cfm/ton of rated capacity (0.0536 $m^3/s/kW$). This practice was consistent for each test unless manufacturer data listed a different flowrate. In this situation, airflow was adjusted to match the manufacturer's value.

After allowing the system to reach steady state, DOE/ARI tests A and B (ARI 1989) were run on the units for a period of 30 minutes. Test A corresponded to an outdoor temperature of 95°F (35°C) and test B corresponded to an outdoor temperature of 82°F (27.8°C). These tests were both steady state, wet coil tests. In addition to these two tests, steady state tests were run at four other outdoor dry bulb temperatures as indicated in Table 5.1. These tests were run to investigate the performance of the units at high outdoor ambient temperatures. Although these higher temperature tests were not ARI standard tests, all ARI measurement procedures were followed (ARI 1989). Data were collected via a data acquisition system at 30 second intervals. The tests involved the measurement

of power factor, total power, refrigerant and air flow rates, temperature, pressure, dew point, and humidity.

***Table 5.1** Room temperature test points.*

Test *	Outdoor db (°F)
1	82
2	95
3	100
4	105
5	110
6	120

* Each test was run at indoor conditions of 80°F (26.7°C) db and 67°F (19.4°C) wb

In addition to the normal measurements taken on the system to determine the capacity of the unit, the condensate from the evaporator coil was collected and measured to provide a further check on the accuracy of the data. This was accomplished by initially running the system until condensate flowed freely from the condensate release port at the base of the coil. An empty bucket was then placed under the drain and condensate was collected for the duration of the test. After the collection period, the bucket of water was weighed and compared to the empty bucket weight to determine the mass of the condensate. This value was then used to determine the latent capacity of the system.

Package-System Testing

To avoid cutting into the system lines on the package units (as requested by EPRI), only air-side measurements were taken. To verify the accuracy of the air-side

measurements, condensate from the evaporator coil was collected and compared to the moisture removal rate calculated for the air-side measurements. All other procedures were identical to those for the split-system air conditioners and heat pumps.

During all testing, the conditions in the psychrometric rooms were maintained within ARI tolerances for testing procedures (ARI 1989). This required that the average dry bulb and wet bulb temperature measurements fall within ± 1.0°F (± 0.56°C) of the desired values.

Calculation Procedures

The cooling capacity of each of the units was calculated in two ways. In accordance with ARI standard testing procedures (ARI 1989), the capacities found using the Air-Enthalpy Method and Refrigerant Flow Method had to agree within ± 6.0% for a test to be considered valid.

The total air-side capacity was determined from the change in enthalpy across the evaporator coil and is the sum of the latent and sensible capacities. The latent capacity was also calculated using the measured condensate from the evaporator coil. The refrigerant-side capacity was determined from the change in enthalpy of the refrigerant through the evaporator. These capacities were found using ASHRAE capacity calculation procedures (ASHRAE 1989). The EER of the unit was calculated by dividing the air-side capacity measurement by the total system power.

For units with no indoor fan, the capacity had to be adjusted to account for indoor fan heat. This was accomplished by subtracting 1250 Btu/h/1000 cfm of evaporator air flow (0.776 kW/m^3/s) in accordance with ARI procedures (ARI 1989). The fan power was calculated as 365 W/1000 cfm of evaporator air flow (771 W/m^3/s). This power was added to the compressor and outdoor fan power to obtain the total power requirement for the system.

Problems Encountered

During the testing of the units, several problems were encountered which were corrected to ensure accurate data measurements for comparison with manufacturers' results. One of the tested units containing an orifice expansion device initially experienced reduced capacity due to a seating problem of the orifice. The manufacturer of the unit was contacted and new orifices were obtained. Three orifices were used before the seating problem was corrected. Another unit had problems with its TXV expansion device. The TXV was not maintaining a constant superheat during operation. To correct the problem, adjustments were made to better secure the temperature sensing bulb to the suction line. A problem also arose due to the orientation of one of the evaporator coils. Initially, the manufacturer of the coil indicated the coil should provide the same capacity whether air flow was horizontal or vertical through the coil. When tested horizontally, however, the measured capacities were more than 10% less than the manufacturer's published capacity values. At this point, the manufacturer said to place the coil in the vertical position. The vertical test measurements decreased the discrepancy between the

rated and tested results. Lastly, the unit providing the largest discrepancy between the manufacturer's and experimental capacities was retested to ensure that the original test results were accurate.

CHAPTER VI

EXPERIMENTAL RESULTS

Ten residential air conditioning systems ranging in capacity from two tons to four tons (7.03 kW to 14.1 kW) were tested and compared to the manufacturers' cooling performance data at high outdoor temperatures. These air conditioners and heat pumps were chosen by the electric utilities involved in the project and exhibit a wide range of hardware characteristics as described in Chapter III. The tests were run in accordance with ARI test procedures (ARI 1989). Indoor conditions of 80°F (26.7°C) db and 67°F (19.4°C) wb were used for each test. Data were taken at outdoor temperatures of 82°F (27.8°C), 95°F (35°C), 100°F (37.8°C), 105°F (40.6°C), 110°F (43.3°C), and 120°F (48.9°C). Data from the experimentation were used to determine air-side capacity, power, and EER which could be compared to manufacturers' data. In addition, power factor measurements were taken on each system.

Manufacturers' cooling performance data were obtained for the tested units at 85°F (29.4°C), 95°F (35°C), 105°F (40.6°C), and 115°F (46.1°C), with the following exceptions. The manufacturer of the H36PTR1H unit did not provide requested capacity data. Another of the units (D24STS1C) consisted of an indoor and outdoor coil from different manufacturers. No manufacturer's capacity data were available for this combination. Experimental capacity data, therefore, were compared to the manufacturers' results only at 95°F (35°C) for these two units using ARI listed ratings (ARI 1994). For the D24STS1C

unit, no system power data of any kind were available. The A42PCS1H unit did not have capacity and power data available at 85°F (29.4°C).

The comparison of experimental and manufacturers' performance data must take into account inherent sources of discrepancy. ARI test procedures (ARI 1989) allow the refrigerant- and air-side capacities to disagree by ±6% and still provide for a valid test. In addition, variations exist in test facilities and individually manufactured units which lead to measurement differences. Thus, measurements taken in this project that satisfied the testing criteria could still show deviations between experimental and manufacturers' data in excess of ±6%. ARI (1989) also allows a -5% variation for manufacturers to account for these situations. Thus, a manufacturer can publish up to a 5% higher capacity than their measured values and still satisfy the tests.

The uncertainty analysis in Appendix A predicts a maximum uncertainty in capacity calculations of ±8.1% and a maximum uncertainty in EER of ±8.1% due to measurement capabilities. Manufacturers' data are only required to meet any standards at 82°F (27.8°C) and 95°F (35°C), which are both required test points. Data at other temperatures are generally provided by computer models. At these higher outdoor temperatures, the experimental capacity and EER uncertainty increases. The percent uncertainty increases because the change in temperature across the evaporator coil decreases with an increase in outdoor temperature. Since the measurement uncertainties of the individual temperatures remain constant (Appendix A), the measurement uncertainty of the temperature change across the coil must also remain constant. This

unit, no system power data of any kind were available. The A42PCS1H unit did not have capacity and power data available at 85°F (29.4°C).

The comparison of experimental and manufacturers' performance data must take into account inherent sources of discrepancy. ARI test procedures (ARI 1989) allow the refrigerant- and air-side capacities to disagree by ±6% and still provide for a valid test. In addition, variations exist in test facilities and individually manufactured units which lead to measurement differences. Thus, measurements taken in this project that satisfied the testing criteria could still show deviations between experimental and manufacturers' data in excess of ±6%. ARI (1989) also allows a -5% variation for manufacturers to account for these situations. Thus, a manufacturer can publish up to a 5% higher capacity than their measured values and still satisfy the tests.

The uncertainty analysis in Appendix A predicts a maximum uncertainty in capacity calculations of ±8.1% and a maximum uncertainty in EER of ±8.1% due to measurement capabilities. Manufacturers' data are only required to meet any standards at 82°F (27.8°C) and 95°F (35°C), which are both required test points. Data at other temperatures are generally provided by computer models. At these higher outdoor temperatures, the experimental capacity and EER uncertainty increases. The percent uncertainty increases because the change in temperature across the evaporator coil decreases with an increase in outdoor temperature. Since the measurement uncertainties of the individual temperatures remain constant (Appendix A), the measurement uncertainty of the temperature change across the coil must also remain constant. This

constant uncertainty value results in a larger percentage uncertainty for smaller temperature drops.

Total Capacity

Measurements allowing the calculation of refrigerant-side and air-side cooling capacity were taken on each of the systems tested. Each set of refrigerant-side and air-side capacities agreed within ±6%, as stipulated in ARI testing procedures (ARI 1989). At 82°F (27.8°C) outdoor temperature, the air-side capacity was estimated to be an average of 3.4% below the refrigerant-side capacity. The average decreased to 2.3% below at 95°F (35°C) outdoor temperature. Only air-side capacity is used by manufacturers to designate the capacity of their units since this capacity is the capacity in which customers are interested. Therefore, only air-side capacities are presented and compared to manufacturers' data.

Table 6.1 lists the deviations in experimental and manufacturer capacity for outdoor temperatures from 85°F (29.4°C) to 115°F (46.1°C). The experimental values at 85°F (29.4°C) and 115°F (46.1°C) were calculated from a curve fit of the measured experimental data. Actual experimental data was used for the calculations at 95°F (35°C) and 105°F (40.6°C).

The experimental capacity measurements agreed with manufacturers' data within ±5% for all units except G48SOR1C at 85°F (29.4°C) outdoor temperature. The experimental values at 85°F (29.4°C) varied from 6.1% below the manufacturer's value to

2.9% above the printed data. Similar results were obtained at 95°F (35°C), where only one unit's capacity calculation (E30STS1C) fell outside the ±5% manufacturer's value. At 105°F (40.6°C), two units differed from the manufacturers' data by more than 5%. Only one of the units, however, differed more than ±6% from the provided data. The 115°F (46.1°C) temperature showed the first multiple results falling outside the ±6% range. Four of the eight units for which data were available resulted in an experimental capacity over 5% less than manufacturer's published value at this temperature.

Table 6.1 *Experimental deviations from manufacturers' published capacity data at various outdoor temperatures.*

	Unit	Deviation by Outdoor Temperature				
		85°F	95°F	105°F	115°F	
4	D36SOS1C	-4.3%	-3.9%	-0.1%	+1.3%	N
3	B42SOR1H	-0.9%	-1.6%	-3.6%	-8.5%	F
8	A42PCS1H		-1.3%	-1.3%	-4.6%	P
1	E42STS1C	-4.2%	-2.6%	-7.5%	-8.7%	N
7	D42POS1C	-0.8%	-0.4%	-2.6%	-6.0%	P
2	E30STS1C	-4.9%	-5.3%	-5.4%	-5.7%	N
5	D42STS1H	+2.9%	+3.4%	+2.0%	+2.7%	F
6	G48SOR1C	-6.1%	-1.7%	-2.4%	-2.1%	N
10	D24STS1C		+1.6%			N
9	H36PTR1H		+0.7%			P
	Average	-2.6%	-1.1%	-2.6%	-4.0%	

As indicated in the table, results were obtained that were below, above, and very similar to manufacturer provided data. A sample of each of these cases will be discussed. Also, the two systems are reviewed for which manufacturers' capacity data were not available.

The greatest positive difference between experimental and manufacturers' published data occurred on the D42STS1H unit (Figure 6.1). This unit was a 12.7 SEER, 3.5 ton (12.3 kW) split-system heat pump with a TXV and a scroll compressor. The capacity of the unit decreased with an increase in outdoor temperature. Differences of between 2.0% and 3.4%were calculated over the temperature range at 105°F (40.6°C) and 95°F (35°C), respectively. The experimental capacity of the system decreased almost 18% over the tested temperature range.

Figure 6.2 shows the results of the unit with the closest experimental and manufacturer's published capacity. This 12 SEER unit, A42PCS1H, was a 3.5 ton (12.3 kW) package heat pump with a capillary tube expansion device and a scroll compressor. The experimental capacity varied from 1.3% to 4.6% below the manufacturer's published value. Between 82°F (27.8°C) and 120°F (48.9°C), the experimental capacity dropped 30%.

The results of the unit E42STS1C exhibited the greatest negative difference compared to the manufacturer's data, as indicated in Figure 6.3. This unit was a 3.5 ton (12.3 kW) split-system air conditioner with a 13 SEER. It had TXV expansion and a scroll compressor. Between 85°F (29.4°C) and 115°F (46.1°C), the experimental results

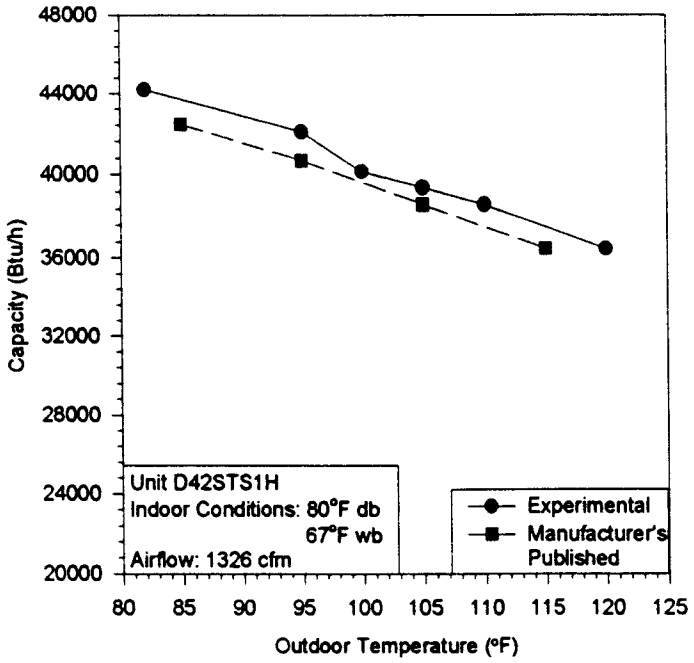

Figure 6.1 D42STS1H capacity comparisons of experimental and manufacturer's published results.

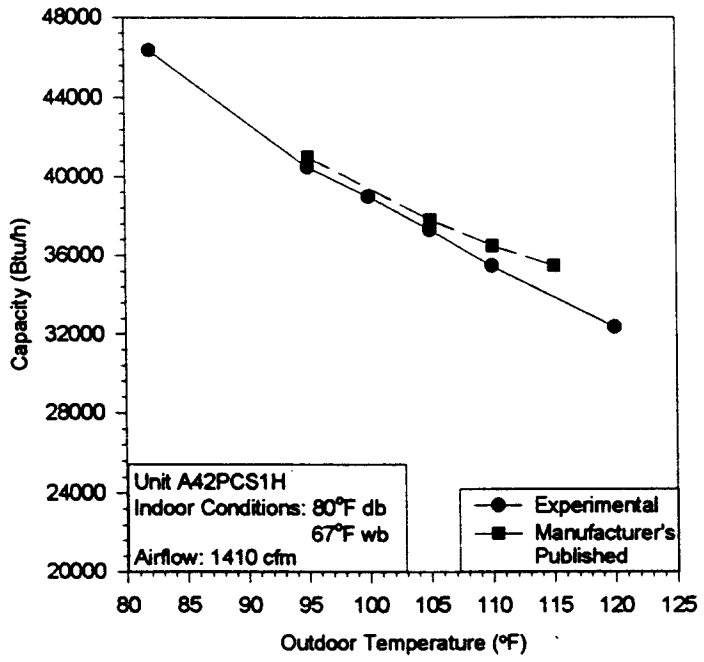

Figure 6.2 A42PCS1H capacity comparisons of experimental and manufacturer's published results.

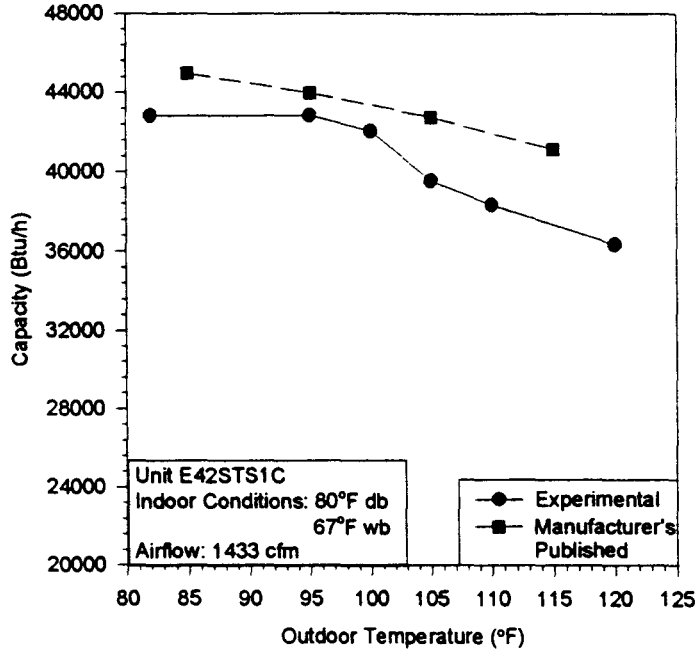

***Figure 6.3** E42STS1C capacity comparisons of experimental and manufacturer's published results.*

ranged from 2.6% to 8.7% below the manufacturer's values at 95°F (35°C) and 115°F (46.1°C), respectively. The experimental capacity dropped 15% between 82°F (27.8°C) and 120°F (48.9°C). The unit E30STS1C had the same experimental and manufacturer's capacity slope, but the experimental values were consistently 5% below that of the manufacturer.

Figures 6.4 and 6.5 show the experimental capacities of units D24STS1C and H36PTR1H. These capacities dropped 16% and 30%, respectively, as the outdoor temperature increased from 82°F (27.8°C) to 120°F (48.9°C). The results of the ten tested units are shown in Figure 6.6. The plot shows experimental capacity divided by manufacturer's capacity for outdoor temperatures between 85°F (29.4°C) and 115°F (46.1°C) as compared to the ideal value of unity (e.g. experimental data = manufacturer's data). The experimental capacity dropped at a faster rate than the manufacturer's capacity with an increase in outdoor temperature. The widest variation occurred at 115°F (46.1°C), where six of the eight listed units had experimental capacities lower than manufacturer's capacities. This may indicate that some of the manufacturers' computer models could be too conservative in estimating the drop in capacity at higher outdoor temperatures.

Table 6.2 compares the average percentage decreases in capacity per degree Fahrenheit for experimental and manufacturers' data for the eight units where this information was known. The experimental drops were based on experimental measurements and were averaged between 82°F (27.8°C) and 120°F (48.9°C). For the

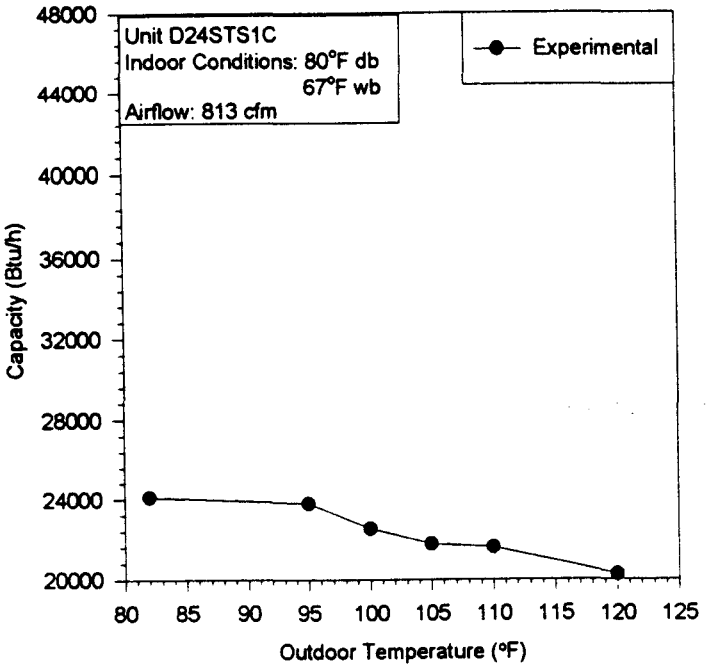

Figure 6.4 *D24STS1C experimental capacity measurements.*

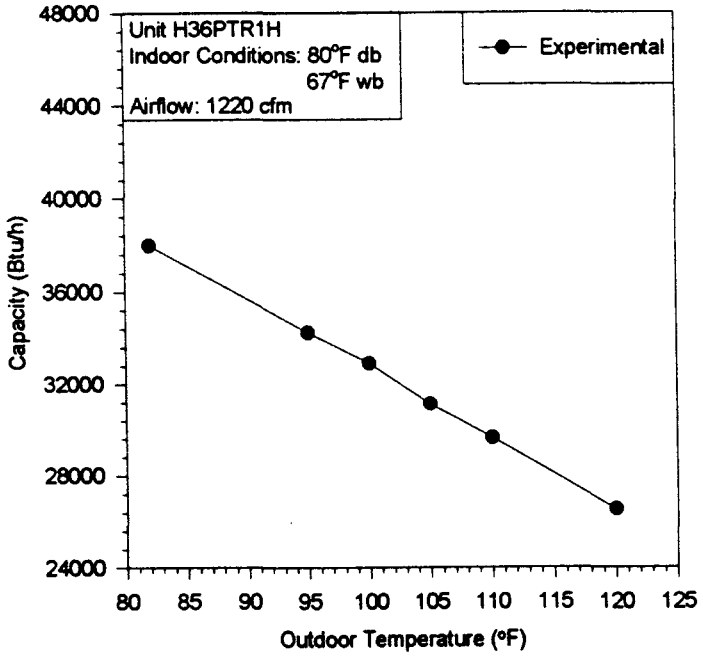

Figure 6.5 *H36PTR1H experimental capacity measurements.*

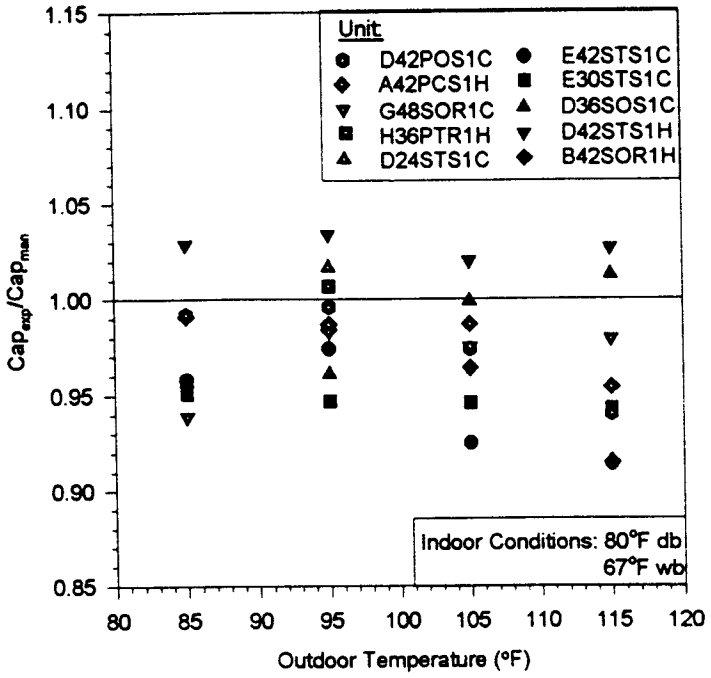

***Figure 6.6** Normalized capacity comparison at various outdoor temperatures.*

manufacturer values, drops were based on data between 85°F (29.4°C) and 115°F (46.1°C), with the exception of the G48SOR1C unit, which used available data from 95°F (35°C) to 115°F (46.1°C).

The experimental percentage drop in capacity per degree Fahrenheit was equal to or greater than the manufacturer's drop for six of the eight units for which comparisons were possible (Table 6.2). The experimental changes ranged from 0.28%/°F to 0.79%/°F, with an average percentage capacity drop of 0.54%/°F over the tested temperature range. The manufacturers' capacity changes varied from 0.28%/°F to 0.74%/°F with an average change of 0.51%/°F.

Table 6.2 *Comparison of experimental and manufacturers' estimated percentage capacity drops per °F.*

Unit	Percentage Drop in Capacity (%/°F)	
	Experimental	Manufacturers' Published
D36SOS1C	0.28	0.42
B42SOR1H	0.71	0.46
A42PCS1H	0.79	0.67 *
E42STS1C	0.39	0.28
D42POS1C	0.76	0.60
E30STS1C	0.42	0.40
D42STS1H	0.47	0.47
G48SOR1C	0.53	0.74
Average	0.54	0.51

* This manufacturer's predicted drop used data between 95°F (35°C) and 115°F (46.1°C)

Table 6.3 compares the experimental decreases for split-system and package units between 82°F (27.8°C) and 120°F (48.9°C). The split-system units had an average capacity

drop of 0.46%/°F between 82°F (27.8°C) and 120°F (48.9°C). For the package systems, the average drop was 0.78%/°F. Each of the package-system units tested dropped in capacity at a faster rate than any of the split-system units. As a result, package units with similar capacities to split-system units at 95°F (35°C) had lower capacities at 120°F (48.9°C).

Table 6.3 *Comparison of split-system and package-system experimental percentage capacity drops per °F from 82°F (27.8°C) to 120°F (48.9°C).*

Unit	Percentage Drop in Capacity (%/°F)	
	Split-System	Package-System
D36SOS1C	0.28	
B42SOR1H	0.71	
E42STS1C	0.39	
E30STS1C	0.42	
D42STS1H	0.47	
G48SOR1C	0.53	
D24STS1C	0.42	
A42PCS1H		0.79
D42POS1C		0.76
H36PTR1H		0.79
Average	0.46	0.78

All units tested in this project were new units. Manufacturers' data from five older package-system units were therefore examined to see if the current capacity drops were similar to those five years ago, before the current minimum efficiency standards took effect. Air conditioners and heat pumps with SEER's ranging from 8.75 to 9.7 experienced an average capacity drop of 0.47%/°F between 85°F (29.4°C) and 115°F (46.1°C) outdoor temperature. The drops varied from 0.32%/°F to 0.58%/°F. This average

drop was 40% below the average for the tested package units.

Total Power

Measurements of total power were taken on each of the systems tested using watt transducers. For units with no indoor fan, the fan power was calculated as 365 W/1000 cfm of evaporator air flow (771 $W/m^3/s$). This power was then added to the measured compressor and outdoor fan power to obtain the total system power. Table 6.4 shows the deviations between experimental and manufacturers' power measurements for outdoor temperatures between 85°F (29.4°C) and 115°F (46.1°C). The experimental values at 85°F (29.4°C) and 115°F (46.1°C) were taken from a curve fit of the experimental data. Experimental values compared at 95°F (35°C) and 105°F (40.6°C) were the measured values.

Table 6.4 *Experimental deviations from manufacturer power data at various outdoor temperatures.*

Unit	Deviation by Outdoor Temperature			
	85°F	95°F	105°F	115°F
D36SOS1C	-3.7%	-3.4%	-2.8%	-1.8%
B42SOR1H	+2.0%	+2.0%	+0.6%	-0.6%
A42PCS1H		-2.7%	-2.0%	+0.2%
E42STS1C	+0.2%	+2.4%	+3.0%	+4.1%
D42POS1C	-3.7%	-1.4%	+2.4%	+3.5%
E30STS1C	-1.8%	-0.8%	-1.3%	-1.7%
D42STS1H	+5.7%	+4.2%	+4.6%	+4.9%
G48SOR1C	+3.6%	+1.0%	-2.1%	-4.8%
H36PTR1H	+0.3%	+1.4%	-0.2%	-1.9%
Average	+0.3%	+0.3%	+0.3%	+0.7%

The experimental and manufacturers' power data showed a closer correlation than those of capacity. This was expected since the total power of the system is easier to measure. The power required by the indoor and outdoor fan varies little over the entire temperature range investigated. The main variable, therefore, is the compressor. Manufacturers generally know compressor performance at different operating temperatures and can therefore accurately predict system power requirements. The power required by the units increased with an increase in outdoor temperature. The experimental and manufacturers' power values only deviated by more than ±5% for one unit at one temperature (85°F (29.4°C)) for all systems tested.

The greatest negative difference between the experimental and manufacturer values occurred for the unit D36SOS1C (see Figure 6.7). The 12 SEER unit was a three ton (10.5 kW) split-system air conditioner with orifice expansion and a scroll compressor. Measured experimental power was between 1.8% and 3.7% less than the manufacturer's published values. Between 82°F (27.8°C) and 120°F (48.9°C), this unit's experimental power increased 45%.

Figure 6.8 shows the results for the unit (H36PTR1H) which was most similar in experimental and manufacturer's power data. This unit was a 12 SEER, three ton (10.5 kW) split-system heat pump with orifice expansion and a reciprocating compressor. Over the experimental temperature range, the experimental results varied from 1.4% above

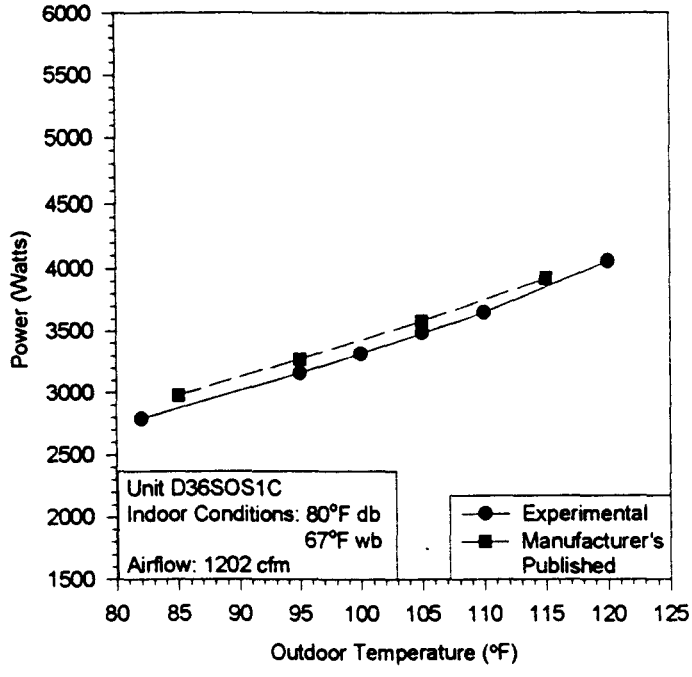

Figure 6.7 D36SOS1C power comparisons of experimental and manufacturer's published results.

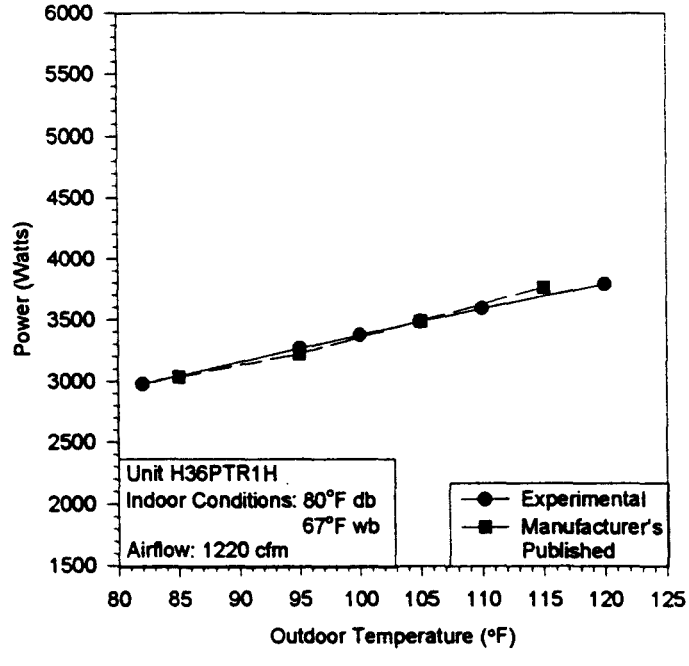

Figure 6.8 H36PTR1H power comparisons of experimental and manufacturer's published results.

the manufacturer's values to 1.9% below the published data. A power increase of 27% occurred between 82°F (27.8°C) and 120°F (48.9°C) during the testing of this unit.

The unit D42STS1H had the biggest positive difference between manufacturer's and experimental power values. This unit was a 12.7 SEER, 3.5 ton (12.3 kW) split-system heat pump with TXV expansion and a scroll compressor. Figure 6.9 shows the experimental and manufacturer power requirements for this unit at different outdoor temperatures. An increase in experimental power of 1.5 kW occurred between 82°F (27.8°C) and 120°F (48.9°C), resulting in a percentage increase of 43%. The difference between the experimental and manufacturer's values varied between 4.2% and 5.7% over the entire temperature range.

Figures 6.10 shows the experimental power measurements of the unit D24STS1C. The power increased 44% between 82°F (27.8°C) and 120°F (48.9°C).

The results of the eight units with known manufacturers' data are summarized in Figure 6.11. The plot shows experimental power divided by manufacturer's power for outdoor temperatures between 85°F (29.4°C) and 115°F (46.1°C). As indicated on the chart, approximately the same number of units had measured powers above and below the manufacturers' data. The greatest variations between experimental and manufacturers' results occurred at the two temperature extremes, namely 85°F (29.4°C) and 115°F (46.1°C). For the two middle temperatures, all ratios fell between 0.95 and 1.05.

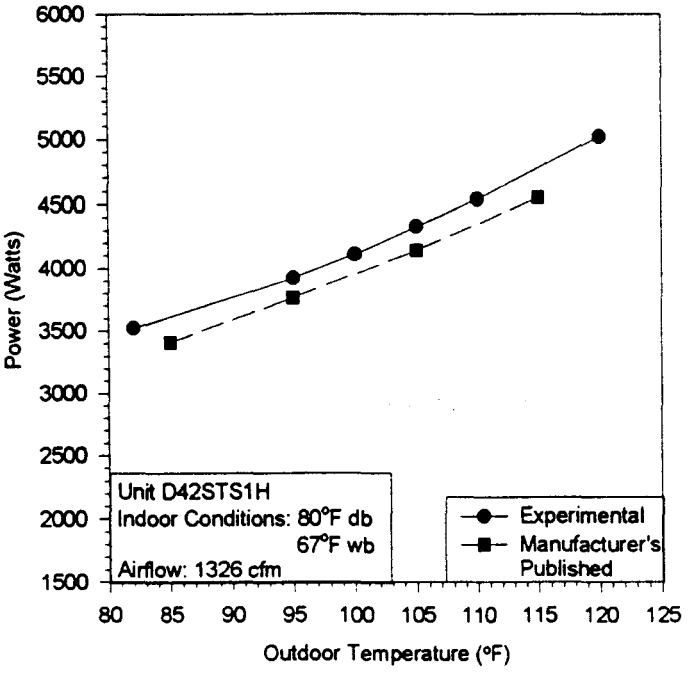

Figure 6.9 *D42STS1H power comparisons of experimental and manufacturer's published results.*

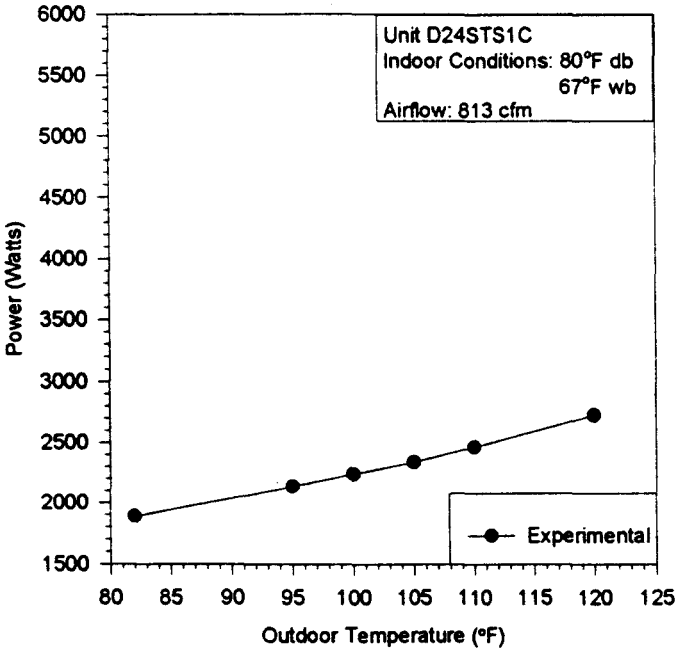

Figure 6.10 *D24STS1C experimental power measurements.*

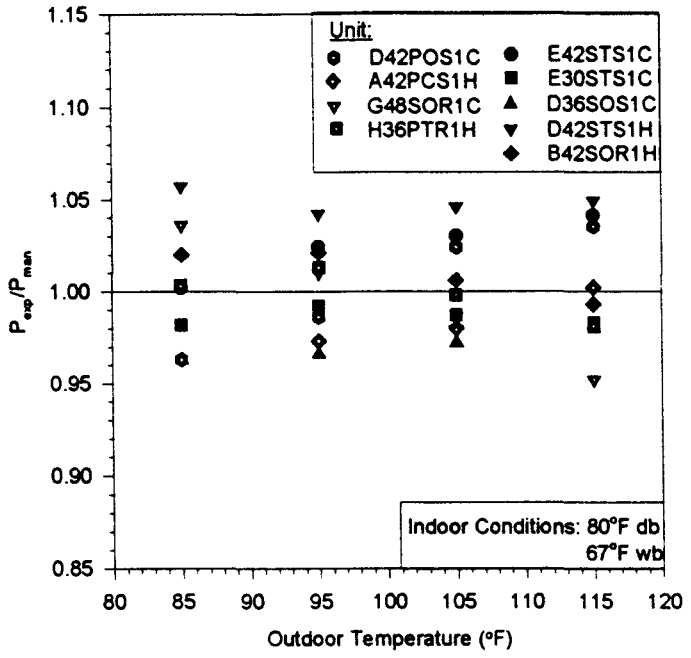

Figure 6.11 Normalized power comparison at various outdoor temperatures.

The experimental and manufacturers' predicted power increases over the outdoor temperature range are listed in Table 6.5. The experimental increases were based on experimental measurements and were averaged between 82°F (27.8°C) and 120°F (48.9°C). For the manufacturers' predicted values, power increases were based on data between 85°F (29.4°C) and 115°F (46.1°C), with the exception of the G48SOR1C unit, which used available data from 95°F (35°C) to 115°F (46.1°C). For six of the nine units listed, the experimental increase was greater than the corresponding manufacturer's increase for the particular unit. An average experimental increase of 1.03%/°F compared to an average manufacturers' predicted change of 0.97%/°F.

***Table 6.5** Comparison of experimental and manufacturers' estimated percentage power increases per °F.*

Unit	Percentage Increase in Power Consumption (%/°F)	
	Experimental	Manufacturers' Published
D36SOS1C	1.18	1.05
B42SOR1H	0.76	0.85
A42PCS1H	1.11	0.85*
E42STS1C	1.34	1.09
D42POS1C	1.32	0.96
E30STS1C	1.08	1.04
D42STS1H	1.13	1.12
G48SOR1C	0.66	0.99
H36PTR1H	0.71	0.80
Average	1.03	0.97

* This manufacturer's predicted increase used data between 95°F (35°C) and 115°F (46.1°C)

Table 6.6 compares the experimental changes of the split-system and package units. The average experimental increase for the split-system units was 1.04%/°F. An average

experimental increase of 1.05%/°F was obtained for the package systems over the tested temperature range. The increases varied from 0.66%/°F to 1.34%/°F for the split systems and 0.71%/°F to 1.32%/°F for the package units, indicating a wide range of power draw for each system type.

Table 6.6 *Comparison of split-system and package-system experimental percentage power increases per °F from 82°F (27.8°C) to 120°F (48.9°C).*

Unit	Percentage Increase in Power Consumption (%/°F)	
	Split-System	Package-System
D36SOS1C	1.18	
B42SOR1H	0.76	
E42STS1C	1.34	
E30STS1C	1.08	
D42STS1H	1.13	
G48SOR1C	0.66	
D24STS1C	1.16	
A42PCS1H		1.11
D42POS1C		1.32
H36PTR1H		0.71
Average	1.04	1.05

Energy Efficiency Ratio

The energy efficiency ratio (EER) was determined by dividing the total air-side capacity in Btu/h of the system by the total power draw in Watts. The differences between experimental and manufacturers' EER's are listed in Table 6.7 for outdoor temperatures between 85°F (29.4°C) and 115°F (46.1°C). The experimental values at 85°F (29.4°C) and 115°F (46.1°C) were taken from a curve fit of the experimental data. Experimental values

compared at 95°F (35°C) and 105°F (40.6°C) were actual measurements.

Table 6.7 Experimental deviations from manufacturers' EER data at various outdoor temperatures.

Unit	Deviation by Outdoor Temperature			
	85°F	95°F	105°F	115°F
D36SOS1C	-0.6%	-0.4%	+2.8%	+3.1%
B42SOR1H	-2.8%	-3.6%	-4.2%	-7.9%
A42PCS1H		+1.4%	+0.7%	-4.8%
E42STS1C	-4.4%	-4.9%	-10.2%	-12.2%
D42POS1C	+3.0%	+1.0%	-4.8%	-9.2%
E30STS1C	-3.1%	-4.5%	-4.2%	-4.1%
D42STS1H	-2.7%	-0.7%	-2.5%	-2.1%
G48SOR1C	-9.3%	-2.7%	-0.4%	+2.8%
H36PTR1H		-0.6%		
Average	-2.8%	-1.7%	-2.9%	-4.3%

At 85°F (29.4°C) and 105°F (40.6°C), only one unit fell outside the ±5% difference in EER. These were the G48SOR1C and E42STS1C units, respectively. None of the experimental EER calculations differed from the manufacturers' published values by more than ±5% at 95°F (35 °C) outdoor temperature. At 115°F (46.1°C), three of the eight units with available data differed in experimental and manufacturers' results by more than 5%. This temperature produced experimental values from 12.2% below to 3.1% above the manufacturers' published data.

The greatest positive discrepancy was found for the D36SOS1C unit (Figure 6.12). This was a 12 SEER, three ton (10.5 kW) split-system air conditioner with orifice

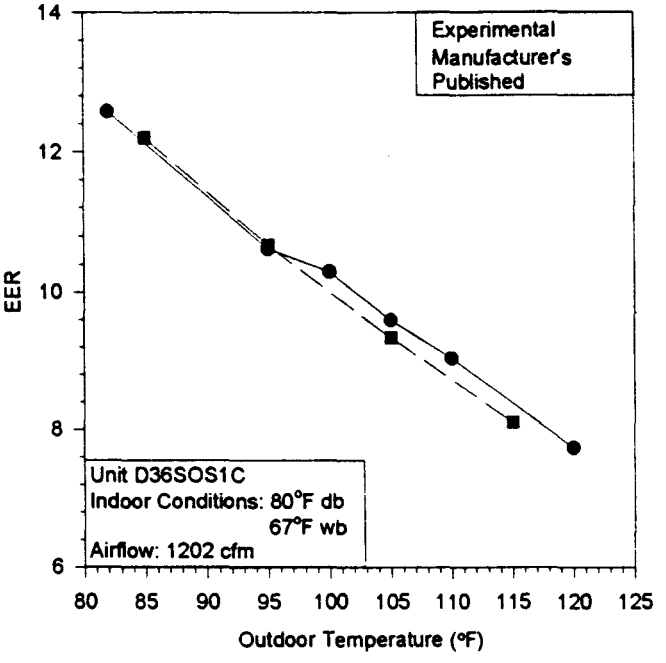

Figure 6.12 *D36SOS1C EER comparisons of experimental and manufacturer's published results.*

expansion and a scroll compressor. The experimental EER varied from 0.6% below the manufacturer's EER at 85°F (29.4°C), to 3.1% above the manufacturer's value at 115°F (46.1°C). Over the tested temperature range, the experimental EER dropped 39%. This same unit had one of the best power performances when compared to the manufacturer's published power requirements. The power directly affects the capacity, so this result was not unexpected.

The experimental EER for the D42STS1H unit followed the manufacturer's EER most closely of any of the units tested, as shown in Figure 6.13. This 12.7 SEER unit was a 3.5 ton (12.3 kW) split-system heat pump with TXV expansion and a scroll compressor. Between 82°F (27.8°C) and 120°F (48.9°C), the experimental EER dropped 42%. This unit had the best capacity performance and worst power performance when compared to the manufacturer's values.

The greatest negative discrepancy between experimental and manufacturers' EER values occurred for the 13 SEER E42STS1C unit, as indicated in Figure 6.14. This was a 3.5 ton (12.3 kW) split-system air conditioner with TXV expansion and a scroll compressor. The experimental EER calculations ranged from 4.4% to 12.2% below the manufacturer's results between 85°F (29.4°C) and 115°F (46.1°C). An overall 44% drop in experimental EER occurred for this system. This same unit had the worst capacity performance when compared to manufacturer's data of any of the tested systems. Since the EER is directly affected by the capacity, this result was also not unexpected.

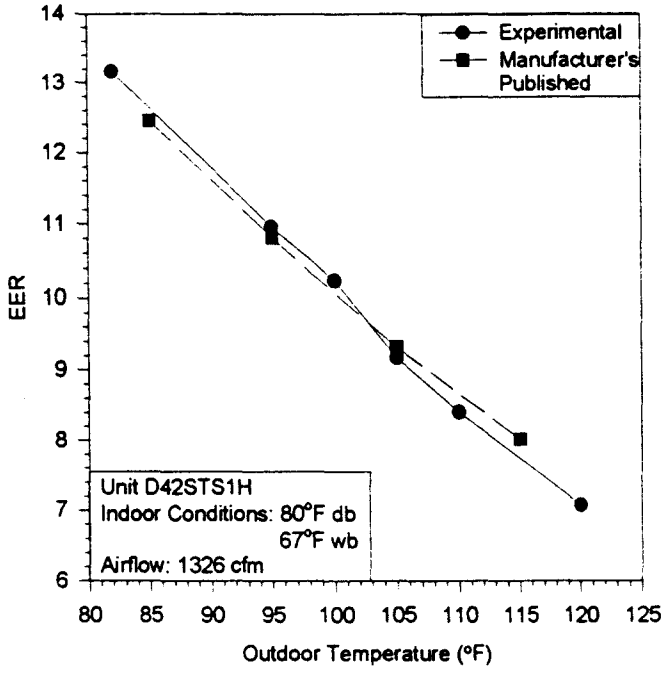

***Figure 6.13** D42STS1H EER comparisons of experimental and manufacturer's published results.*

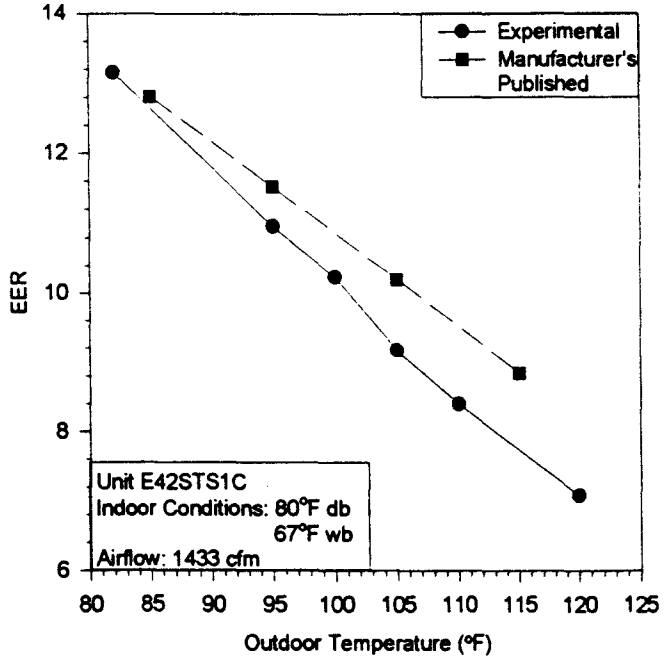

***Figure 6.14** E42STS1C EER comparisons of experimental and manufacturer's published results.*

Figures 6.15 and 6.16 show the experimental EER measurements of units D24STS1C and H36PTR1H. Over the tested temperature range, the EER's of these units lowered 42% and 45%, respectively.

The EER results of the nine units with known manufacturers' EER's are summarized in Figure 6.17. The plot shows the ratio of experimental EER to manufacturer's EER for outdoor temperatures between 85°F (29.4°C) and 115°F (46.1°C). After 105°F (40.6°C), there was an obvious decline in the experimental EER as compared to the manufacturers' predicted EER.

Table 6.8 shows the comparison of experimental and manufacturers' EER drops over the tested temperature range. The experimental drops were based on experimental measurements and were averaged between 82°F (27.8°C) and 120°F (48.9°C). For the manufacturers' values, EER decreases were based on data between 85°F (29.4°C) and 115°F (46.1°C), with the exception of the G48SOR1C unit, which used available data from 95°F (35°C) to 115°F (46.1°C). Five of the eight units listed had a higher experimental drop than manufacturers' drop. The average experimental decline was 1.18%/°F compared to an average manufacturers' drop of 1.17%/°F.

In Table 6.9, the split system EER drop is compared to that of the package systems. The average experimental EER decline between 82°F (27.8°C) and 120°F (48.9°C) was 1.12%/°F for the split-system units and 1.23%/°F for the package-system

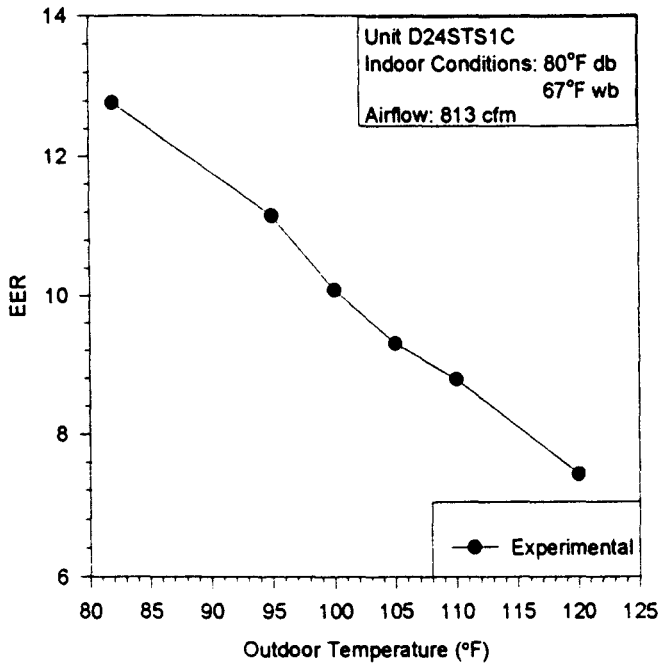

Figure 6.15 D24STS1C EER comparisons of experimental and manufacturer's published results.

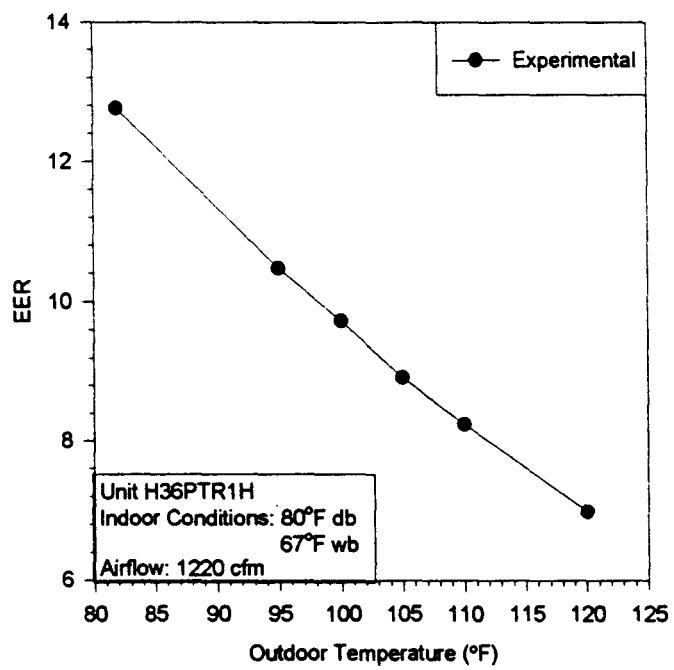

Figure 6.16 H36PTR1H EER comparisons of experimental and manufacturer's published results.

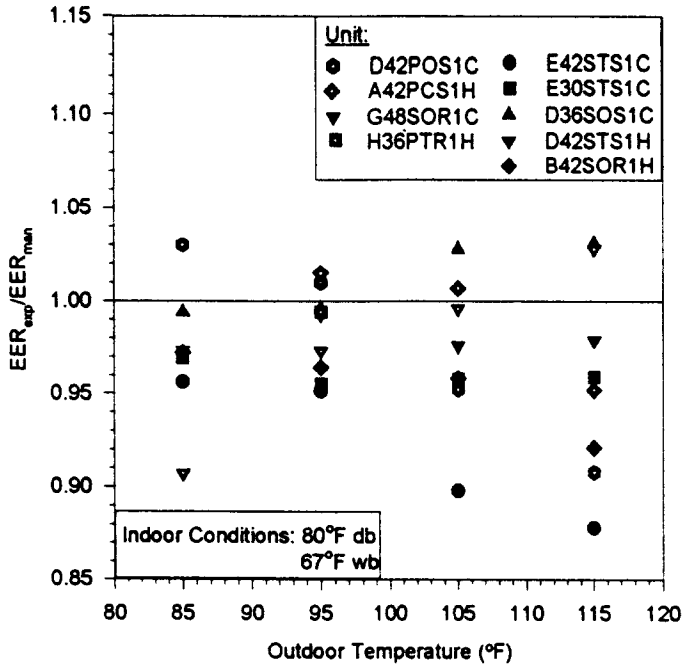

Figure 6.17 Normalized EER comparison at various outdoor temperatures.

units. Each of the package units experienced a greater decline in EER than any of the split-system units, with the exception of the D42STS1H unit.

Table 6.8 *Comparison of experimental and manufacturers' estimated percentage EER drops per °F.*

Unit	Percentage Decrease in EER (%/°F)	
	Experimental	Manufacturers' Published
D36SOS1C	1.03	1.12
B42SOR1H	1.13	1.04
A42PCS1H	1.34	1.30*
E42STS1C	1.16	1.03
D42POS1C	1.37	1.21
E30STS1C	1.08	1.10
D42STS1H	1.37	1.20
G48SOR1C	0.94	1.33
Average	1.18	1.17

* This manufacturer's predicted drop used data between 95°F (35°C) and 115°F (46.1°C)

Table 6.9 *Comparison of split-system and package-system experimental percentage EER drops per °F from 82°F (27.8°C) to 120°F (48.9°C).*

Unit	Percentage Drop in EER (%/°F)	
	Split-System	Package-System
D36SOS1C	1.03	
B42SOR1H	1.13	
E42STS1C	1.16	
E30STS1C	1.08	
D42STS1H	1.37	
G48SOR1C	0.94	
D24STS1C	1.11	
A42PCS1H		1.30
D42POS1C		1.21
H36PTR1H		1.18
Average	1.12	1.23

Power Factor

The power factor is the ratio (between zero and one) of the real power, which does the work in the system, to the apparent power, which the utility supplies. The higher the power factor, the less power which must be supplied by the utility. Power factor data were not available for residential unitary air conditioners and heat pumps. Therefore, all data listed were experimental values. Table 6.10 shows the power factor changes between 82°F (27.8°C) and 120°F (48.9°C) for the ten tested units. The average power factor change for the split-system units was 0.8% and for the package units was 1.4%. All units exhibited changes of less than 2% over the temperature range.

Table 6.10 *Comparison of split-system and package-system power factor changes between 82°F (27.8°C) and 120°F (48.9°C).*

Unit	Power Factor Change	
	Split-System	Package-System
D36SOS1C	-0.8%	
B42SOR1H	-0.4%	
E42STS1C	+0.4%	
E30STS1C	+0.5%	
D42STS1H	+0.7%	
G48SOR1C	-1.5%	
D24STS1C	+1.3%	
A42PCS1H		+1.6%
D42POS1C		-0.8%
H36PTR1H		-1.8%
Average Absolute Change	0.8%	1.4%

Figures 6.18 and 6.19 show the power factor measurements for the split-system and package-system units, respectively. All units had power factors above 0.95 between

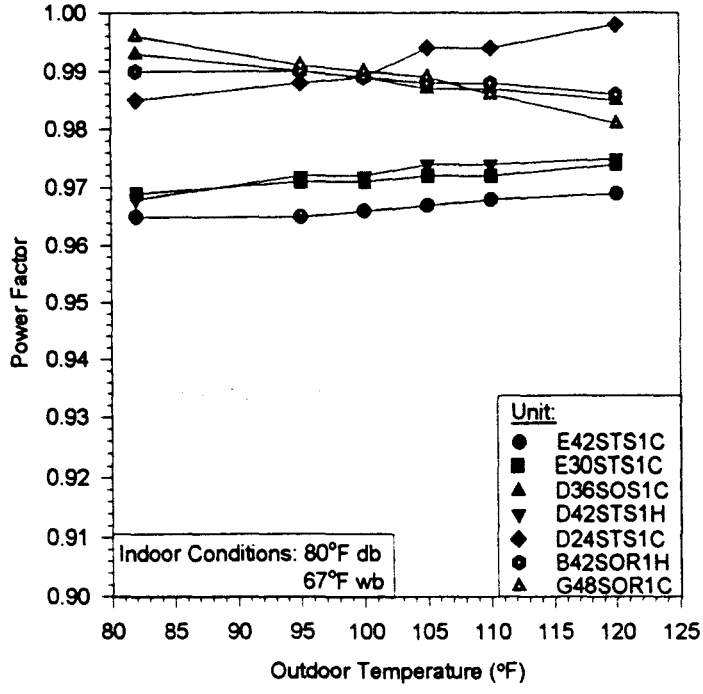

Figure 6.18 Power factor measurements for split-system units.

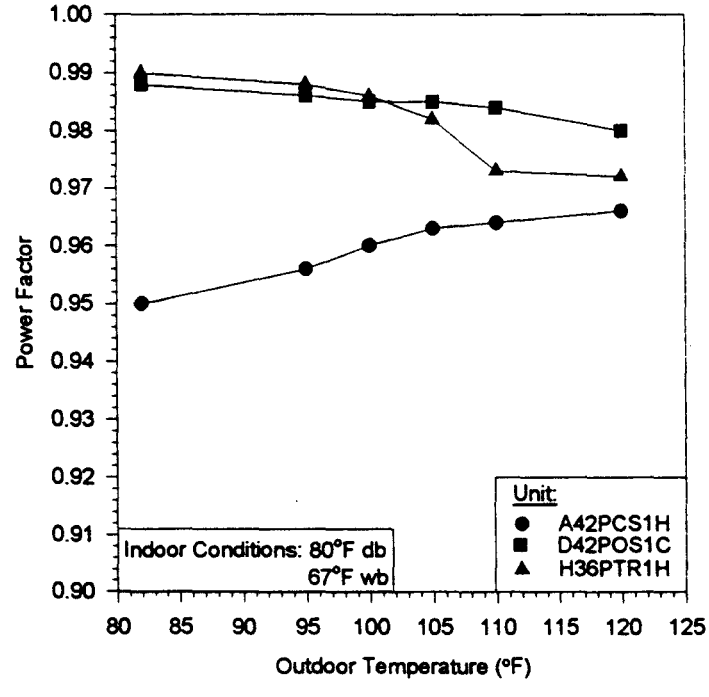

Figure 6.19 Power factor measurements for package-system units.

82°F (27.8°C) and 120°F (48.9°C) outdoor temperature. This indicated that the manufacturers were concerned with lowering the demand of their units. All units tested utilized capacitors to overcome the inefficiencies of the various system hardware (e.g. compressor, indoor fan motor, outdoor fan motor).

Summary

The experimental measurements of capacity, power, and EER produced results which were above and below manufacturers' values. Between 85°F (29.4°C) and 115°F (46.1°C), 15% of the experimental and manufacturers' published results differed by more than ±5%. Half of these differences were less than ±6%, and two-thirds of the differences were at temperatures greater than 95°F (35°C), which are not required test points. For each of the units tested, capacity and power decreased with an increase in outdoor temperature, and system power increased with an increase in outdoor temperature.

CHAPTER VII

HARDWARE CONFIGURATION ANALYSIS

The cooling performance data from five manufacturers were analyzed to determine if there was a statistically significant relationship between the hardware configuration of an air conditioning system and system performance at high outdoor temperatures. A total of 230 air conditioning systems were examined with the hardware distribution indicated in Table 7.1. The analysis involved units with nominal cooling capacities between three and four tons (10.5 to 14.1 kW).

***Table 7.1** Hardware distribution of air-conditioning units.*

System Characteristic	Number of Units
Split System	200
Package System	30
Air Conditioner	124
Heat Pump	106
Scroll Compressor	77
Reciprocating Compressor	153
Single-Speed Compressor	212
Two-Speed Compressor	18
TXV Expansion	141
Orifice Expansion	77
Capillary Expansion	12

One part of the analysis investigated possible relationships between the steady-state and cyclic performance of air conditioning systems through the use of the EER and

SEER. The second analysis looked at only steady-state performance at various outdoor temperatures. Each method is discussed below.

In the analysis, linear curve fits of the data were obtained which fit the following linear regression model:

$$y = b(0) + b(1)x \tag{7.1}$$

In this model, b(0) is the y-intercept of the data and b(1) is the slope of the data. A representative value of the correlation, r^2, was obtained for each curve fit. The r^2 value represents the percentage of the variability in y explained by the linear model and is obtained by the following equation:

$$r^2 = \frac{S_{yy} - SSE}{S_{yy}} \tag{7.2}$$

where: S_{yy} = total variability in y

SSE = random variability in y about the linear model

R^2 provides a measure of the linear relation between x and y and provides an indication of the dependence of the variable y on x. The more horizontal the curve fit, the less y depends on the value of x. As a result, horizontal lines produce low r^2 values, despite their linearity.

For each table with data in it in the chapter, the following codes were used to distinguish hardware:

S:	Split-system unit
P:	Package-system unit
r:	Reciprocating compressor
s:	Scroll compressor
o:	Orifice expansion device
t:	TXV expansion device
Cap:	Capillary tube expansion device
c:	Air conditioner
h:	Heat pump
2:	Two-Speed compressor
tot:	Total two-speed air conditioners and heat pumps

The designations not containing the number 2 refer only to units with single-speed compressors. All two-speed units had reciprocating compressors and TXV expansion devices. Also, the data shown for all two-speed units correspond to operation at the higher compressor speed. This speed is the speed which would be expected during electric utility peak load conditions.

Steady-State/Cyclic Analysis

In this analysis, possible relationships between steady-state and cyclic cooling performance were analyzed. The EER is a measure of the steady-state performance of an air conditioning system and is the ratio of the capacity of the unit to the system power requirements during steady-state operation. The SEER includes cycling losses that occur during normal operation and is a measure of the total cooling provided by the system over a period of time divided by the electrical use during the same time frame. During start-up, an air conditioning system provides less cooling than it does during steady-state operation.

As a result, the SEER at a given temperature is lower than the corresponding EER value at that same temperature. For this analysis, the SEER value analyzed is always the SEER at 82°F (27.8°C), which is a required rating point for a given system. Although there is no physical basis for a consistent relationship between the EER and SEER for different units, prior research (Nguyen et al 1981) has indicated a statistical relationship does exist.

EER vs. SEER

This section examines the relationship between the EER at 95°F (35°C) and the SEER for air conditioning units with various hardware configurations. Units with a range of SEER values were analyzed and compared to their EER's at 95°F (35°C). The 95°F (35°C) outdoor temperature was examined because it is a required test point. EER's at higher temperatures are often based on computer models. It is believed that investigating the units based on the EER at 95°F (35°C) provides a more accurate representation of system performance.

This analysis demonstrates how higher SEER units perform compared to lower SEER units. The consumer's primary information is the SEER of the system. In general, it is expected that higher SEER units provide better performance during the cooling season than lower SEER units, resulting in lowered energy costs. For electric utilities, performance (higher EER's) at higher outdoor ambient temperatures is important because these conditions usually coincide with peak summer electrical demand. For a given capacity, a lower EER means lower power requirements and therefore inherent reductions

in the overall demand. The ideal situation for both consumers and utilities would occur when an increase in the SEER of a unit also resulted in an increase in the EER and maintained a fairly constant slope over the range of SEER values on the market.

Table 7.2 lists the fits for the EER data as a function of the SEER data for varying hardware configurations. The table lists the hardware configurations in order of decreasing slope, with the largest slopes listed first. The slope of each line was positive, indicating an increase in EER at 95°F (35°C) with an increase in SEER. For a given capacity, the EER can only be increased by a reduction in the steady-state power draw. As the SEER is increased, fast power reduction results in a large slope of the EER vs. SEER line. Larger slopes are therefore ideal for electric utilities.

***Table 7.2** Fits for EER@95°F as a function of SEER.*

Hardware Configuration	b(0)	b(1)	r^2
Sr	1.3800	0.7928	0.796
So	1.3249	0.7913	0.755
Ss	1.1084	0.7908	0.879
Sh	1.8522	0.7364	0.870
Sc	2.0991	0.7254	0.833
St	2.0594	0.7211	0.864
Pc	2.0483	0.6956	0.879
Pt	2.2038	0.6788	0.851
Pr	2.3662	0.6657	0.851
PCap	2.6372	0.6289	0.872
Ps	3.1954	0.5857	0.730
2c	2.5753	0.5817	0.955
Ph	3.3305	0.5742	0.733
2tot	4.6711	0.4312	0.712
2h	6.7199	0.2810	0.467

In Table 7.2, b(1) specifies the increase in EER corresponding to a one integer increase in SEER for the different hardware configurations. The slopes ranged from 0.793 for the split-system units with reciprocating compressors to 0.281 for the two-speed heat pump systems. All six of the single-speed split-system unit combinations had higher slopes than the package-system or two-speed units. This indicates that increases in SEER for single-speed split-system units generally corresponded to greater power reduction than for other types of systems. With the exception of the package heat pumps, all package systems had higher slopes than the units with two-speed compressors.

One possible reason for the package units exhibiting worse performance than their split-system counterparts may lie in the greater emphasis placed on split-system units in recent years. Between 1972 and 1992, the number of U.S. shipments of unitary split-system air conditioners rose 67% (ARI 1993). During this same time frame, the number of shipments of package-system units only rose 18%. Due to the apparent increase in demand for split-system units, manufacturers may have put more research into improving these types of systems.

Inherent natural heat and air leakage also exists in package systems which affect their performance. In package units, the evaporator and condenser are in a single assembly. They are generally separated by a sheet metal wall along with attached insulation. Because of the close proximity of the two assemblies, any leakage of air from one side to the other has immediate effects on system operation. Hot air from the

condenser side mixed with cooler air on the evaporator side lowers the cooling capacity and the efficiency of the unit.

Correlation r^2 values for the lines ranged from 0.955 for the two-speed air conditioners to 0.467 for the two-speed heat pumps. The two-speed heat pumps had a lower r^2 value for two reasons: the scatter was greater for these units and the fit was more horizontal than for any of the other combinations. The small number of data points for the two-speed units also lowered the r^2. Individual scatter in the data points had a much greater effect than for systems with a large data set.

Figures 7.1 to 7.15 show the EER/SEER relationship for different hardware configurations. Although the data showed definite trends in terms of general slope, the variability in the data was often significant. Figure 7.1, for example, shows the relationship of EER at 95°F (35°C) to the SEER for split-system units with reciprocating compressors. The EER at 95°F (35°C) ranged from approximately 8.5 at a SEER of 10 to 12.6 at an SEER of 14.3. A significant variation also occurred in the EER's at corresponding SEER's. At an SEER of 10, the EER at 95°F (35°C) for the different units varied from 8.5 to more than 10. Variations likewise occurred in the SEER needed to obtain a specific EER value. An EER of 10.2 was obtained with an SEER of 10 for one unit and an SEER of 12.2 for another unit. For this case, the increase in SEER did not result in an improvement in steady state performance at 95°F (35°C).

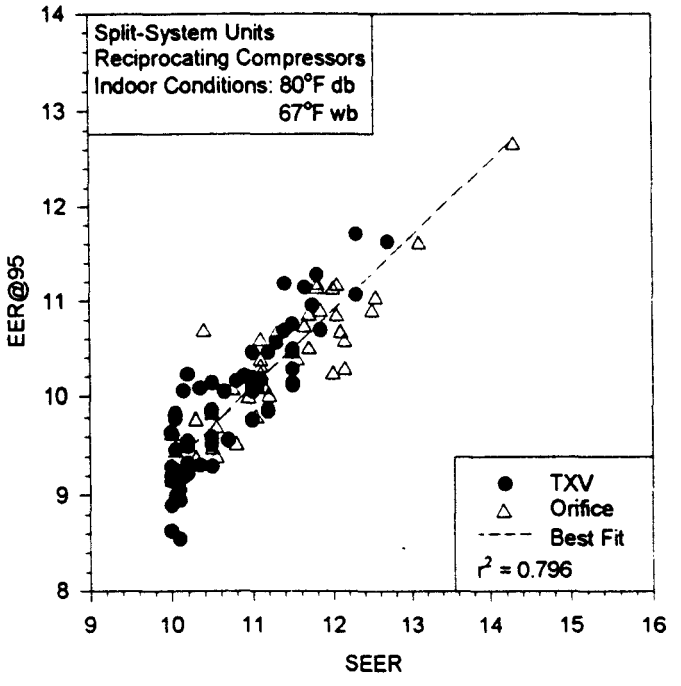

Figure 7.1 EER@95°F vs. SEER for split-system units with reciprocating compressors.

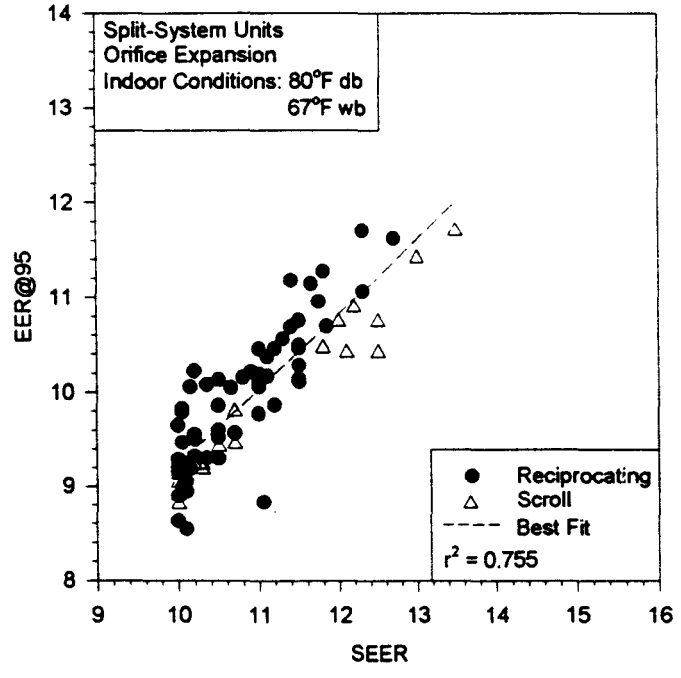

Figure 7.2 EER@95°F vs. SEER for split-system units with orifice expansion.

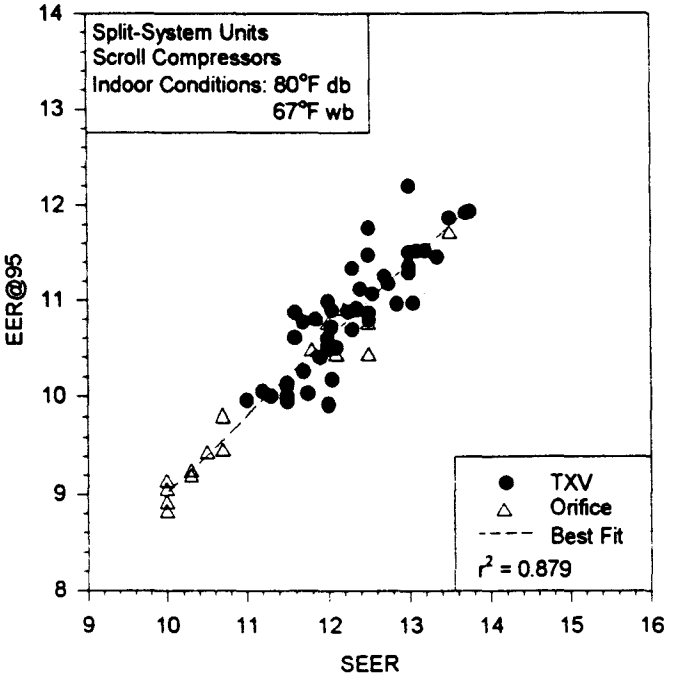

Figure 7.3 EER@95°F vs. SEER for split-system units with scroll compressors.

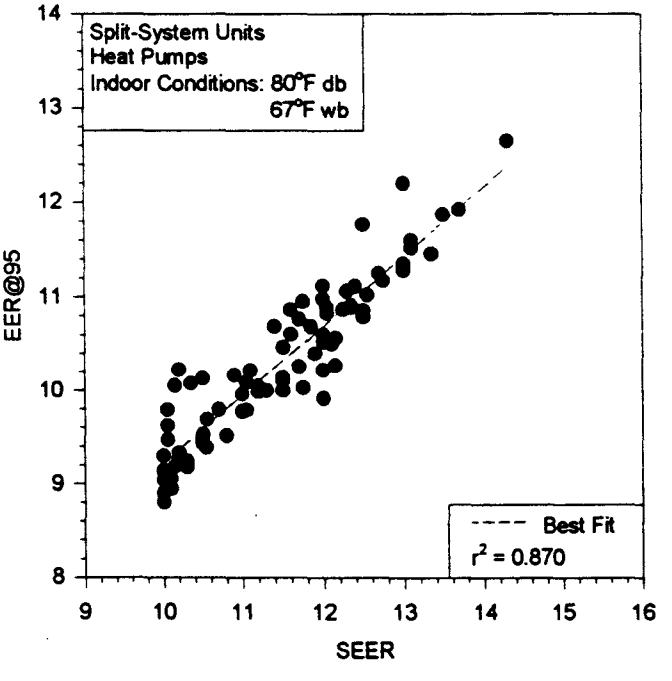

Figure 7.4 EER@95°F vs. SEER for split-system heat pumps.

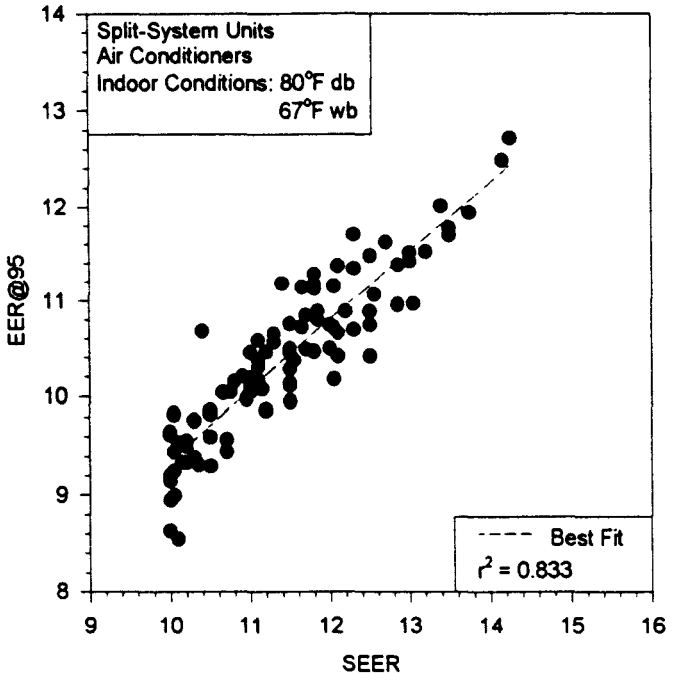

Figure 7.5 EER@95°F vs. SEER for split-system air conditioners.

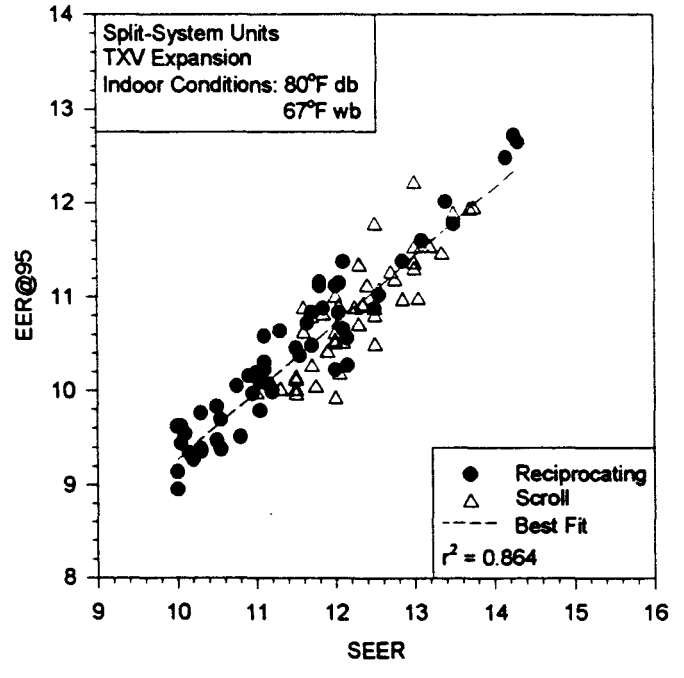

Figure 7.6 EER@95°F vs. SEER for split-system units with TXV expansion.

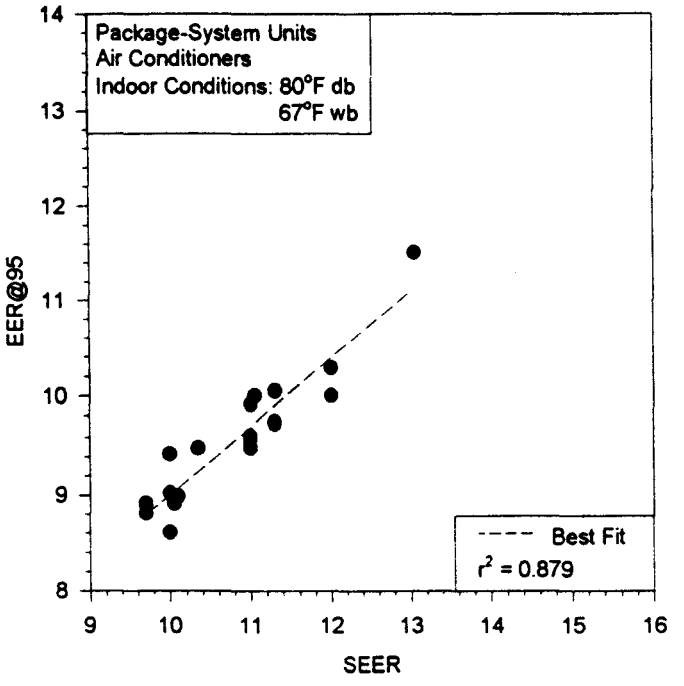

Figure 7.7 EER@95°F vs. SEER for package-system air conditioners.

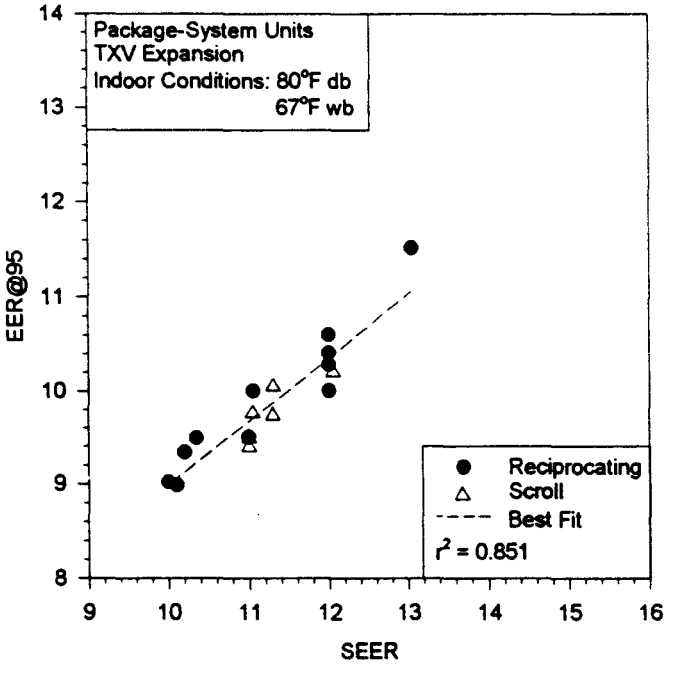

Figure 7.8 EER@95°F vs. SEER for package-system units with TXV expansion.

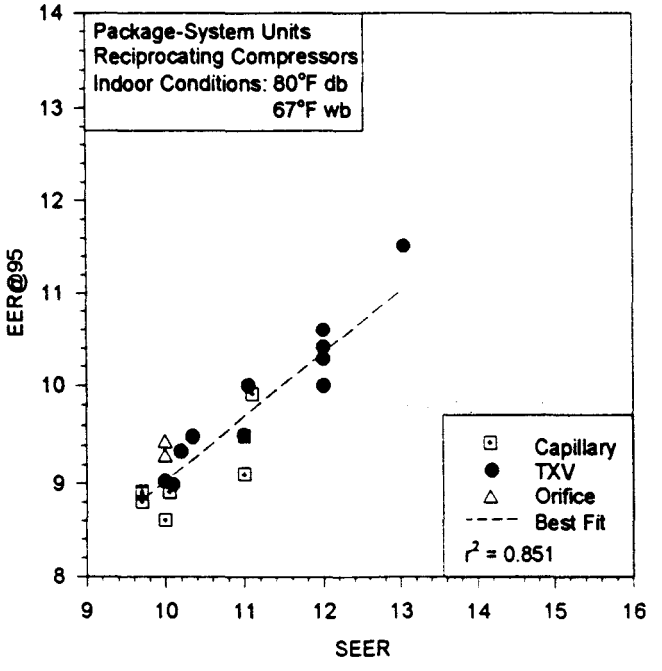

Figure 7.9 EER@95°F vs. SEER for package-system units with reciprocating compressors.

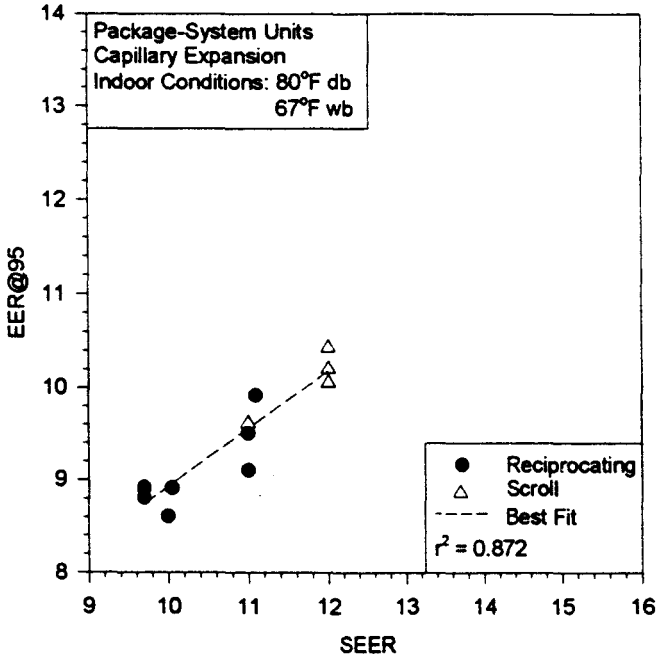

Figure 7.10 EER@95°F vs. SEER for package-system units with capillary tube expansion.

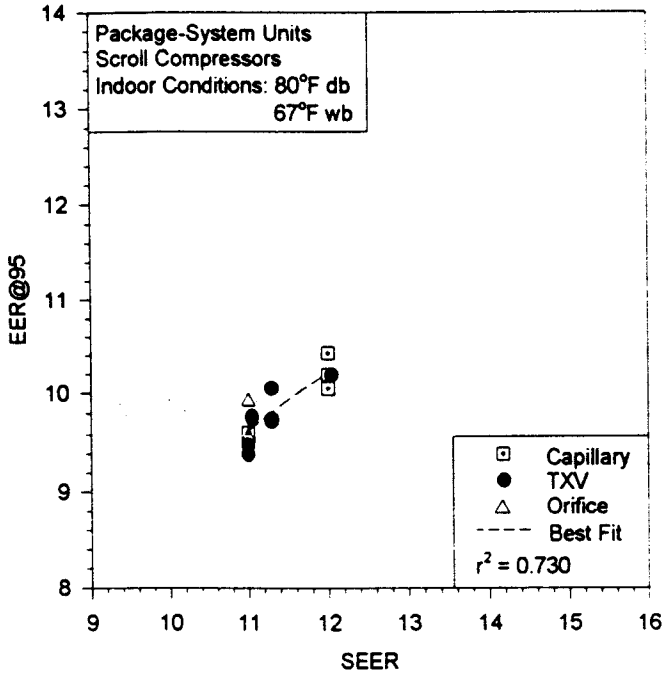

Figure 7.11 *EER@95°F vs. SEER for package-system units with scroll compressors.*

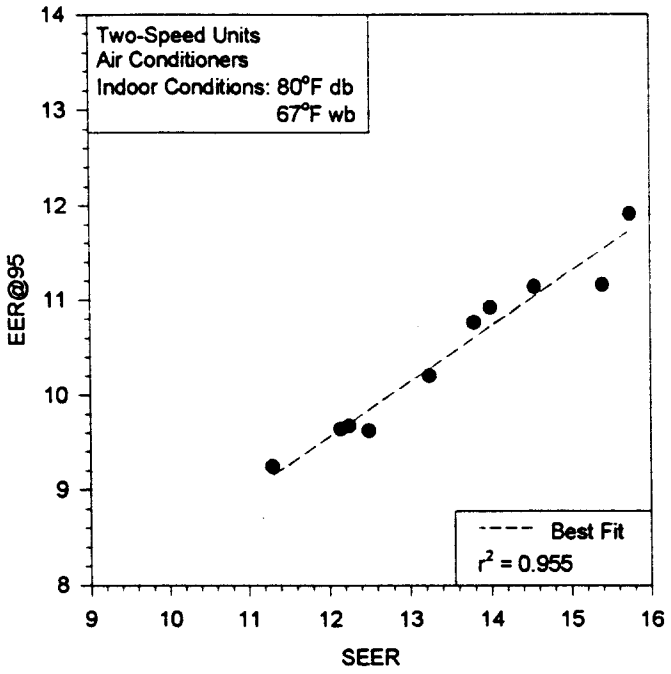

Figure 7.12 *EER@95°F vs. SEER for two-speed air conditioners.*

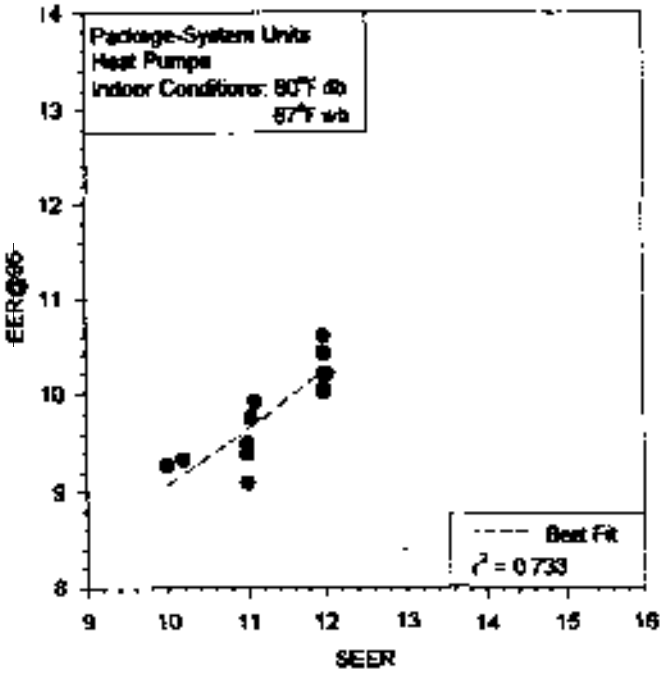

Figure 7.13 EER@95°F vs. SEER for package-system heat pumps.

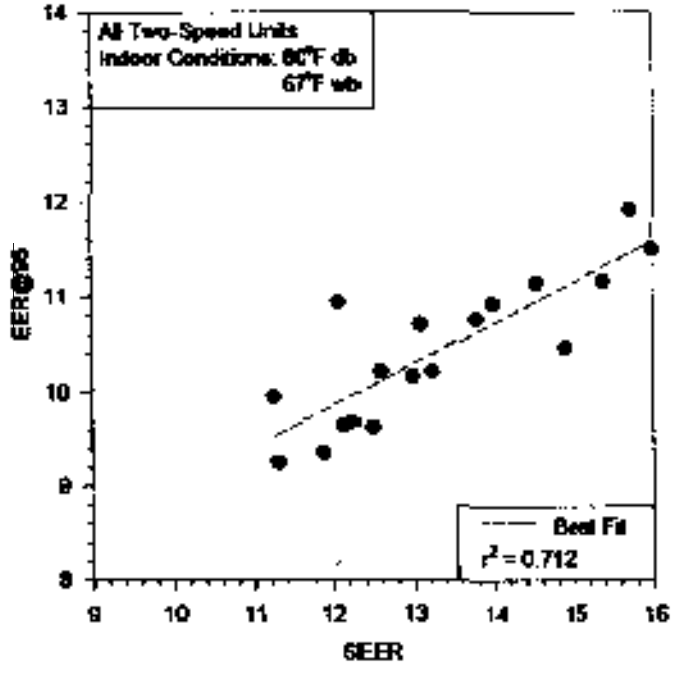

Figure 7.14 EER@95°F vs. SEER for all two-speed units.

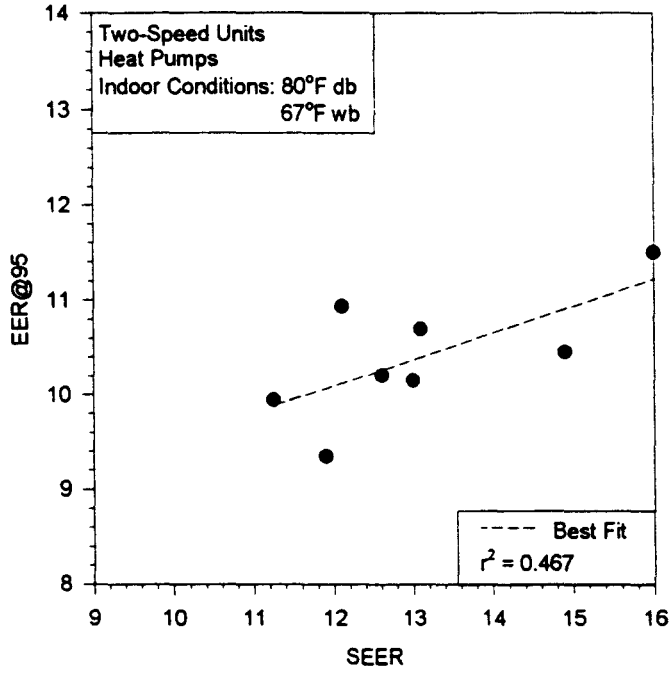

Figure 7.15 *EER@95°F vs. SEER for two-speed heat pumps.*

The results indicated that an electric utility could offer a rebate for a 12 SEER split-system unit with a reciprocating compressor, for example, which would provide the same EER at 95°F (35°C) as a 10 SEER unit of the same hardware configuration. Higher SEER values for this hardware combination did not always result in higher EER values. Similar results occurred for the various hardware distributions, indicating a possible need for a new approach to rebate policies which are currently based only on the SEER of a unit.

Figure 7.1 shows the affect of the type of expansion device on system performance for split-system units containing reciprocating compressors. The units with orifice expansion possessed a flatter fit than those with TXV expansion, indicating the TXV's provided a greater increase in system performance for a given increase in SEER. In Figure 7.2, the two compressor types are shown for the split-system units possessing orifice expansion. While both types of compressors experienced similar slopes, the scroll compressors were shifted to the right. This is an indication that the scroll compressors were not providing improved steady state performance at 95°F (35°C) over the reciprocating compressors with increases in the SEER. The higher SEER units had scroll compressors, but they had the same EER at 95°F (35°C) as some of the lower SEER units with reciprocating compressors. Figure 7.3 shows different expansion devices for split-system units with scroll compressors. The units with orifice expansion made up the lower SEER units and possessed a slightly flatter fit than the TXV units. The difference between expansion devices was not as severe, however, as for the units with reciprocating

compressors. Figure 7.6 shows the two compressor types for split-system units with TXV expansion. In this case, the scroll compressors experienced a much steeper slope than the reciprocating compressors. For units with TXV expansion, the scroll compressors provided better steady state performance than the reciprocating compressors with increases in the SEER.

The slopes of the systems discussed in the previous paragraph are listed in Table 7.3. The table shows that the type of hardware configuration of an air conditioning system has a definite effect on system performance.

***Table** 7.3 Fits for EER@95°F as a function of SEER--comparison of compressor and expansion device.*

Figure	Hardware Configuration	b(0)	b(1)	r^2
7.1	Srt	0.1123	0.9127	0.784
7.1	Sro	2.1101	0.7244	0.827
7.2	Sor	0.2123	0.8991	0.731
7.2	Sos	1.503	0.7508	0.960
7.3	Sst	1.251	0.7808	0.755
7.3	Sso	1.466	0.7537	0.959
7.6	Str	1.666	0.7629	0.915
7.6	Sts	1.343	0.7720	0.748

The package units with TXV expansion are shown in Figure 7.8. With the smaller number of data points for the package units, it was difficult to draw definite conclusions on the differences between the performance of the scroll and reciprocating compressors. The lower SEER units for this combination generally possessed reciprocating

compressors. Figure 7.9 shows package-system units with reciprocating compressors separated by type of expansion device. The lower SEER units had mostly capillary tubes, whereas the higher SEER units had mostly TXV's. The TXV units had the same slope as the capillary tube units, but had higher EER performance at similar SEER's. In Figure 7.10, the package units with capillary tube expansion are shown by type of compressor. The higher SEER units possessed scroll compressors. Figure 7.11 shows different expansion devices for package-system units with scroll compressors. No significant difference between the performance of the expansion devices could be determined. However, a 12 SEER capillary tube unit provided no steady state performance improvement at 95°F (35°C) over a 11 SEER orifice unit.

EER@95/SEER vs. SEER

This section examines the relationship between the EER at 95°F (35°C) divided by the SEER as compared to the SEER alone. Average values were sought for the ratio of EER/SEER for various hardware configurations. It was hoped that these average values would be consistent for different SEER values so that a common ratio could be found for a given hardware system. This average could then be used to predict the EER at 95°F (35°C) and the corresponding power requirements (assuming the nominal capacity is known) at this outdoor temperature based only on the SEER. This average could also be compared to prior research to investigate how the average has changed over the past ten to fifteen years.

Table 7.4 lists the hardware configurations analyzed. This table is organized in terms of increasing slopes, with the smallest slope listed first in the table. Smaller slopes indicate less variation over the range of SEER values examined, and generally indicate better concurrence with the average EER/SEER value obtained.

As can be seen from Table 7.4, all slopes were slightly negative. This drop in slope corresponded to a drop in the average EER/SEER ratio with increasing SEER values, indicating the EER did not rise at as fast a rate as the SEER. The split-system units with scroll compressors had the slope closest to zero and hence the most consistent EER/SEER ratio of any of the hardware configurations. The two-speed heat pumps exhibited the least consistent averages.

Table 7.4 Fits for EER@95°F/SEER vs. SEER.

Hardware Configuration	b(0)	b(1)	r^2	EER/SEER Average
Ss	0.9792	-0.00796	0.099	0.883
So	1.0216	-0.00993	0.055	0.913
Sr	1.0343	-0.01050	0.075	0.919
Sh	1.0619	-0.01418	0.235	0.899
2c	0.9669	-0.01425	0.708	0.775
St	1.0716	-0.01474	0.273	0.897
Sc	1.0836	-0.01515	0.218	0.910
Pc	1.0765	-0.01759	0.348	0.857
Pt	1.0811	-0.01826	0.346	0.875
Pr	1.1048	-0.02022	0.381	0.886
PCap	1.1242	-0.02309	0.505	0.875
Ps	1.1383	-0.02385	0.366	0.867
2tot	1.1292	-0.02577	0.582	0.786
Ph	1.1830	-0.02770	0.436	0.868
2h	1.2829	-0.03684	0.694	0.800

For the hardware combinations considered, the r^2 values ranged from 0.055 for the split-system units with orifice expansion to 0.708 for the two-speed air conditioners. In these cases, r^2 was more a predictor of horizontality than variability. While variability about the curve fits definitely existed, the general horizontal nature of most of these curves resulted in extremely low r^2 values. The small data set of package-system and two-speed units also contributed to this small value. Figures 7.16 to 7.30 show the linear curve fits for the hardware configurations listed in Table 7.4.

EER/SEER is the slope of Figures 7.1 to 7.15. Since EER/SEER decreased with an increase in SEER values in Figures 7.16 to 7.30, the slope of EER as a function of SEER should be non-linear and concave downward. This indicates that as the SEER of units increases, further improvements in the SEER result in less and less EER improvement. Second-order curve fits of this performance, however, did not show any significant correlation improvement over the linear fits because of the small curvature over the range of SEER's investigated. For simplicity, therefore, linear fits were used for all data analyzed.

Table 7.5 lists the average EER/SEER values in decreasing order. Five of the six hardware configurations examined involving single-speed split-system units exhibited the highest average values of EER at 95°F (35°C) divided by the SEER. Both the split-system and package-system units had higher average values than the two-speed units. The two-speed units had low averages because the performance analyzed involved the units operating at high speed. This provided a lower EER value, but kept the same high SEER.

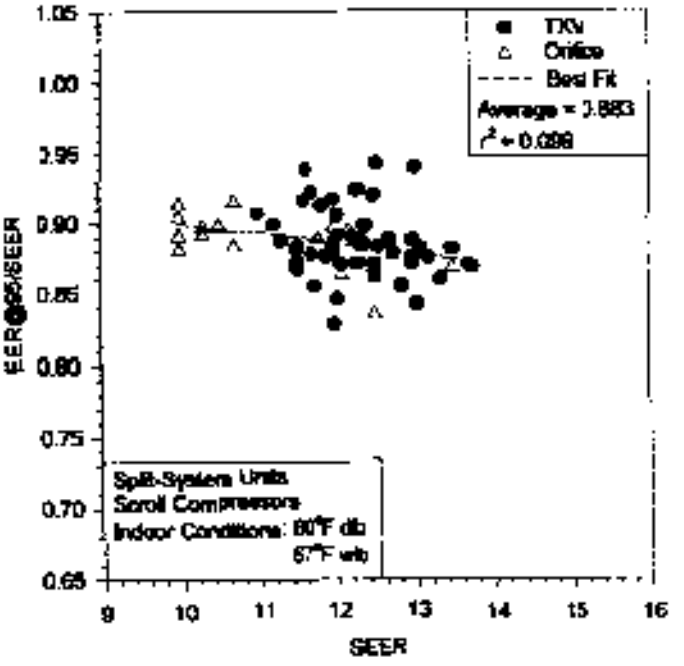

Figure 7.16 EER@95°F/SEER vs. SEER for split-system units with scroll compressors.

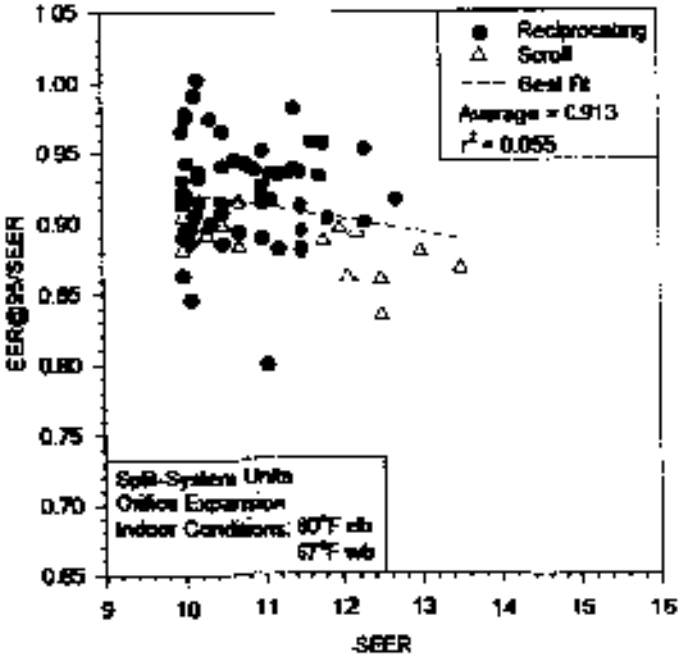

Figure 7.17 EER@95°F/SEER vs. SEER for split-system units with orifice expansion.

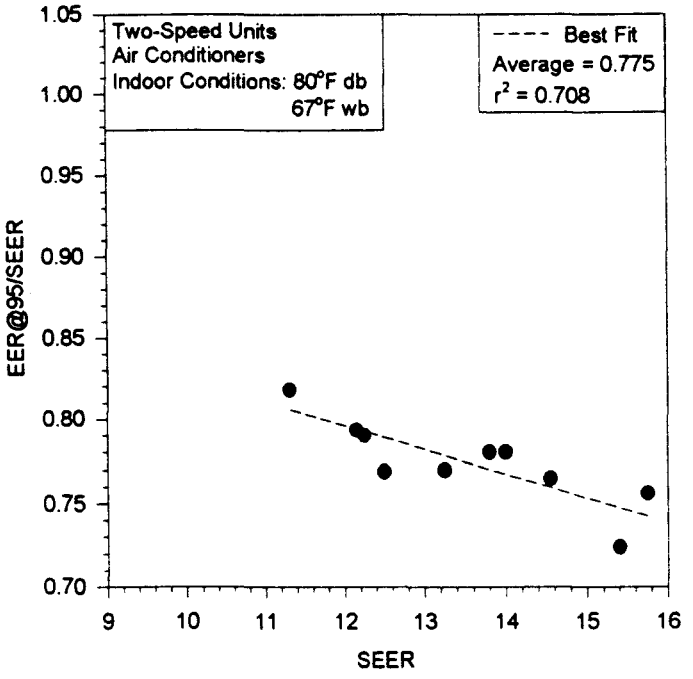

Figure 7.20 EER@95°F/SEER vs. SEER for two-speed air conditioners.

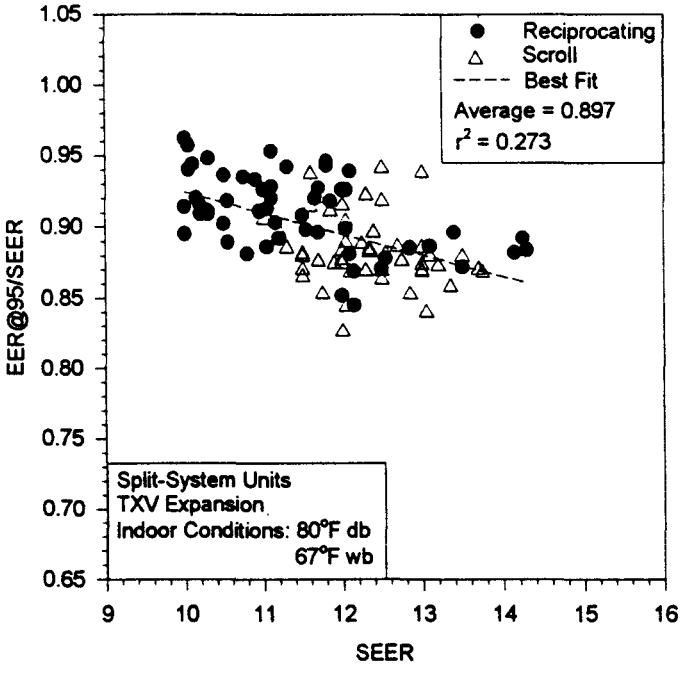

Figure 7.21 EER@95°F/SEER vs. SEER for split-system units with TXV expansion.

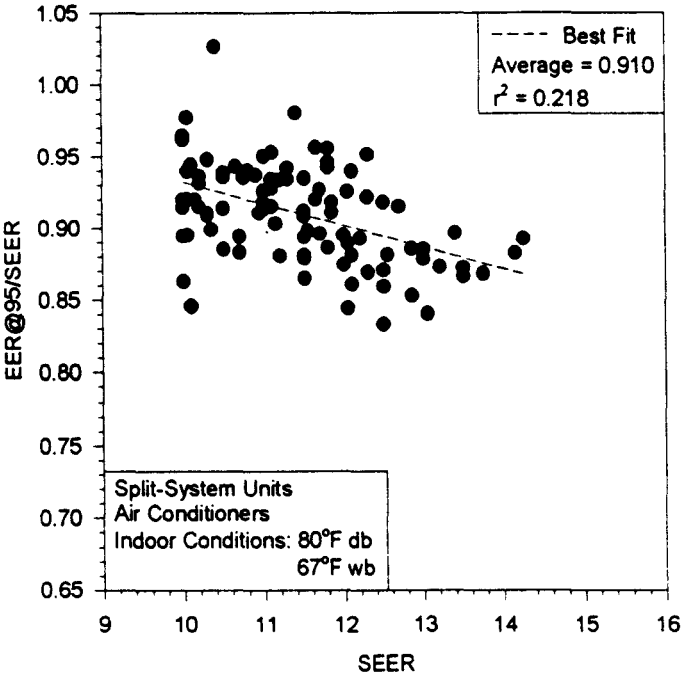

Figure 7.22 *EER@95°F/SEER vs. SEER for split-system air conditioners.*

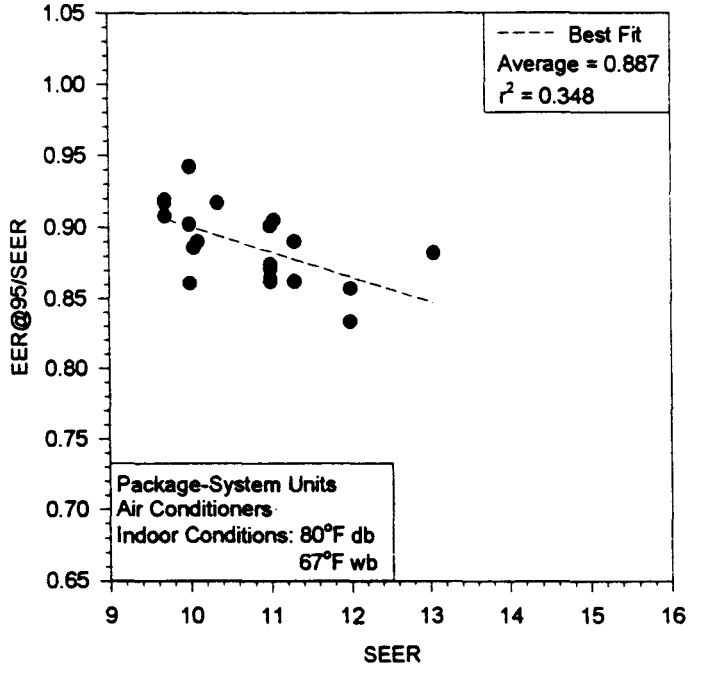

Figure 7.23 *EER@95°F/SEER vs. SEER for package-system air conditioners.*

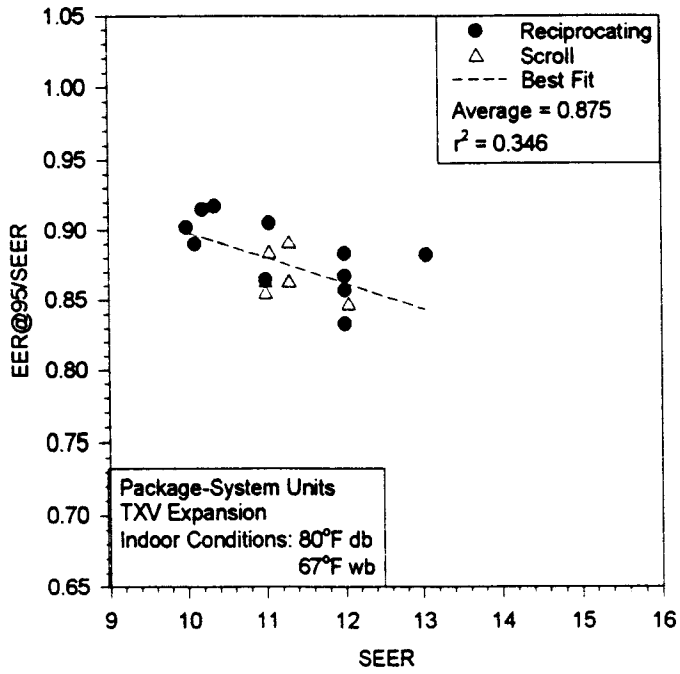

Figure 7.24 EER@95°F/SEER vs. SEER for package-system units with TXV expansion.

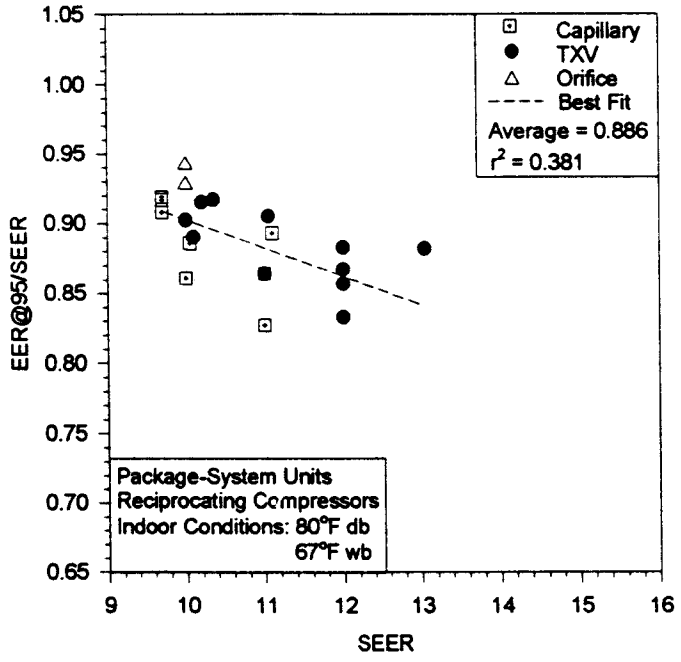

Figure 7.25 EER@95°F/SEER vs. SEER for package-system units with reciprocating compressors.

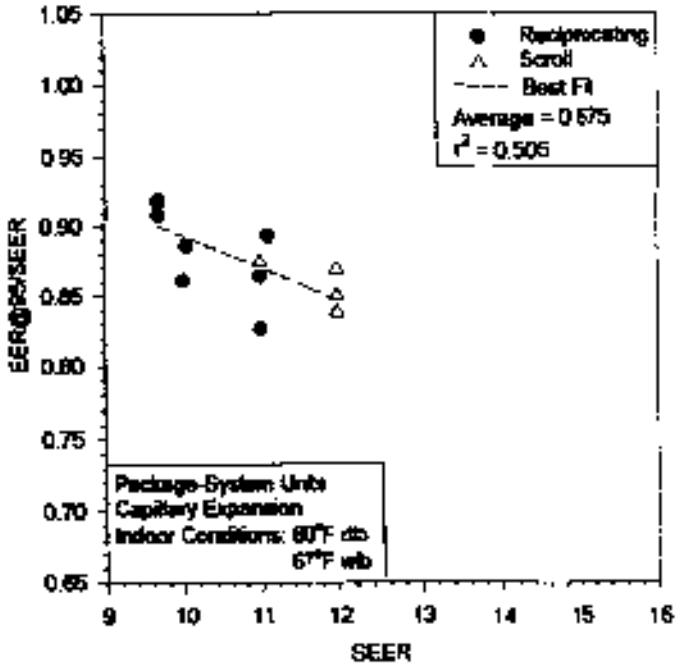

Figure 7.26 EER@95°F/SEER vs. SEER for package-system units with capillary tube expansion.

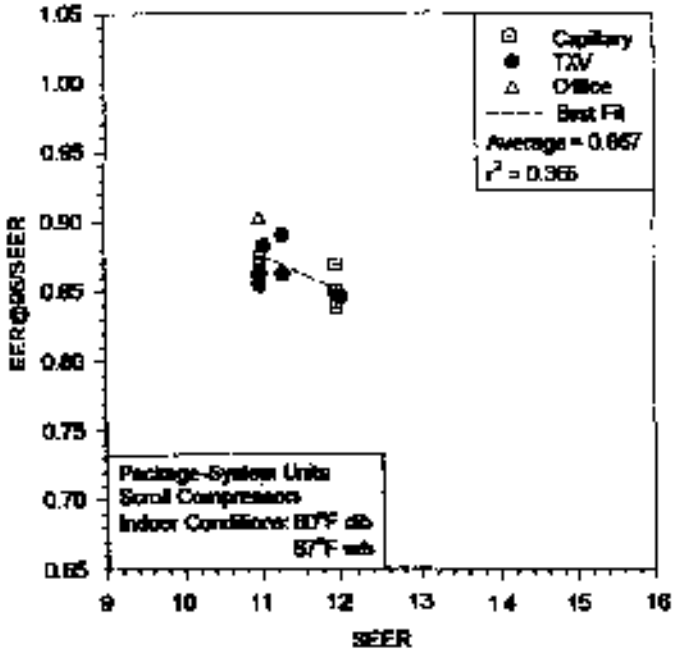

Figure 7.27 EER@95°F/SEER vs. SEER for package-system units with scroll compressors.

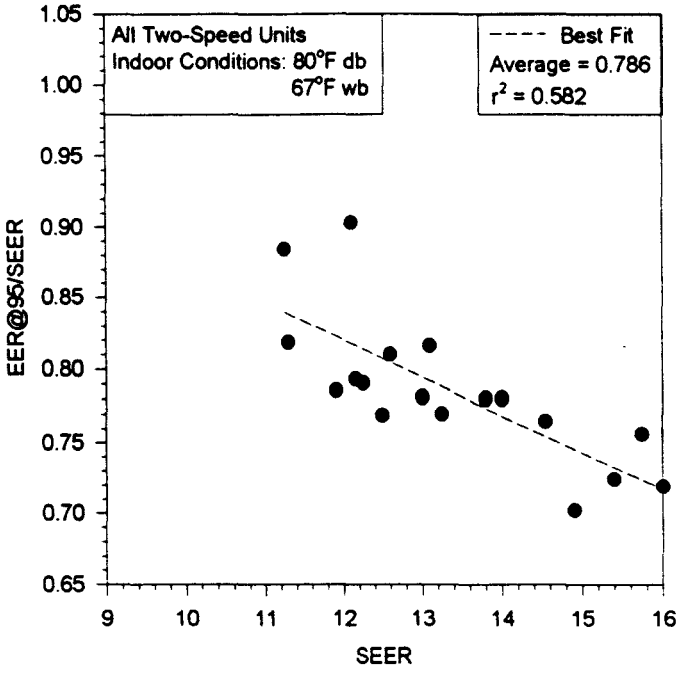

Figure 7.28 *EER@95°F/SEER vs. SEER for all two-speed units.*

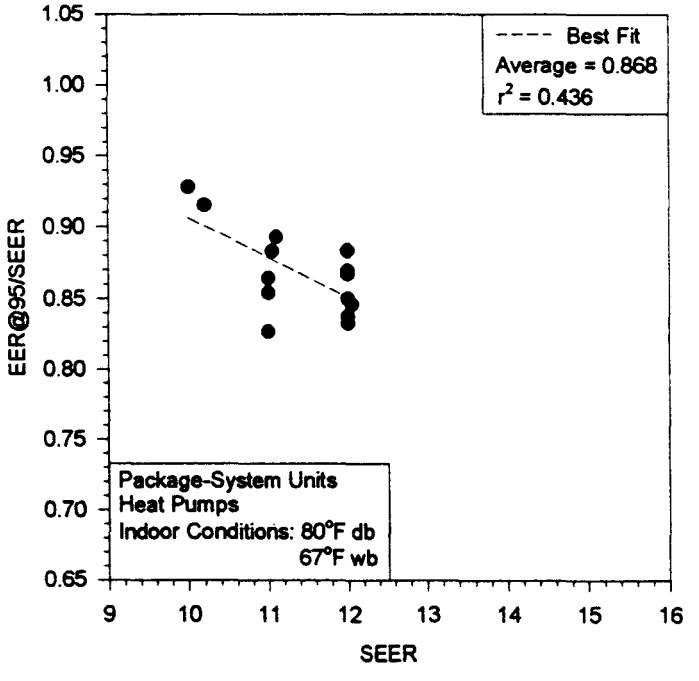

Figure 7.29 *EER@95°F/SEER vs. SEER for package-system heat pumps.*

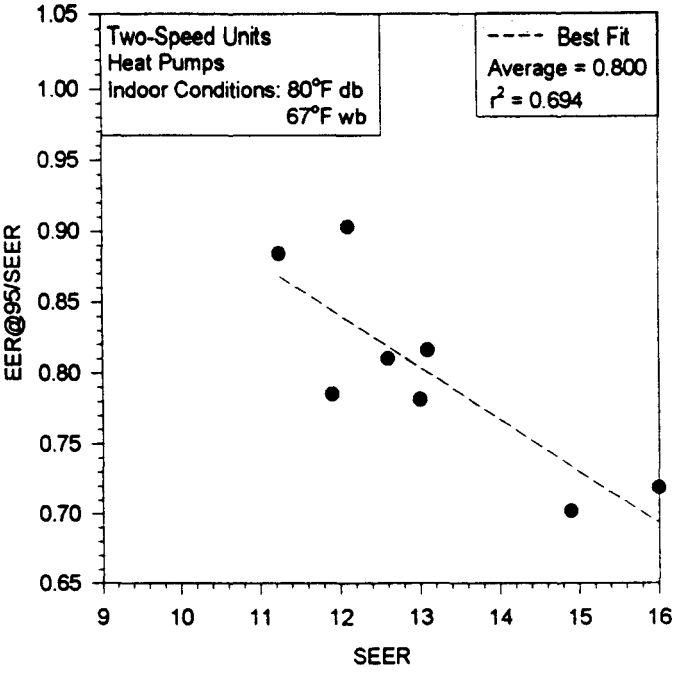

Figure 7.30 *EER@95°F/SEER vs. SEER for two-speed heat pumps.*

The calculation of the SEER of two-speed units involves compressor operation at both speeds, resulting in a higher SEER value than if it were based on only high speed operation. Consistently high average values of EER/SEER over a range of SEER's are good for electric utility companies. For a given capacity, these higher averages correspond to lower system power requirements.

Table 7.5 Average EER/SEER values for various hardware configurations.

Hardware Configuration	EER@95°F/SEER Average
Sr	0.919
So	0.913
Sc	0.910
Sh	0.899
St	0.897
Pc	0.887
Pr	0.886
Ss	0.883
Pt	0.875
PCap	0.875
Ph	0.868
Ps	0.867
2h	0.800
2tot	0.786
2c	0.775

Figure 7.17 shows the split-system units with orifice expansion divided by their type of compressor. The units with scroll compressors had consistently lower averages than those with reciprocating compressors. This indicates that the EER at 95°F (35°C) for

units with scroll compressors was often lower than that for units with reciprocating compressors at equivalent SEER values.

The split-system units had an average EER/SEER of 0.904, while the package-system units had an average of 0.876. For the two-speed units investigated, the EER/SEER ratio was 0.787. Table 7.6 compares the average EER/SEER values found in this experiment to similar results obtained in work by Nguyen et al (1981).

***Table 7.6** Comparison of EER@95°F/SEER for current and previous research.*

Data Sample	EER@95°F/SEER (Nguyen et al 1981)	EER@95°F/SEER (Current)	Percent Change
Split-Systems	0.947	0.904	-4.5%
Package-Systems	0.941	0.876	-6.9%
TXV Units	0.929	0.886	-4.6%
Orifice Units	0.941	0.913	-3.0%
Capillary Tube Units	0.959	0.875	-8.8%
All Single-Speed Units	0.946	0.890	-5.9%

The current values of EER/SEER ranged from 3.0% to 8.8% below those found by Nguyen et al in 1981. For all single-speed units, the average value was 5.9% less than the prior research. Several possible reasons exist for this change. Since the initial study, manufacturers have had over a decade to improve the seasonal efficiency of air conditioning systems. During this time, a number of technologies such as scroll compressors, variable speed motors, higher efficiency motors, and internally finned tubes

have been implemented into air conditioning system design. Thus, the average SEER of residential unitary air conditioning units improved from 7.78 in 1981 to 10.61 in 1994 (ARI 1995). As mentioned earlier, these increases in SEER do not always correspond to increases in EER. As a result, the ratio of EER to SEER has decreased.

Steady-State Analysis

In this analysis, only steady-state cooling performance was examined to determine a relationship between capacity, power, or EER, and outdoor temperature. The purpose of this analysis was to provide a method of predicting system cooling performance at various outdoor temperatures based on the hardware configuration of the system. System performance at 85°F (29.4°C), 95°F (35°C), 105°F (40.6°C) and 115°F (46.1°C) outdoor temperatures divided by the performance at 95°F (35°C) was examined for various hardware configurations. The outdoor temperature 95°F (35°C) was chosen for several reasons. First of all, this temperature is the temperature at which the cooling capacity of the system is rated. As a result, the nominal capacity of a unit at this temperature is known. Since capacity rating occurs at this temperature, the temperature is also a required test point. Power requirements and EER at this temperature are therefore known. Finally, one set of manufacturer data only listed performance of temperatures at 95°F (35°C) and above.

Normalized Capacity

This section of the analysis looked at normalized capacity values between 85°F

(29.4°C) and 115°F (46.1°C) outdoor temperature. Table 7.7 lists the linear curve fits and r^2 correlation values for each of the hardware configurations analyzed. All slopes of the data were negative, showing a decrease in capacity with an increase in outdoor temperature. The table is organized in order of increasingly negative slopes, with the smallest negative slope listed first. Smaller negative slopes indicate a smaller decrease in capacity with an increase in outdoor temperature. Air conditioners with two-speed compressors exhibited the smallest capacity drop over the temperature range, while package heat pumps showed the largest capacity drop.

The slope of the figures indicates the change in the normalized capacity value per °F, and can be thought of as a percentage drop of the capacity at 95°F (35°C). For example, for the two-speed air conditioners, each increase in outdoor temperature of 1°F (0.56°C) resulted in a decrease in capacity of 0.43% of the capacity rating at 95°F (35°C), as indicated in the following equation:

$$\Delta\text{Capacity} = \frac{100\% * b(1) * \text{Capacity@95}}{^\circ\text{F}} \qquad (7.2)$$

where: ΔCapacity = Change in capacity of unit

Capacity@95 = Capacity of unit at 95°F

b(1) = slope of normalized capacity from Table 7.7

The average slopes obtained for the various types of systems were -0.00585 for the

split-system units, -0.00609 for the package-system units, and -0.00503 for the two-speed units. This indicates that on average, two-speed units showed the smallest decrease in capacity with an increase in outdoor temperature, followed by split-system units and two-speed units.

Table 7.7 Fits for normalized capacity.

Hardware Configuration	b(0)	b(1)	r^2
2c	1.4500	-0.00434	0.990
Ps	1.5211	-0.00472	0.795
Pc	1.5937	-0.00497	0.853
2h	1.4944	-0.00507	0.990
Sr	1.5364	-0.00515	0.974
Pt	1.6128	-0.00520	0.848
So	1.5065	-0.00524	0.968
Ss	1.4109	-0.00537	0.979
Sc	1.4953	-0.00554	0.953
2tot	1.4732	-0.00568	0.985
Pr	1.6952	-0.00629	0.899
Sh	1.4865	-0.00645	0.960
St	1.4804	-0.00735	0.949
PCap	1.7431	-0.00744	0.907
Ph	1.7030	-0.00790	0.876

The correlation values ranged from 0.795 for package systems with scroll compressors to 0.990 for the two-speed air conditioners and heat pumps. An overall average r^2 of 0.928 was found for the hardware configurations investigated. This average can be divided into an average r^2 of 0.964 for the split-system unit combinations, 0.863 for the package-system unit combinations, and 0.988 for the two-speed unit combinations. These values indicate the two-speed units showed the most consistent capacity drop

pattern for the different outdoor temperatures, followed by the split-system units and the package-system units, respectively.

Figures 7.31 through 7.45 show the linear fits of normalized capacity data at outdoor temperatures from 85°F (29.4°C) to 115°F (46.1°C). The figures are listed in the order they appear in Table 7.7.

Normalized Power

Normalized system power was analyzed at the different outdoor temperatures for the hardware configurations shown in Table 7.8. The positive slopes for each hardware system describe the increase in power requirements which occurred with an increase in outdoor temperature. Table 7.8 is organized by increasing slopes with the smallest slope listed first. In this case, smaller slopes indicate less dependence of the power on outdoor temperature and smaller increases in power requirements with an increase in outdoor temperature. The two-speed heat pumps showed the smallest rise in power over the temperature range, while the two-speed air conditioners showed the biggest rise.

R-squares for the normalized power curves varied from 0.892 for the package heat pumps to 0.988 for the split-system units with scroll compressors. The average r^2 values were 0.946 for the split-system units, 0.926 for the package-system units, and 0.968 for the two-speed units. These averages resulted in an overall average r^2 of 0.942.

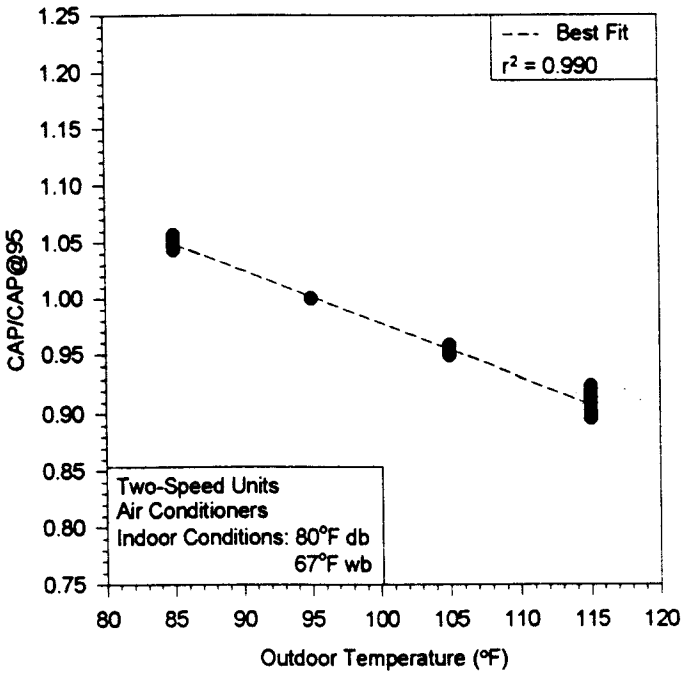

Figure 7.31 *Normalized capacity at various outdoor temperatures for two-speed air conditioners.*

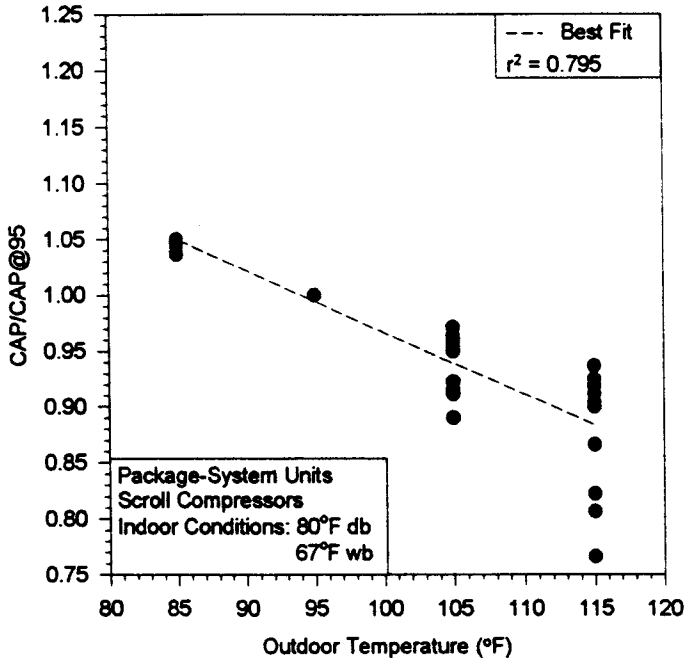

Figure 7.32 *Normalized capacity at various outdoor temperatures for package-system units with scroll compressors.*

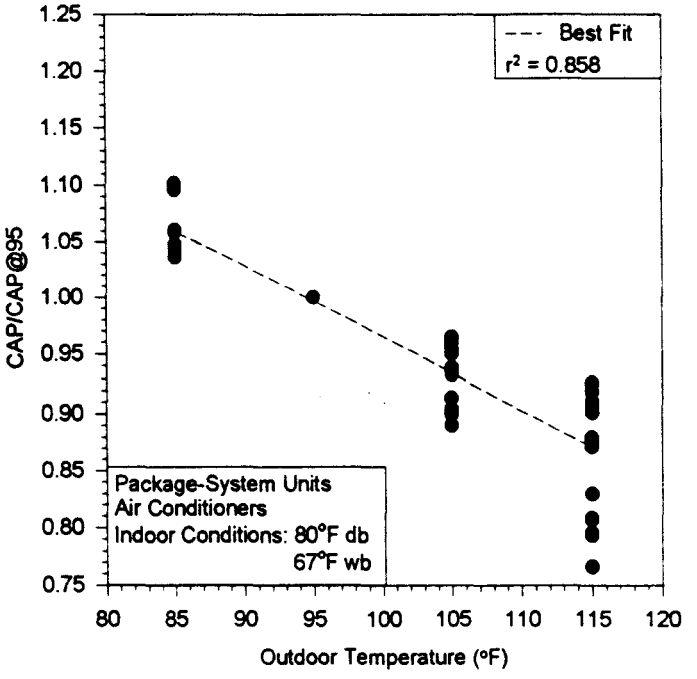

Figure 7.33 *Normalized capacity at various outdoor temperatures for package-system air conditioners.*

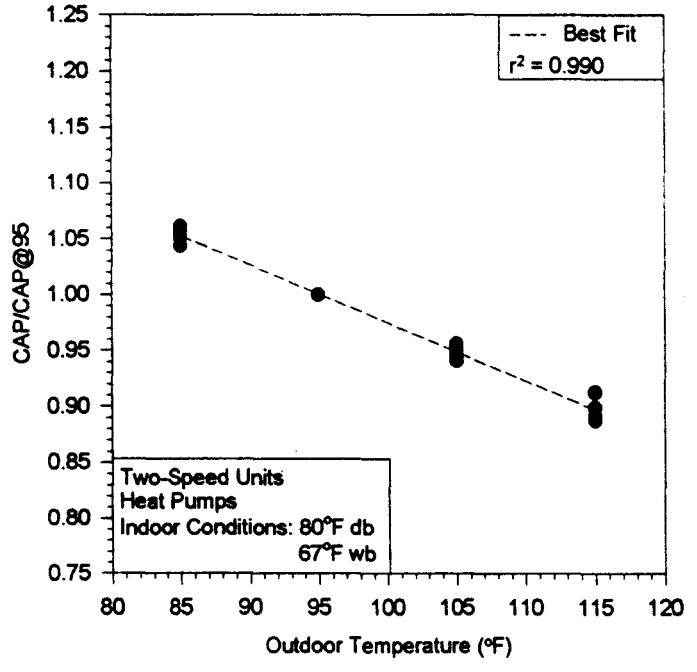

Figure 7.34 *Normalized capacity at various outdoor temperatures for two-speed heat pumps.*

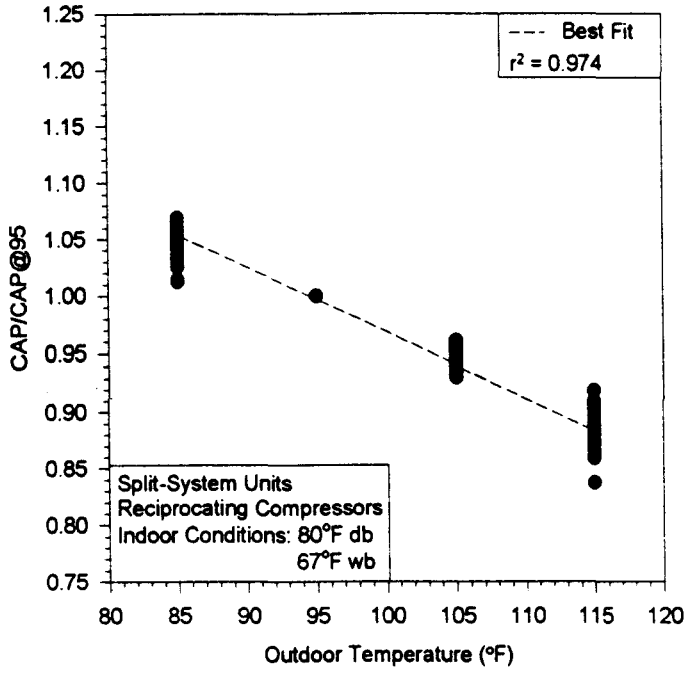

Figure 7.35 *Normalized capacity at various outdoor temperatures for split-system units with reciprocating compressors.*

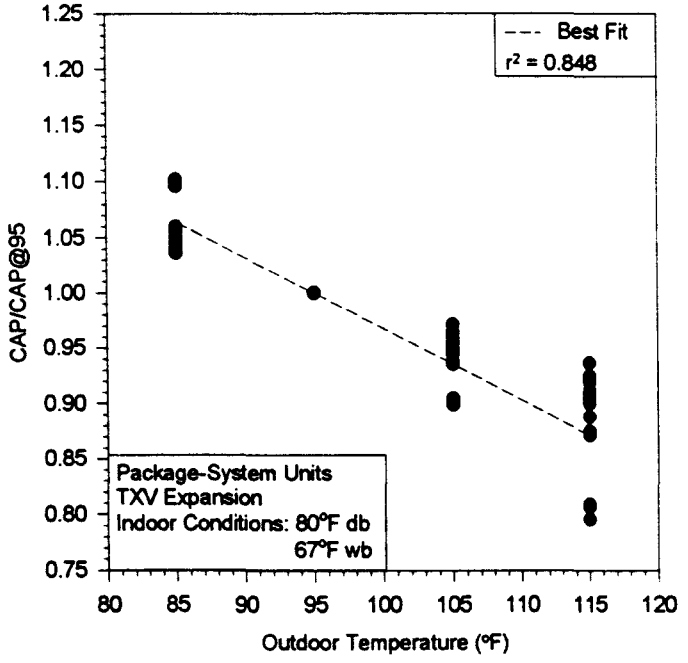

Figure 7.36 *Normalized capacity at various outdoor temperatures for package-system units with TXV expansion.*

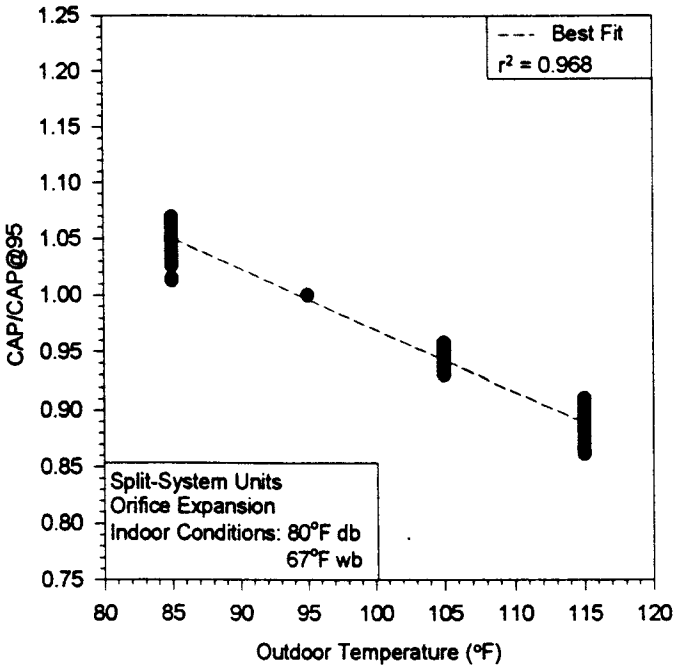

***Figure 7.37** Normalized capacity at various outdoor temperatures for split-system units with orifice expansion.*

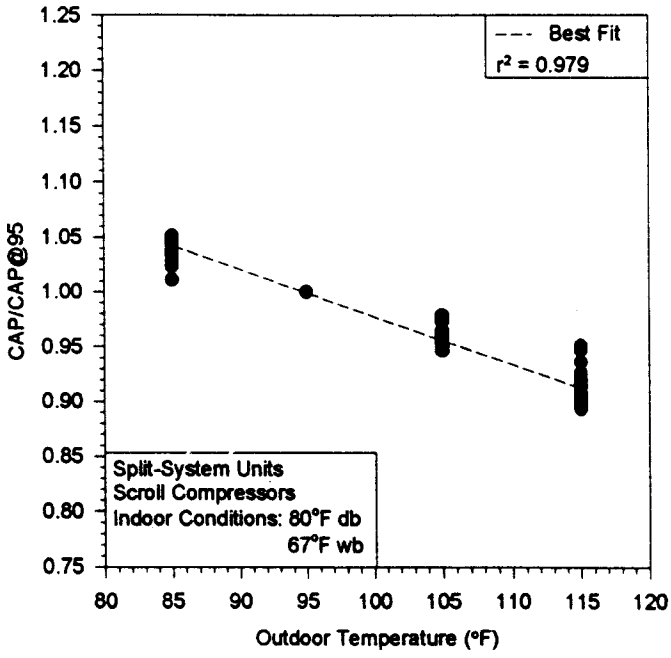

***Figure 7.38** Normalized capacity at various outdoor temperatures for split-system units with scroll compressors.*

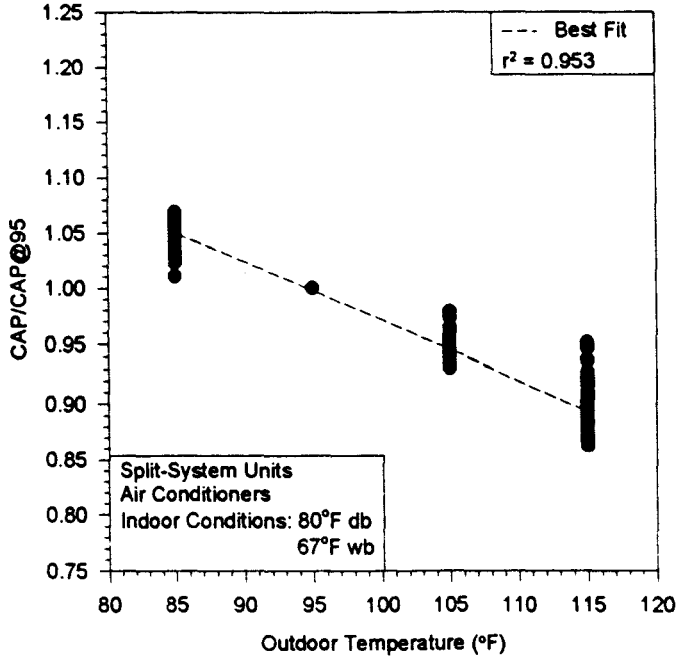

Figure 7.39 Normalized capacity at various outdoor temperatures for split-system air conditioners.

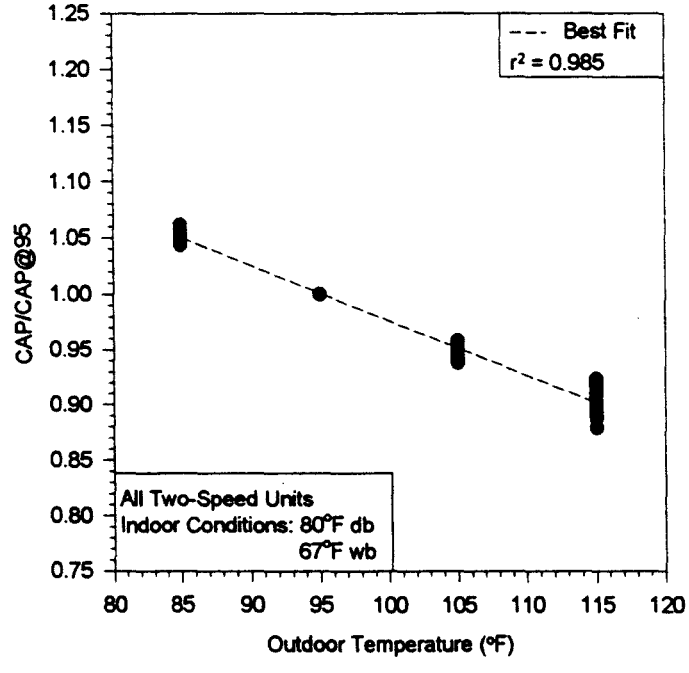

Figure 7.40 Normalized capacity at various outdoor temperatures for all two-speed units.

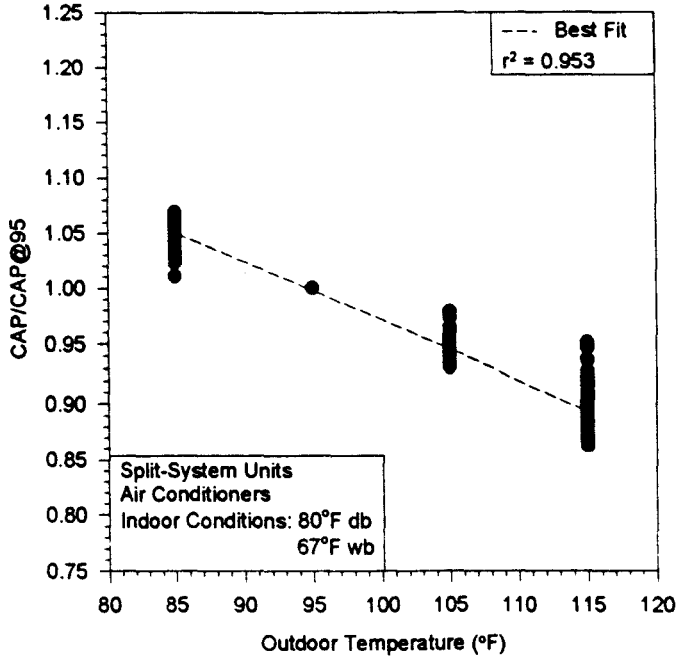

Figure 7.39 Normalized capacity at various outdoor temperatures for split-system air conditioners.

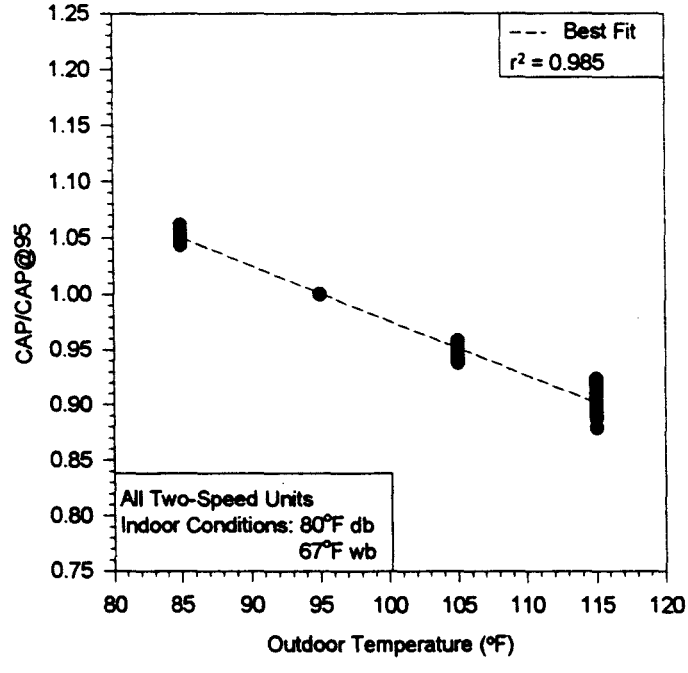

Figure 7.40 Normalized capacity at various outdoor temperatures for all two-speed units.

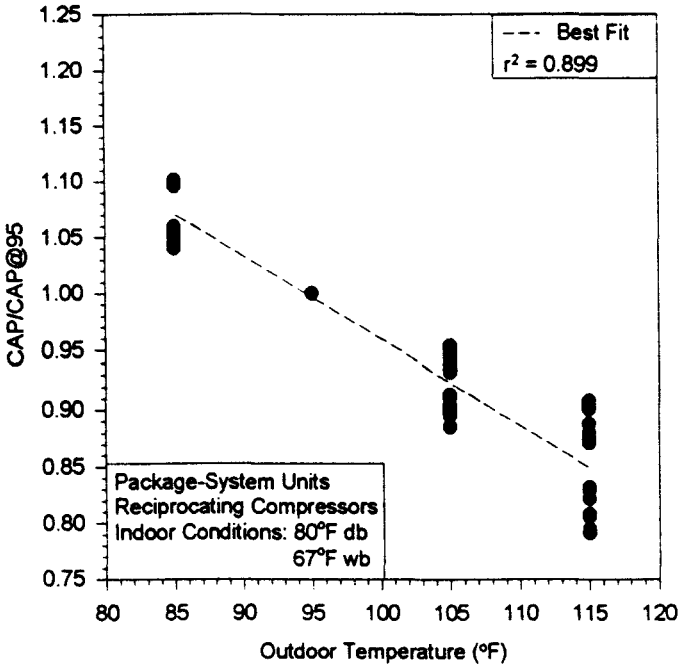

Figure 7.41 Normalized capacity at various outdoor temperatures for package-system units with reciprocating compressors.

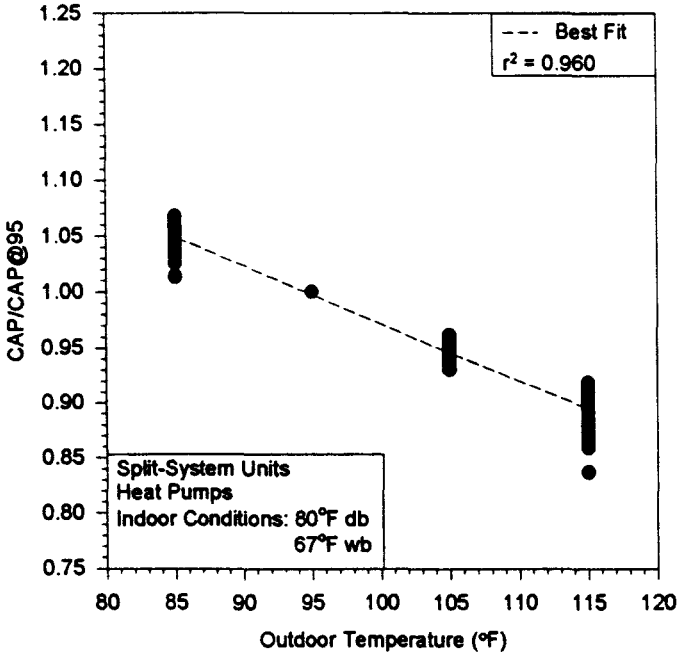

Figure 7.42 Normalized capacity at various outdoor temperatures for split-system heat pumps.

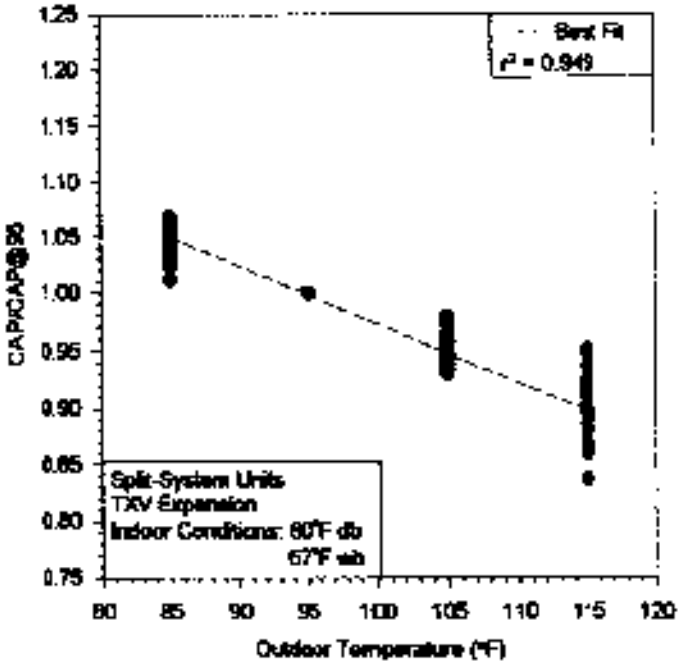

Figure 7.43 Normalized capacity at various outdoor temperatures for split-system units with TXV expansion.

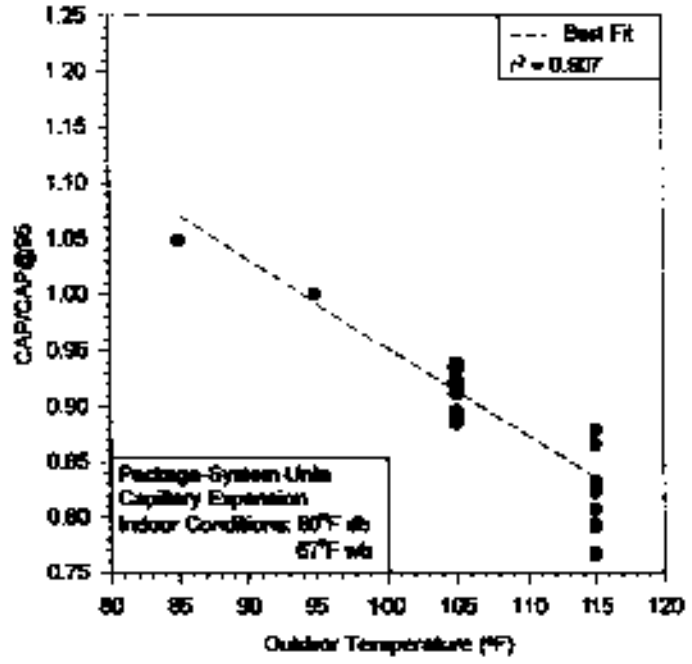

Figure 7.44 Normalized capacity at various outdoor temperatures for package-system units with capillary tube expansion.

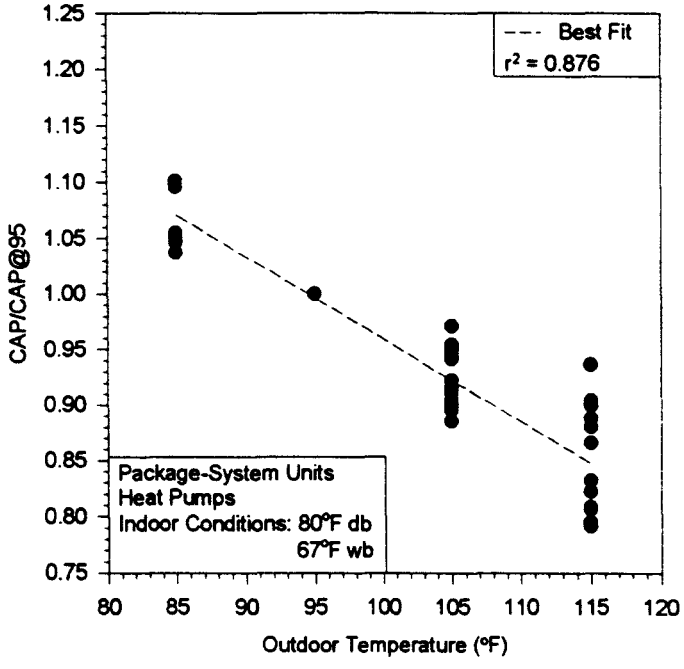

Figure 7.45 *Normalized capacity at various outdoor temperatures for package-system heat pumps.*

Table 7.8 Fits for normalized power.

Hardware Configuration	b(0)	b(1)	r^2
2h	0.0812	0.00662	0.972
Pr	0.3731	0.00662	0.936
St	0.2230	0.00738	0.927
Sr	0.3714	0.00747	0.966
PCap	0.2676	0.00754	0.945
2tot	0.1859	0.00756	0.951
Pt	0.2871	0.00770	0.892
Sc	0.2842	0.00774	0.927
Sh	0.2174	0.00782	0.931
Ss	0.0585	0.00822	0.988
Ps	0.1263	0.00827	0.959
Pc	0.3016	0.00863	0.926
So	0.2918	0.00925	0.936
Ph	0.2620	0.00980	0.895
2c	0.2697	0.00998	0.981

The split-system units had an average slope of 0.00798, the package-system units had an average slope of 0.00809, and the two-speed units had an average slope of 0.00805. On average, therefore, split-system units had the smallest increase in power with an increase in outdoor temperature, followed by two-speed units and package units, respectively. The increase in power with an increase in outdoor temperature can be obtained from Equation 7.3.

$$\Delta\text{Power} = \frac{100\% * b(1) * \text{Power@95}}{^{\circ}\text{F}} \tag{7.3}$$

where: ΔPower = Change in power requirements of unit

Power@95 = Power requirements of unit at 95°F

b(1) = slope of normalized power from Table 7.8

The normalized power data are listed in Figures 7.46 to 7.60 along with their linear fits. The figures are listed as they appear in Table 7.8.

An investigation by Proctor et al (1994) examined the power requirements of scroll and reciprocating compressors at high outdoor temperatures. The report concluded that although scroll compressors initially drew less power than reciprocating compressors of the same nominal capacity at lower outdoor temperatures, after 100°F (37.8°C) scroll compressors drew more power. The current analysis indicated a similar trend. As shown in Table 7.8, units with reciprocating compressors (both split-system and package units) had smaller slopes of normalized power than scroll compressors, indicating smaller increases in power with an increase in outdoor temperature.

Normalized EER

The ratio of EER at various outdoor temperatures to the EER at 95°F (35°C) was analyzed for outdoor temperatures between 85°F (29.4°C) and 115°F (46.1°C) for the hardware configurations listed in Table 7.9. The slopes of all curves were negative, indicating a decrease in EER with an increase in outdoor temperature. The table lists linear curve fits in order of increasingly negative slopes, with the least negative slope shown first. Less negative slopes correspond to smaller decreases in EER with an increase in outdoor temperature.

The average r^2 for the set of hardware configurations was 0.982. This resulted

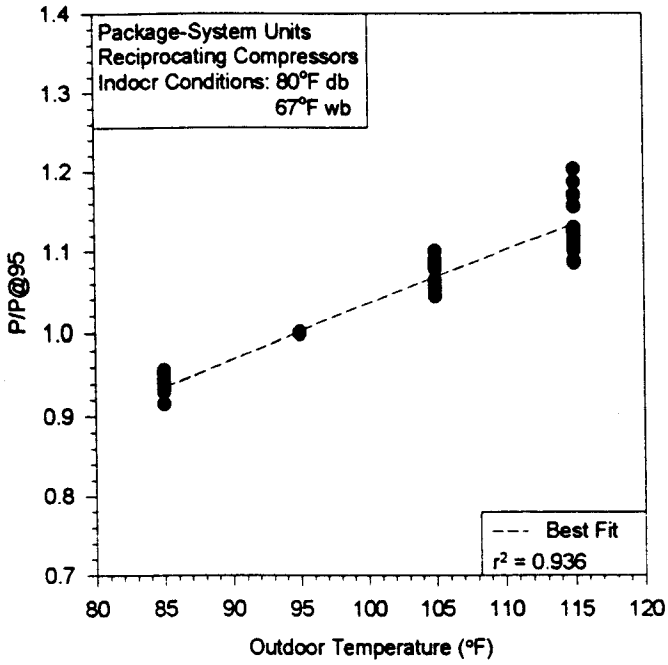

Figure 7.46 *Normalized power at various outdoor temperatures for package-system units with reciprocating compressors.*

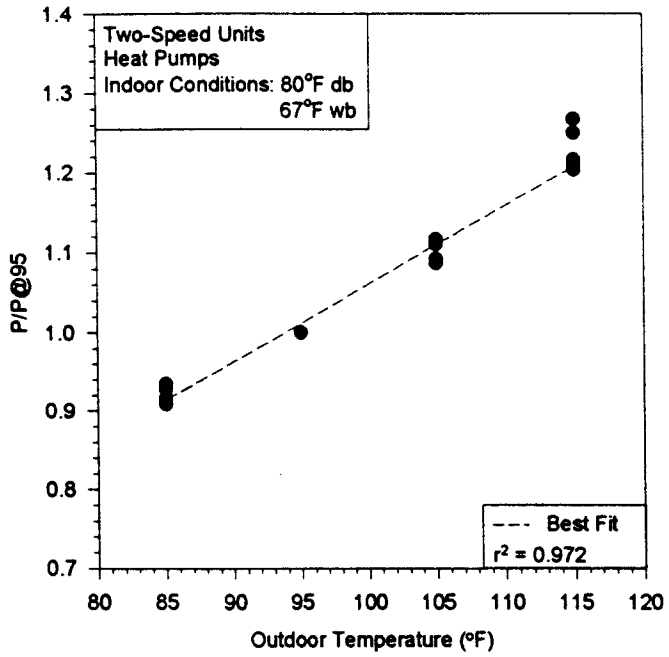

Figure 7.47 *Normalized power at various outdoor temperatures for two-speed heat pumps.*

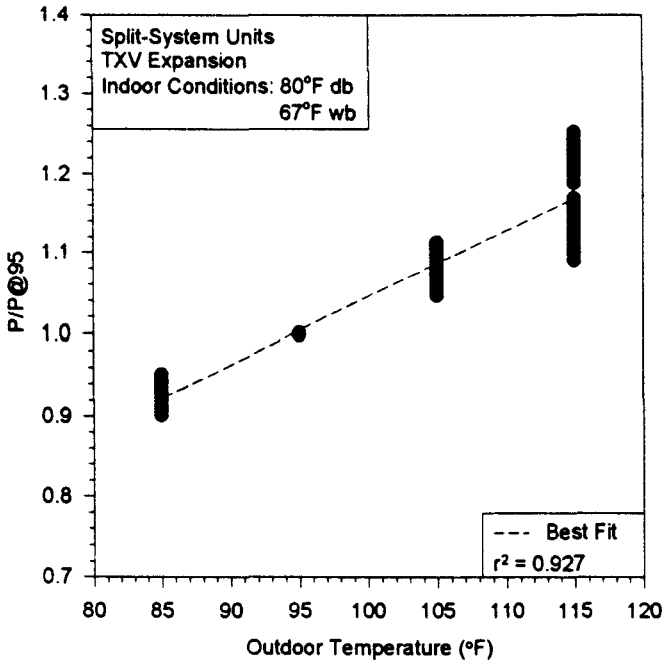

Figure 7.48 Normalized power at various outdoor temperatures for split-system units with TXV expansion.

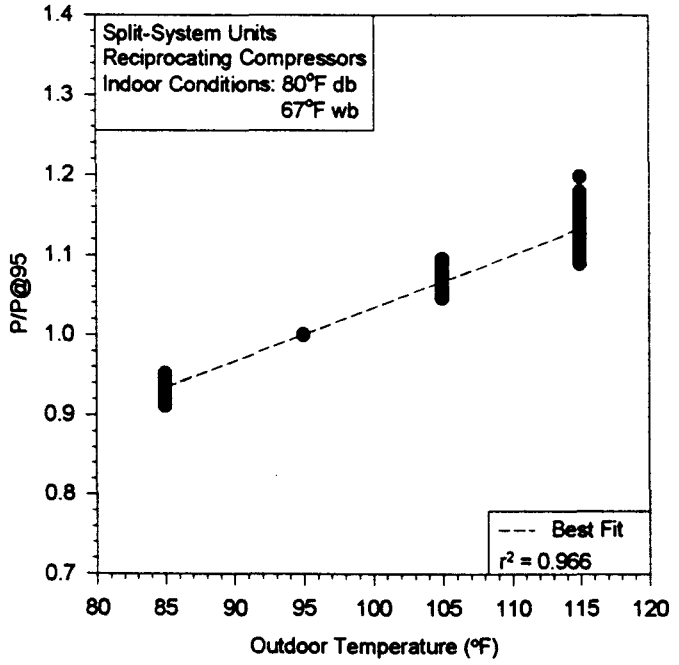

Figure 7.49 Normalized power at various outdoor temperatures for split-system units with reciprocating compressors.

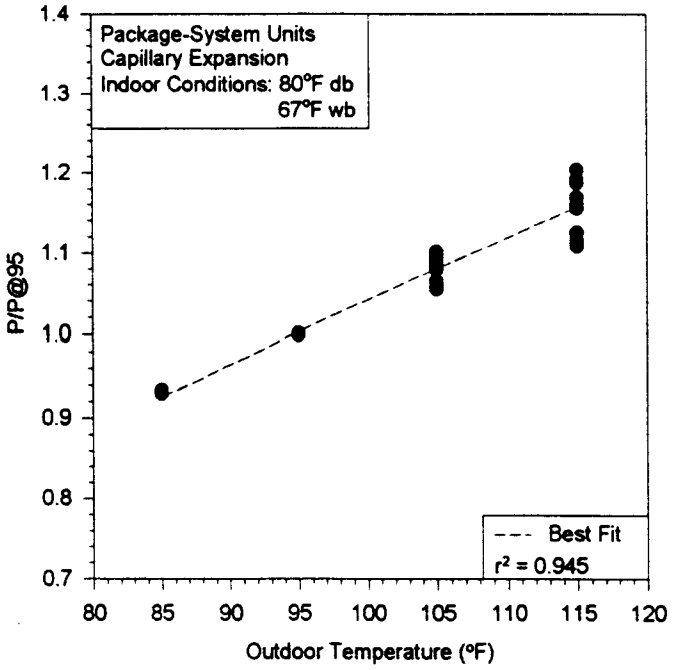

Figure 7.50 Normalized power at various outdoor temperatures for package-system units with capillary tube expansion.

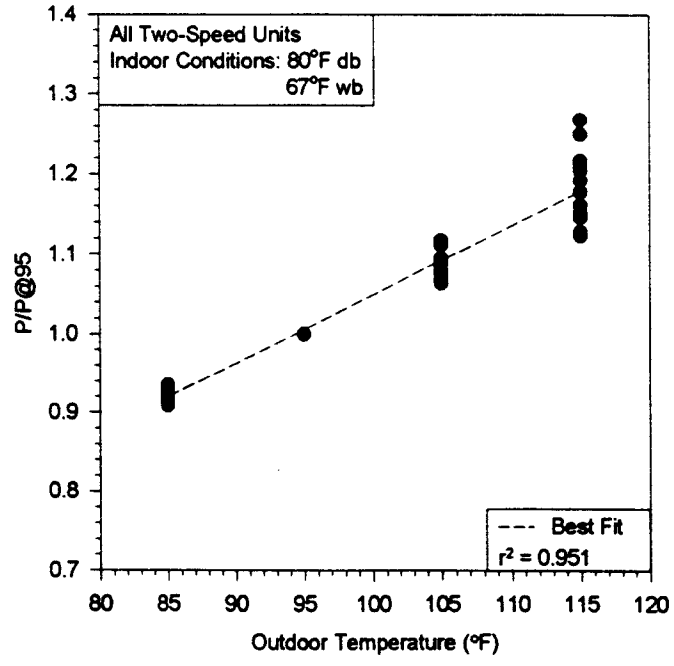

Figure 7.51 Normalized power at various outdoor temperatures for all two-speed units.

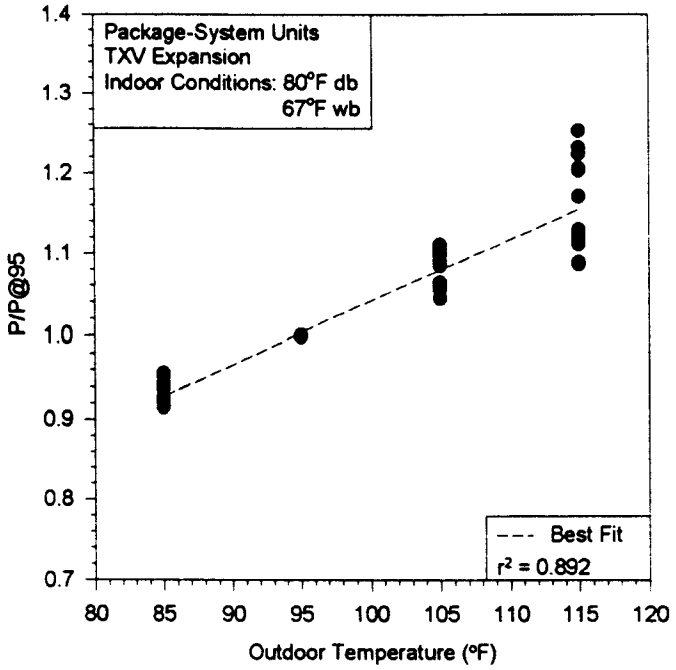

***Figure 7.52** Normalized power at various outdoor temperatures for package-system units with TXV expansion.*

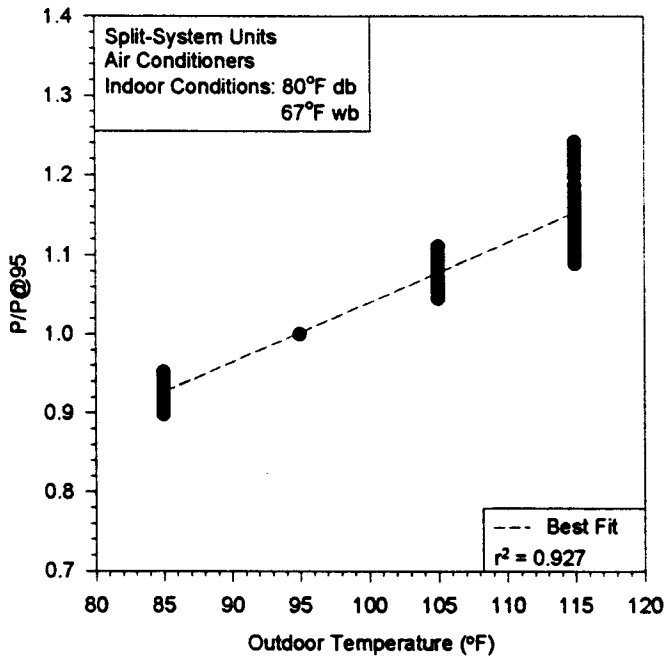

***Figure 7.53** Normalized power at various outdoor temperatures for split-system air conditioners.*

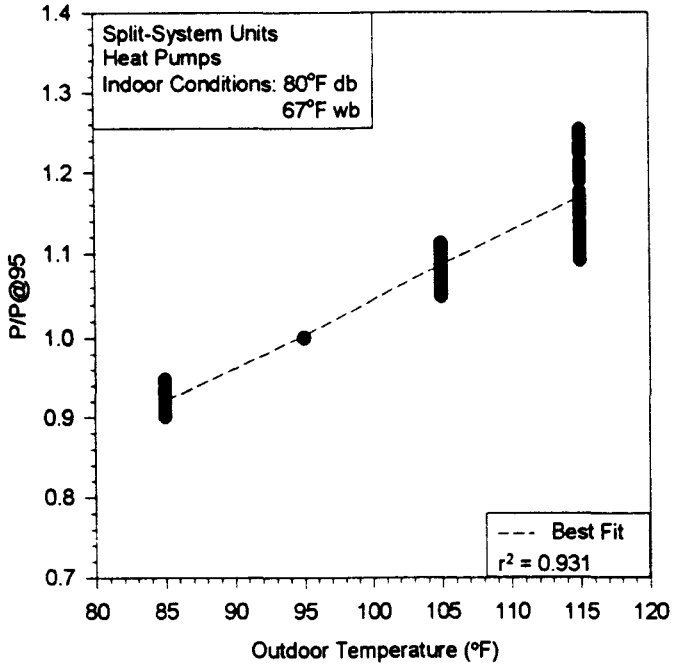

Figure 7.54 Normalized power at various outdoor temperatures for split-system heat pumps.

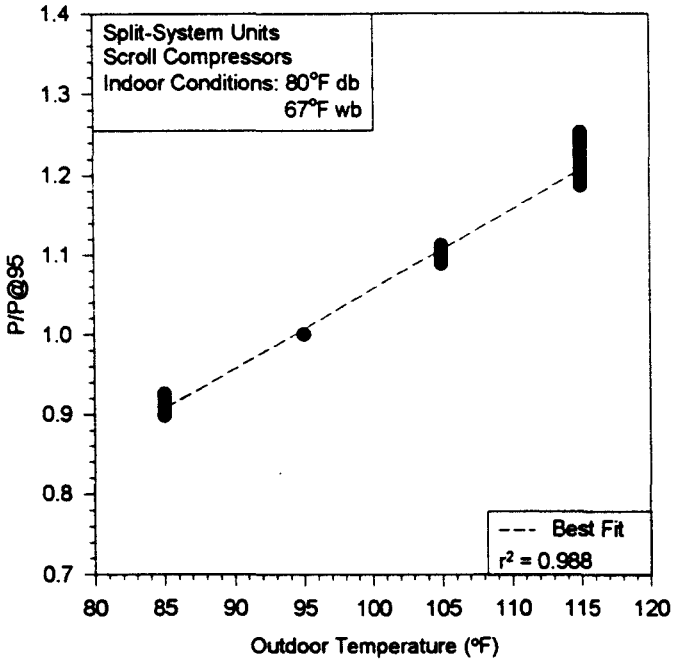

Figure 7.55 Normalized power at various outdoor temperatures for split-system units with scroll compressors.

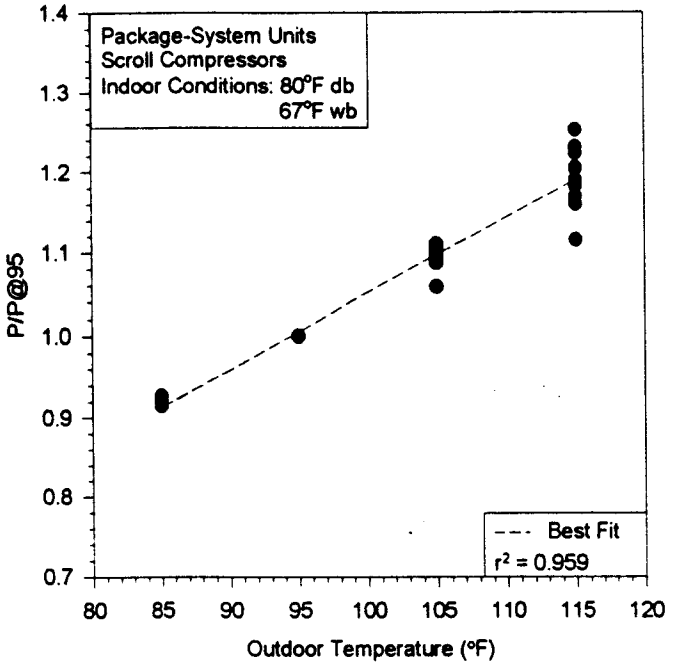

***Figure 7.56** Normalized power at various outdoor temperatures for package-system units with scroll compressors.*

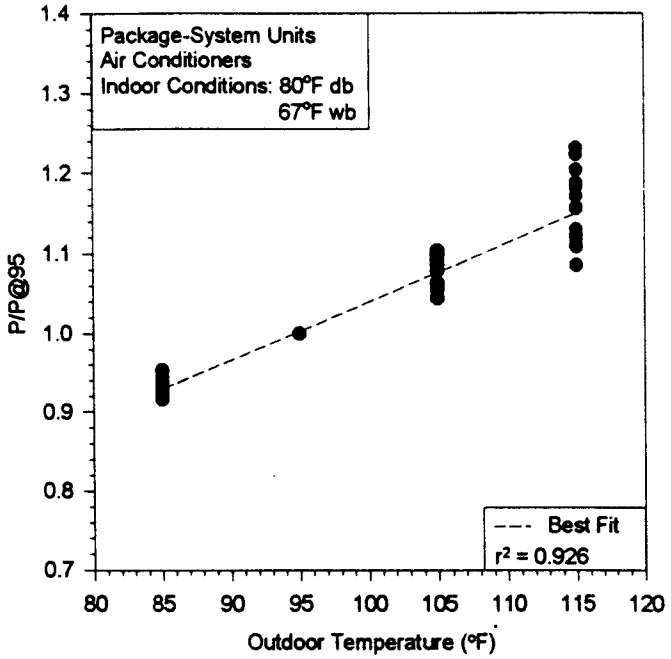

***Figure 7.57** Normalized power at various outdoor temperatures for package-system air conditioners.*

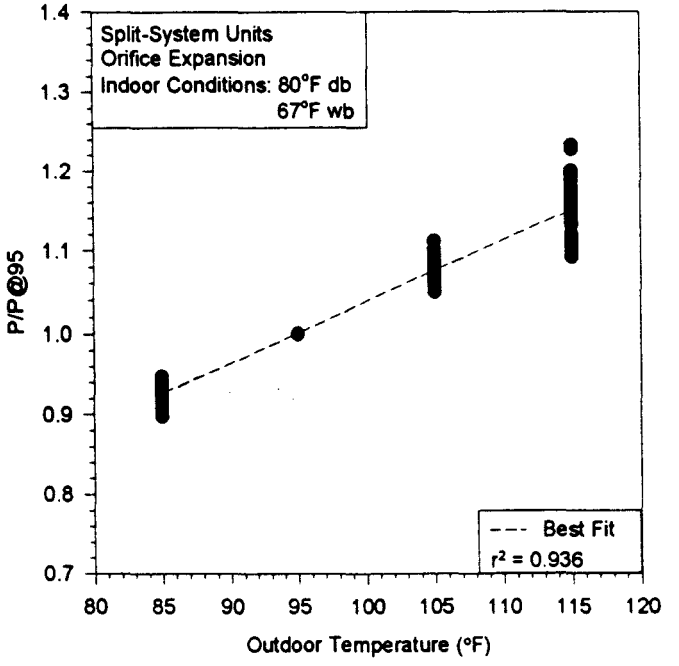

Figure 7.58 *Normalized power at various outdoor temperatures for split-system units with orifice expansion.*

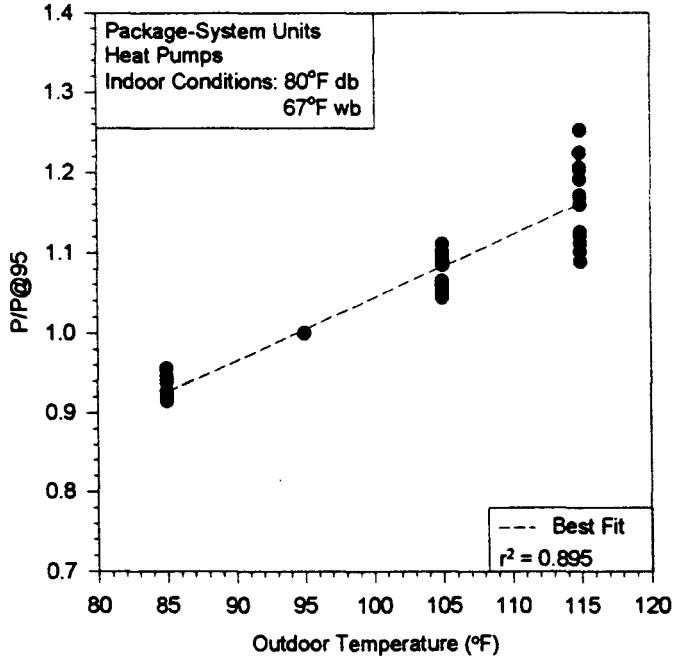

Figure 7.59 *Normalized power at various outdoor temperatures for package-system heat pumps.*

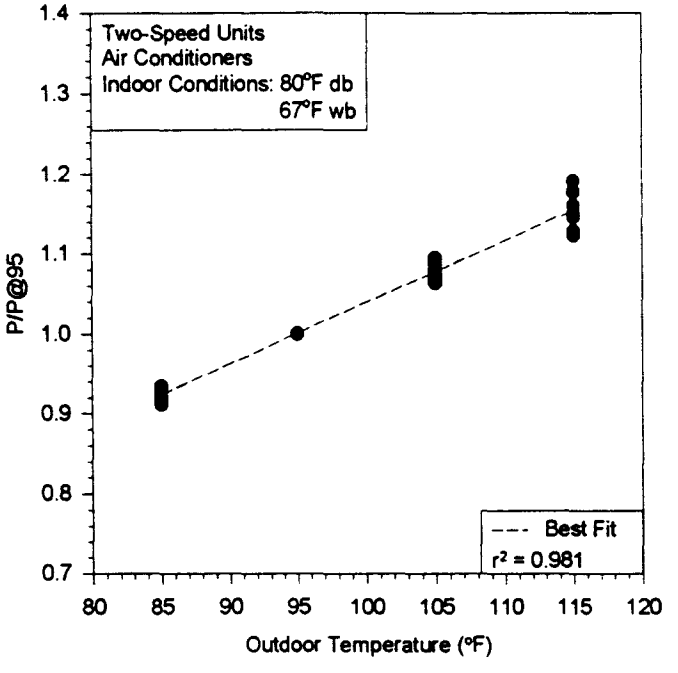

***Figure 7.60** Normalized power at various outdoor temperatures for two-speed air conditioners.*

from an average split-system r^2 of 0.992, an average package-system r^2 of 0.968, and an average two-speed r^2 of 0.992. The correlation value varied from 0.950 for package-system units with reciprocating compressors to 0.998 for the two-speed heat pumps.

Table 7.9 Fits for normalized EER.

Hardware Configuration	b(0)	b(1)	r^2
Sr	2.1040	-0.01158	0.992
2c	2.1160	-0.01164	0.992
Sc	2.1348	-0.01190	0.990
So	2.1414	-0.01197	0.991
St	2.1680	-0.01224	0.990
Sh	2.1800	-0.01237	0.991
2tot	2.1868	-0.01243	0.986
Pc	2.1877	-0.01248	0.963
Pt	2.2226	-0.01281	0.964
Pr	2.2276	-0.01290	0.950
Ss	2.2345	-0.01295	0.996
Ps	2.2625	-0.01330	0.986
2h	2.2754	-0.01341	0.998
Ph	2.3189	-0.01388	0.970
PCap	2.3168	-0.01393	0.973

The slopes of the linear EER fits allow the determination of the decrease in EER with an increase in outdoor temperature as shown in Equation 7.4.

$$\Delta EER = \frac{100\% * b(1) * EER@95}{^{\circ}F} \tag{7.4}$$

where: ΔEER = Change in EER of unit

EER@95 = EER of unit at 95°F

b(1) = slope of normalized EER from Table 7.9

The smallest negative slope occurred for the split-system units with reciprocating compressors, indicating the smallest decrease in EER with an increase in outdoor temperature. The package-system units with capillary tube expansion possessed the most negative slope. Average slopes of -0.01217 for the split-system units, -0.01322 for the package-system units, and -0.01249 for the two-speed units were obtained in the analysis. These results indicate that, in general, split-system units showed the smallest decrease in EER with an increase in outdoor temperature, followed by two-speed units, and package-system units, respectively.

Figures 7.61 to 7.75 show the EER/EER@95°F (35°C) data with best fit lines. The figures are listed as they appear in Table 7.9.

Summary

Table 7.10 shows the average r^2 values for the normalized performance curves discussed above. For each of the performance parameters investigated, the two-speed units showed the most consistent performance, followed by the split-system units and the package-system units. It should be noted, however, that all two-speed units analyzed were from the same manufacturer, increasing the probability of similar performance.

The normalized EER curves had the highest average correlation coefficients,

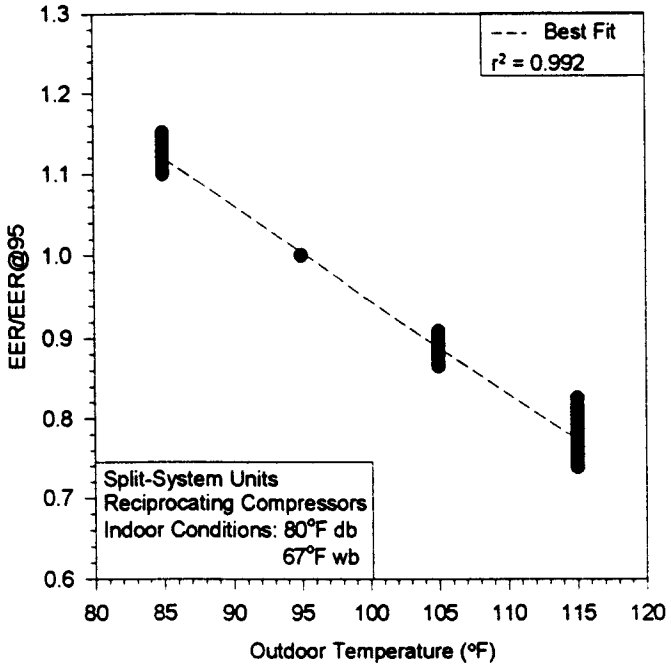

Figure 7.61 *Normalized EER at various outdoor temperatures for split-system units with reciprocating compressors.*

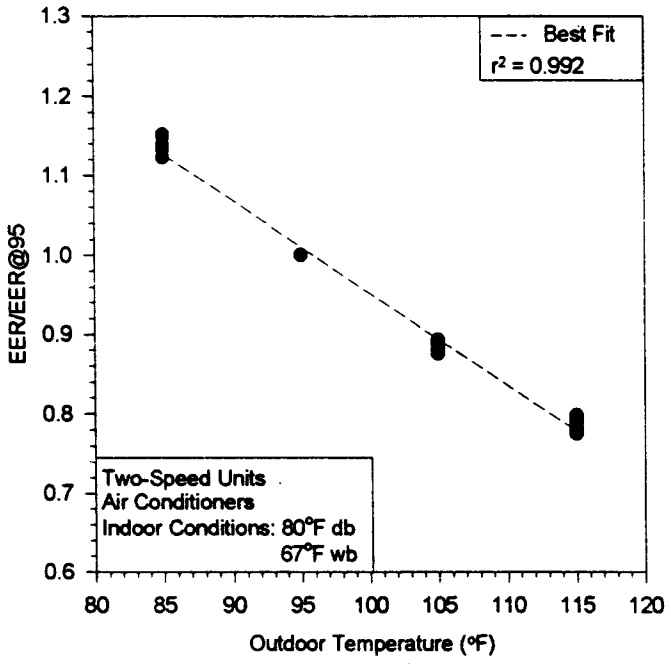

Figure 7.62 *Normalized EER at various outdoor temperatures for two-speed air conditioners.*

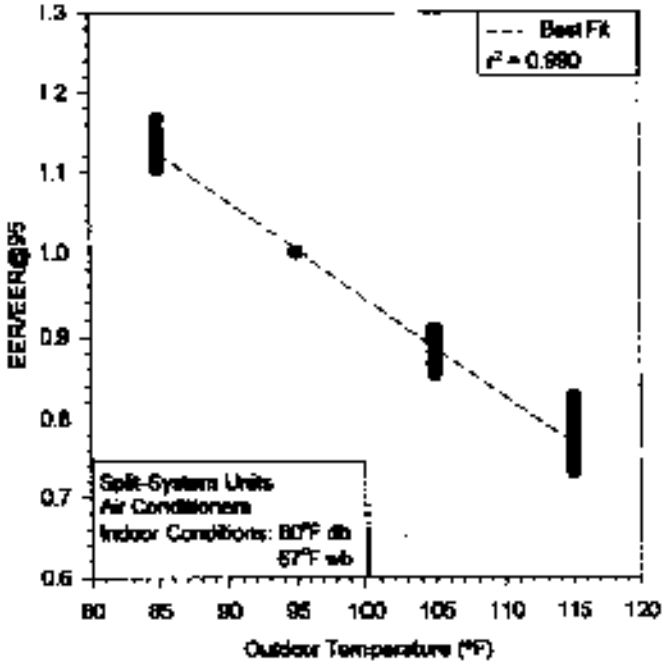

Figure 7.63 Normalized EER at various outdoor temperatures for split-system air conditioners.

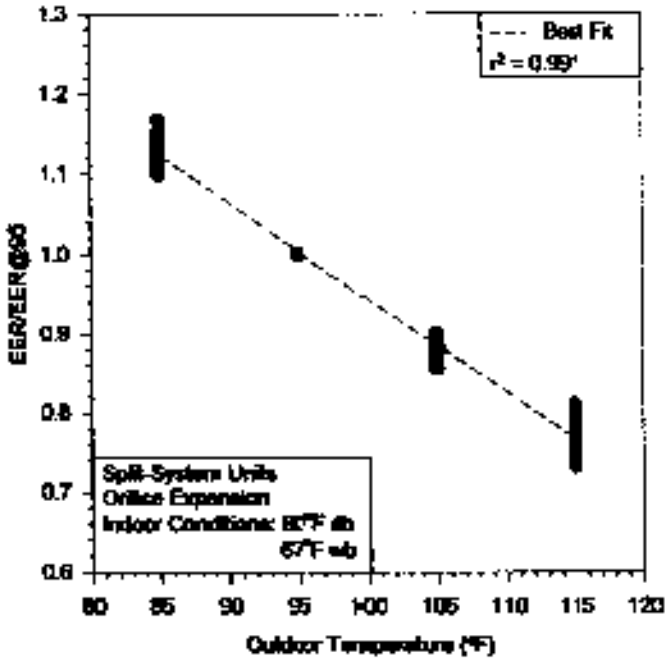

Figure 7.64 Normalized EER at various outdoor temperatures for split-system units with orifice expansion.

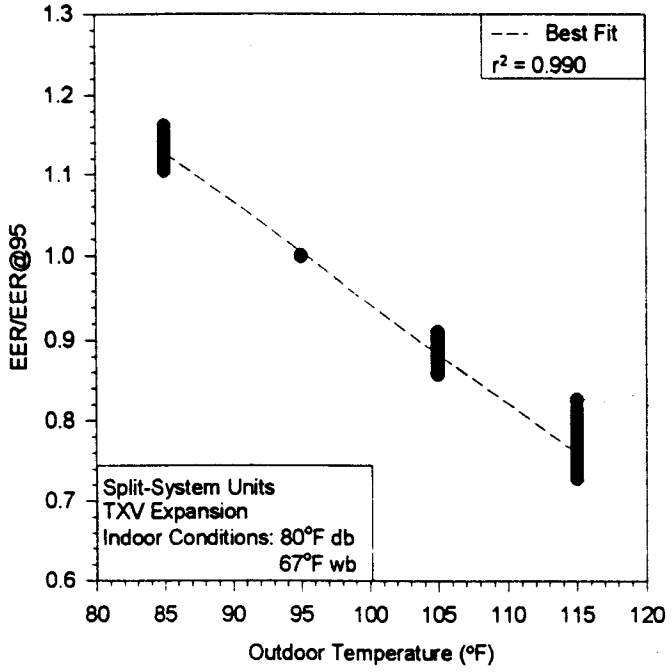

Figure 7.65 *Normalized EER at various outdoor temperatures for split-system units with TXV expansion.*

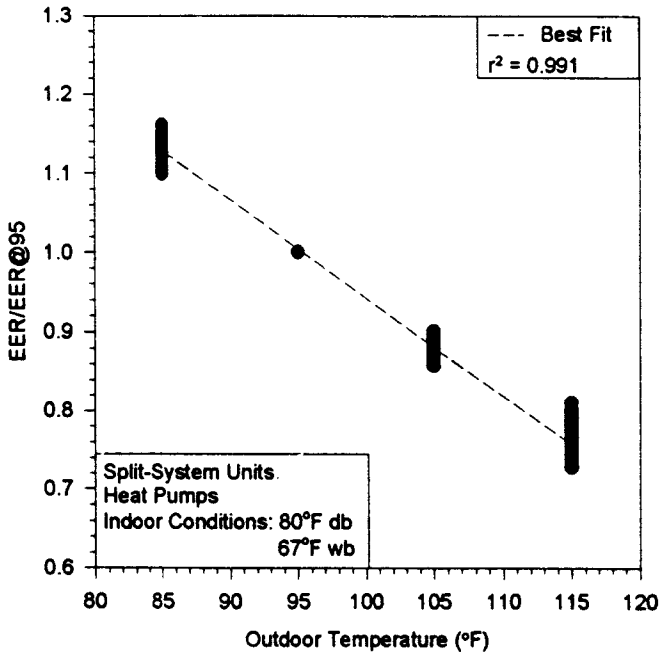

Figure 7.66 *Normalized EER at various outdoor temperatures for split-system heat pumps.*

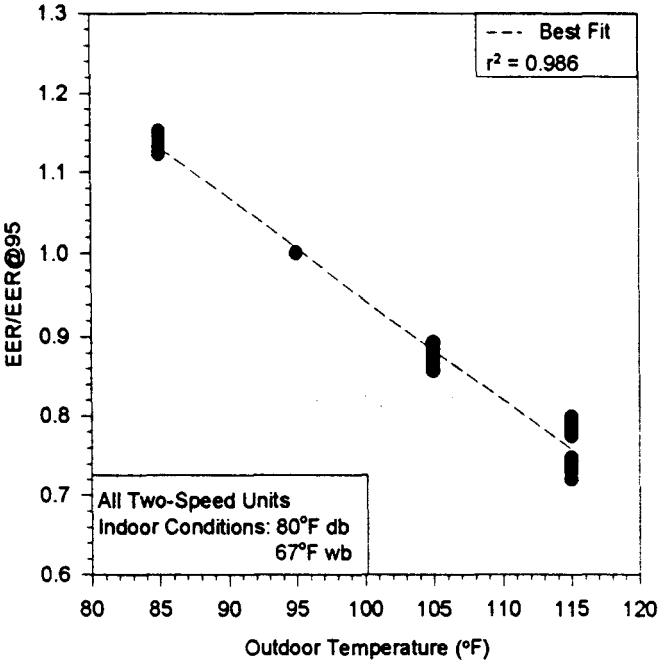

Figure 7.67 *Normalized EER at various outdoor temperatures for all two-speed units.*

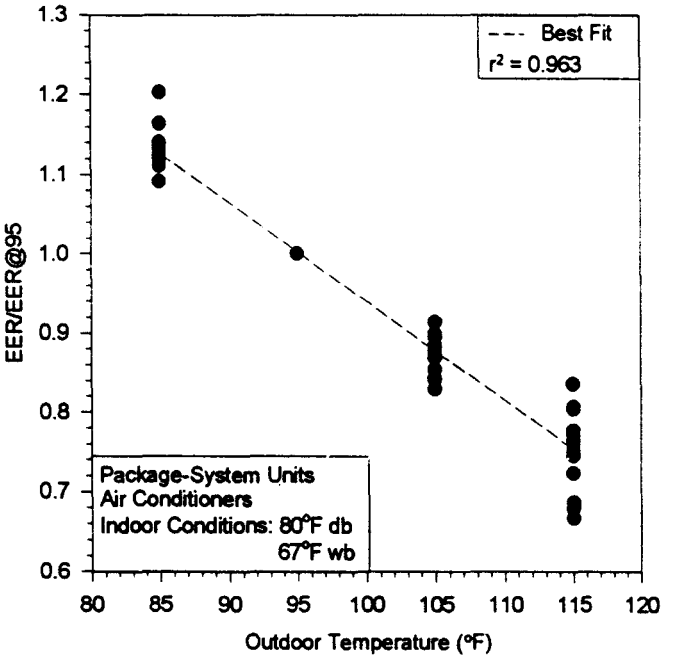

Figure 7.68 *Normalized EER at various outdoor temperatures for package-system air conditioners.*

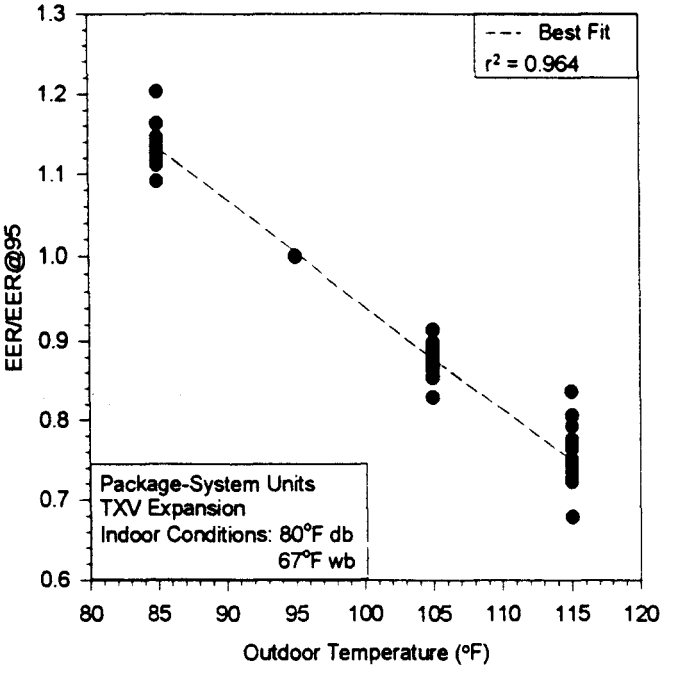

Figure 7.69 *Normalized EER at various outdoor temperatures for package-system units with TXV expansion.*

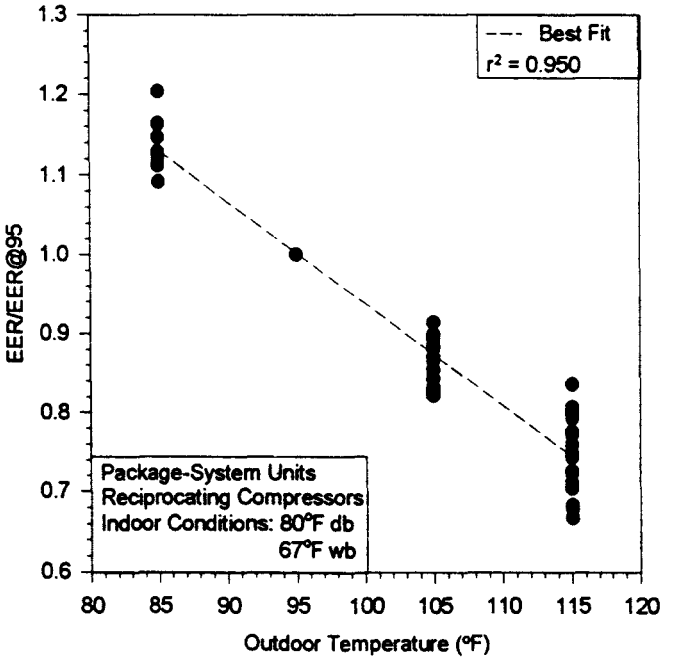

Figure 7.70 *Normalized EER at various outdoor temperatures for package-system units with reciprocating compressors.*

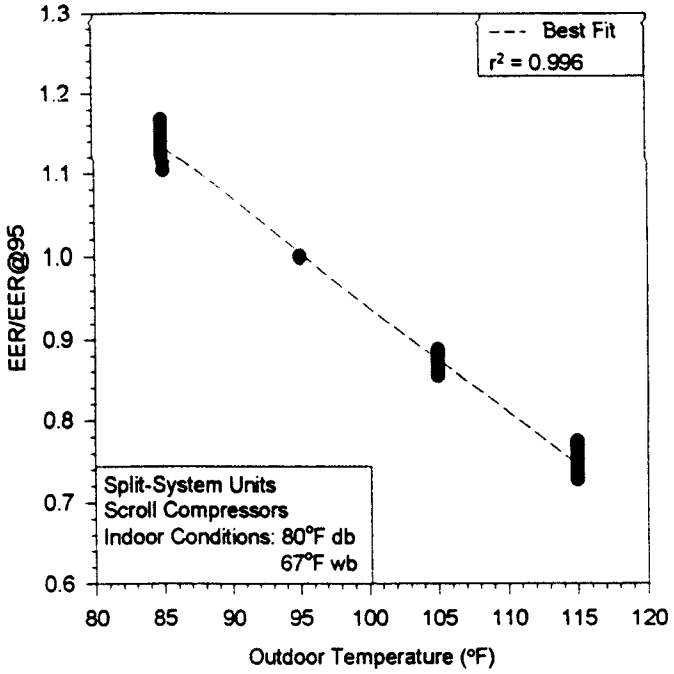

Figure 7.71 *Normalized EER at various outdoor temperatures for split-system units with scroll compressors.*

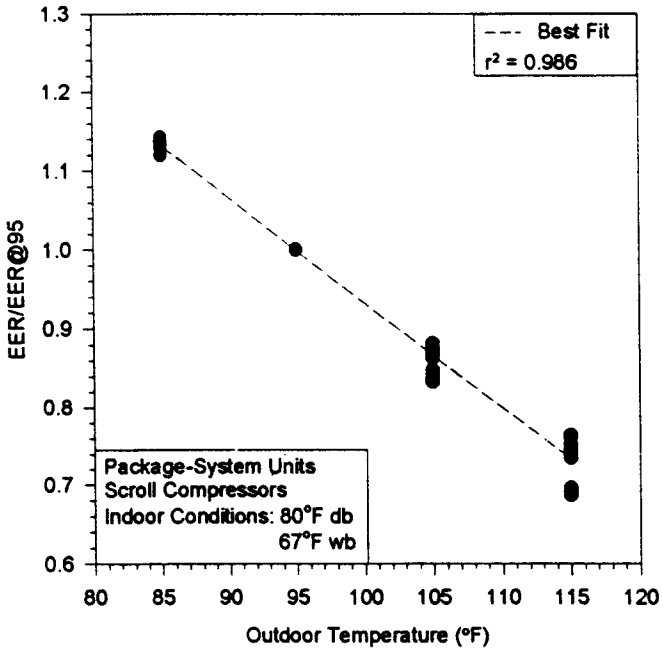

Figure 7.72 *Normalized EER at various outdoor temperatures for package-system units with scroll compressors.*

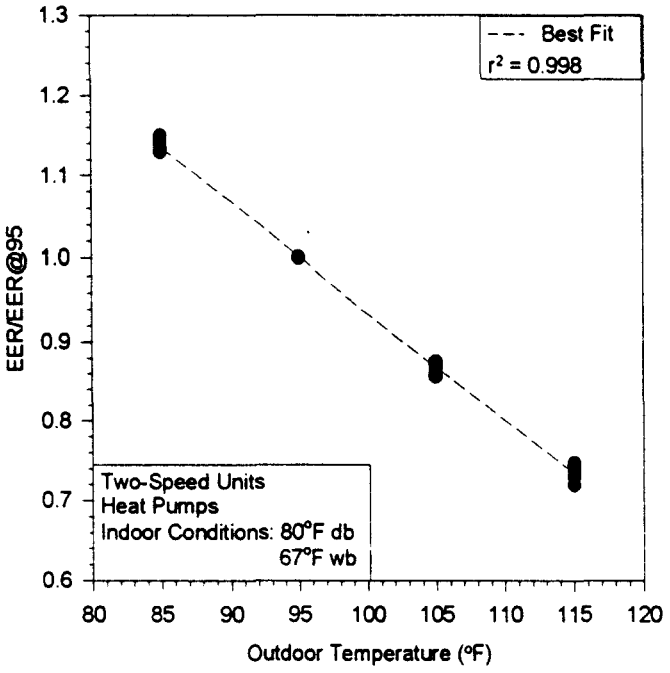

Figure 7.73 Normalized EER at various outdoor temperatures for two-speed heat pumps.

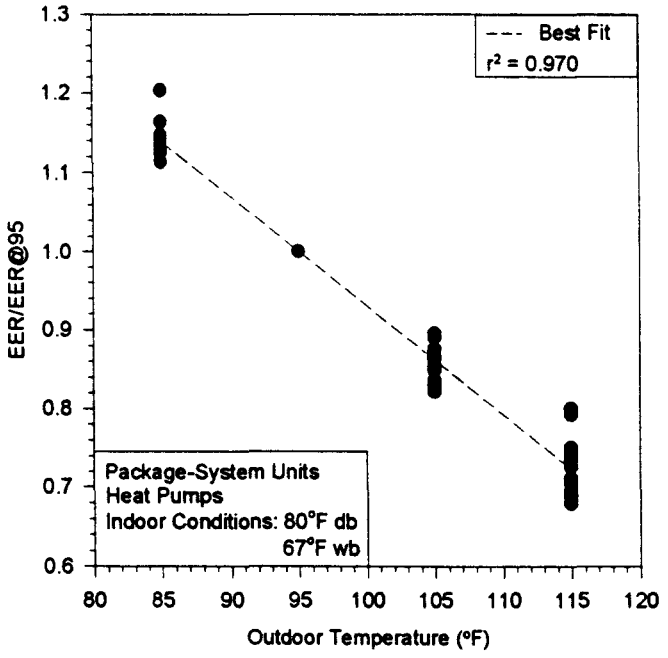

Figure 7.74 Normalized EER at various outdoor temperatures for package-system heat pumps.

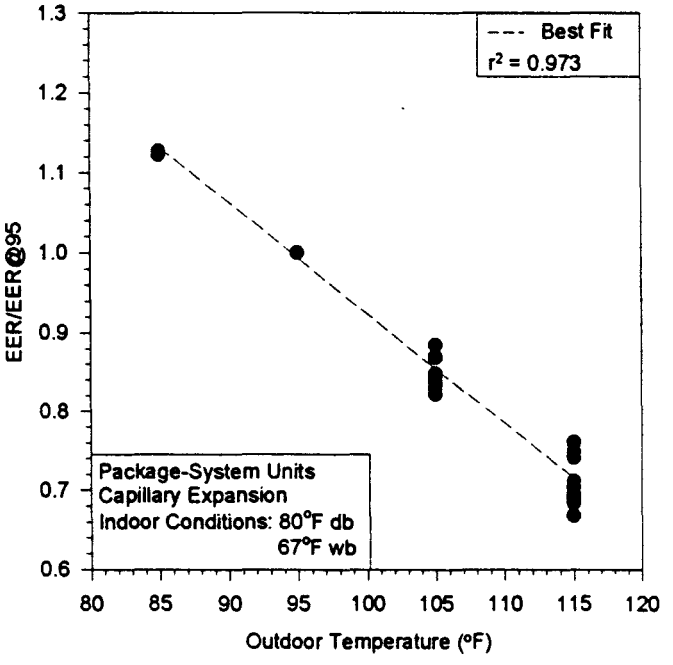

Figure 7.75 Normalized EER at various outdoor temperatures for package-system units with capillary tube expansion.

followed by the normalized power and normalized capacity. Units with smaller decreases in capacity with an increase in outdoor temperature tended to have larger decreases in power over the same temperature range. This resulted in EER curves providing a better fit of the data despite their direct dependence on the power and capacity values. Even though the overall average power r^2 value was greater than the overall average capacity r^2 value, the average r^2 for the split-system and two-speed units were higher for the normalized capacity. The averages of all three sets of these normalized performance curves were above 0.9, indicating a good prediction of system performance.

Table 7.10 *Average correlation coefficients (r^2) for fits of normalized capacity, power, and EER at various outdoor temperatures.*

	Capacity	Power	EER
Split-System Units	0.964	0.946	0.992
Package-System Units	0.863	0.926	0.968
Two-Speed Units	0.988	0.968	0.992
Average	0.928	0.942	0.982

Table 7.11 shows which type of units experienced the smallest to largest change in capacity, power, and EER with an increase in outdoor temperature. Capacity and EER values are listed in order of decreases and power values are listed in order of increases with respect to the outdoor temperature increase. The table demonstrates that, on average, the package units performed worst under each category. They exhibited the largest decrease in normalized capacity and EER over the outdoor temperature range investigated. Also, the package-system units showed the largest increase in power with an increase in

temperature. The two-speed units had the smallest decrease in capacity with the outdoor temperature increase. For both the normalized power and EER values, the split-system units performed most ideally, providing smaller power increases and smaller EER decreases over the temperature range.

Table 7.11 *Order of average changes in normalized capacity, power, and EER with an increase in outdoor temperature for split-system, package-system, and two-speed units.*

	Capacity (Decrease)	Power (Increase)	EER (Decrease)
Smallest	Two-Speed	Split	Split
Middle	Split	Two-Speed	Two-Speed
Largest	Package	Package	Package

Total Units

This section looks at the performance of air conditioning systems under broader categories. The normalized capacity, power, and EER curves were analyzed in Figures 7.76 through 7.81 for the entire group of split-system and package-system units. Table 7.12 lists the fits for the normalized data examined. With the exception of the package-system capacity, all fits had r^2 values greater than 0.9. This suggests the possibility of accurately estimating performance based only on the type of overall system (i.e. split or package).

The average correlation value for the split-system units is 0.958 and for the package-system units is 0.910. These values are consistent with values obtained in earlier

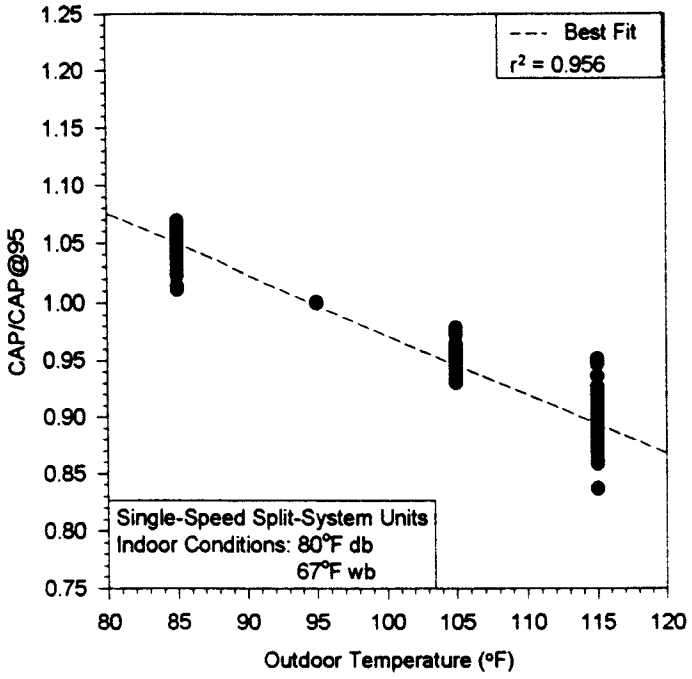

Figure 7.76 Normalized capacity for all single-speed split-system units.

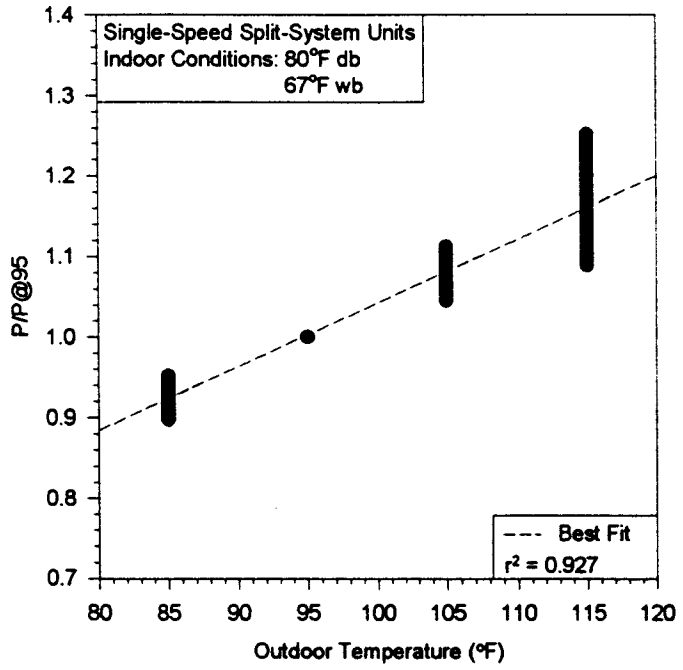

Figure 7.77 Normalized power for all single-speed split-system units.

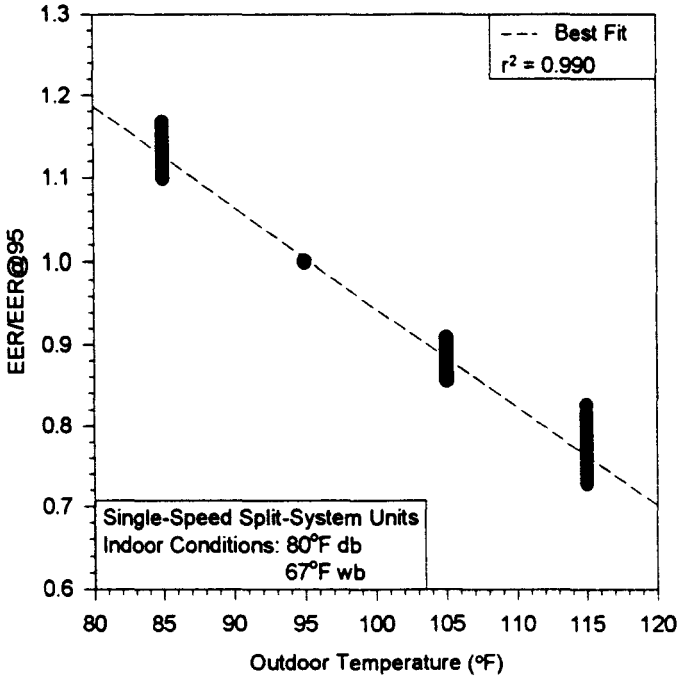

Figure 7.78 Normalized EER for all single-speed split-system units.

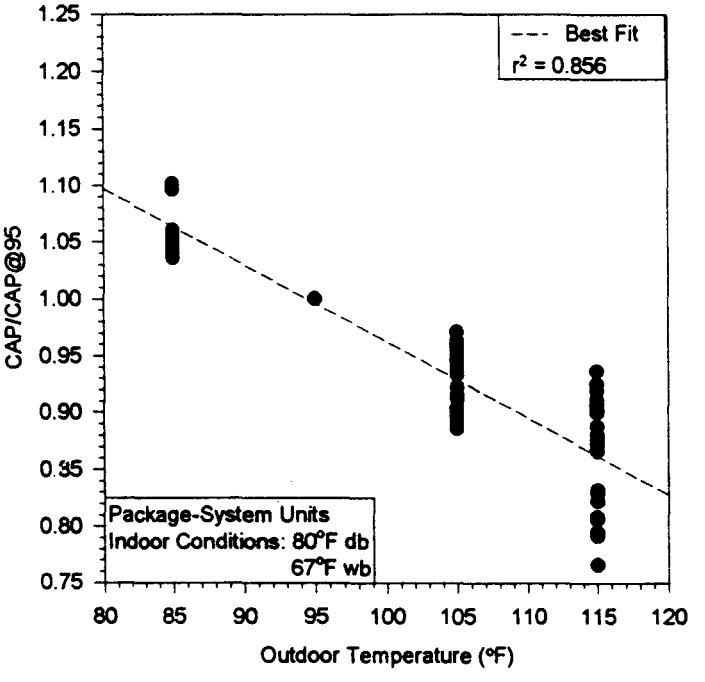

Figure 7.79 Normalized capacity for all package-system units.

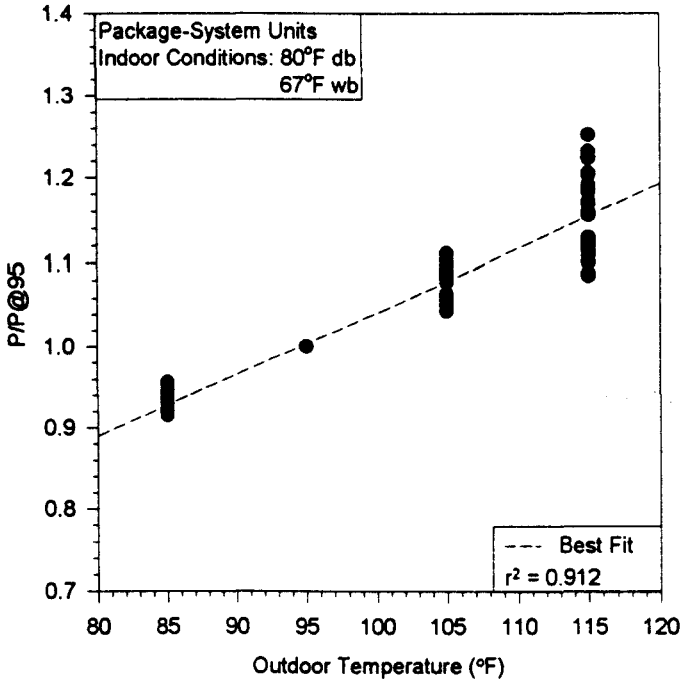

Figure 7.80 *Normalized power for all package-system units.*

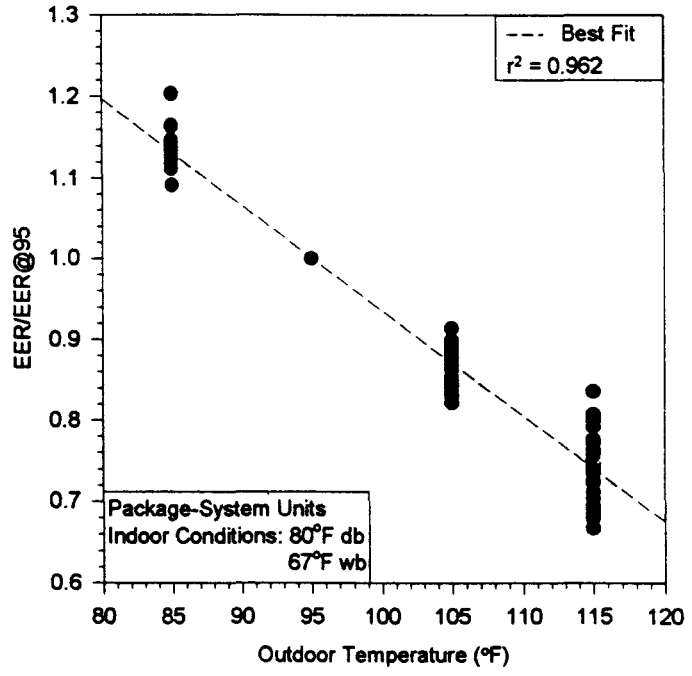

Figure 7.81 *Normalized EER for all package-system units.*

sections and indicate that the performance of package-system units tends to vary more than the performance of split-system units. As indicated by the slopes of the curves, the total split-system units have the ideal capacity and EER performance in that these values drop slower with an increase in outdoor temperature than for the package systems. The total set of package units, however, does not increase in power requirements as fast as the split-system units over the same temperature range.

Table 7.12 Fits of normalized capacity, power, and EER for split-system and package-system units.

Hardware Configuration	b(0)	b(1)	r^2
Total Split-Cap	1.4912	-0.005196	0.956
Total Split-Pwr	0.2530	0.007892	0.927
Total Split-EER	2.1559	-0.01212	0.990
Total Package-Cap	1.6355	-0.006731	0.856
Total Package-Pwr	0.2854	0.007557	0.912
Total Package-EER	2.2402	-0.01304	0.962

Summary

The results discussed above suggest several possible methods of predicting system performance. The steady-state/cyclic analysis provided a method of determining the EER at 95°F (35°C) based on the SEER of the system. This could be accomplished in two ways. The appropriate average value listed in Table 7.5 could be multiplied by the SEER of the unit to give an estimate of the EER at 95°F (35°C) for a given hardware configuration. For more accurate results, the fits of the data shown in Table 7.4 could be used with the SEER to determine the approximate EER value. The steady-state analysis

temperatures from 85°F (29.4°C) to 115°F (46.1°C). With the EER at 95°F (35°C) predicted as indicated earlier, the EER at various outdoor temperatures could be estimated. The total system power could be approximated in a similar manner. The fits of the normalized power (Power/Power@95°F (35°C)) are shown in Table 7.8. With the EER at 95°F (35°C) and the nominal capacity at 95°F (35°C) known, the power requirements at 95°F (35°C) could be estimated. This value could then be used with the linear fits to find the system power draw at different outdoor temperatures. Capacity could be estimated using the same procedure and the known nominal capacity for a given unit. Quicker but slightly less accurate indications of system performance could be obtained through the use of the equations in Table 7.12.

CHAPTER VIII

CONCLUSIONS AND RECOMMENDATIONS

To determine a relationship between the hardware configuration and cooling system performance of air conditioning systems at high outdoor temperatures, an experimental and statistical investigation was performed which looked at a wide range of systems.

Summary

For the experimental work, measurements were taken to determine total capacity, system power requirements, EER, and power factor. These results were then compared to manufacturers' predicted values. For the capacity, the experimental results were an average of 2.6% below the manufacturers' published values for outdoor temperatures from 85°F (29.4°C) to 115°F (46.1°C). Split-system units dropped in capacity an average of 0.46%/°F over the temperature range compared to an average drop of 0.78%/°F for the package systems. Experimental power measurements were on average 0.4% above manufacturers' listed results. The increase in power with an increase in outdoor temperature was 1.04%/°F and 1.05%/°F for the split-system and package-system units, respectively. Power and capacity measurements resulted in experimental EER's which were an average of 2.9% less than the manufacturers' predicted values from 85°F (29.4°C) to 115°F (46.1°C). A split-system EER drop of 1.12%/°F with an increase in outdoor

temperature compared to an EER drop of 1.23%/°F for the package systems. The power factors of all units were above 0.95 for the entire range of outdoor temperatures tested.

In the analysis of manufacturers' published data, relationships between steady-state performance, cyclic performance, and hardware configuration were investigated for a variety of air conditioning units. The single-speed split-system units generally possessed greater increases in EER for a given increase in SEER than the package-system or two-speed units. Averages values of EER/SEER for EER's at 95°F (35°C) were highest for the split-system units, followed by the package and two-speed units, respectively. These EER/SEER averages were 5.9% lower than equivalent averages obtained in 1981 (Nguyen et al 1981). Normalized capacity, power, and EER curves were investigated at outdoor temperatures from 85°F (29.4°C) to 115°F (46.1°C). On average, the two-speed units showed the smallest decrease in capacity with an increase in outdoor temperature, followed by the split-system and package-system units. The smallest power increase and smallest EER decrease with an increase in outdoor temperature were exhibited by the split-system units, followed by the two-speed units and package-system units. The EER curves possessed the highest correlation coefficients.

Conclusions

The results of the experimental tests of the ten air conditioning units indicated manufacturers' published values for capacity, power, and EER at high outdoor temperatures, which are generally based on computer models, are acceptable and can be used by electric utilities. Between 85°F (29.4°C) and 115°F (46.1°C), 15% of the

experimental and manufacturers' published results differed by more than ±5%. Half of these differences, however, were less than ±6%. Due to the experimental uncertainty involved in the testing of the units as well as the variations in testing facilities and units and the allowances of ARI (1989) discussed in Chapter VI, variations of ±6% should not be unexpected. Three of the units tested did experience more severe discrepancies between experimental and manufacturers' capacities at higher outdoor temperatures. These values, however, never differed by more than 10%. For each of the units tested, capacity and power decreased with an increase in outdoor temperature, and system power increased with an increase in outdoor temperature.

The results also indicated a statistical relationship between the EER and SEER of an air conditioning system. Linear fits of the ratio EER/SEER were found which decreased with an increase in the SEER. The averages of this ratio for different hardware configurations has decreased over the last ten to fifteen years, indicating more emphasis may have been placed on improving the SEER than on improving steady-state performance. Fits of EER as a function of SEER indicated variability in data for similar hardware configurations and possible problems with providing rebates for air conditioning systems based only on the SEER of the unit. For similar types of configuration, higher SEER units did not always result in higher EER's at 95°F (35°C). Certain hardware configurations performed more ideally than others.

An analysis of the normalized capacity, power, and EER data indicated the possibility of predicting system cooling performance based only on the hardware

configuration. An average r^2 was found of 0.928 for the capacity, 0.942 for the power, and 0.982 for the EER. In general, the single-speed split-system units had the highest correlation values. However, these units were also part of the largest data sets.

Recommendations

Future investigations are recommended in several areas of this study. This experiment involved the testing of ten units from six different manufacturers. Additional work involving a larger group of manufacturers would be helpful in verifying system performance. Since no units possessing two-speed or variable-speed compressors were tested, this might also be an interesting area to explore.

The analysis of manufacturers' cooling performance data involved 230 units from five manufacturers. Additional manufacturers and units would enhance the validity of current fits. The addition of data for package-system and two-speed units would be especially beneficial.

REFERENCES

AMCA. 1985. *AMCA/ANSI Standard 210-85, Laboratory Methods of Testing Fans for Rating.* Arlington Heights, IL: Air Movement and Control Association.

Appliance Energy Efficiency Standards Hearing. 1981. Washington, D. C.: United States House Committee on Energy and Commerce.

ARI. 1989. *ARI Standard 210/240, Standard for Unitary Air-Conditioning and Air-Source Heat Pump Equipment.* Arlington, VA: Air Conditioning and Refrigeration Institute.

ARI. 1985. *Comparison Study of Energy Efficiency Ratios.* Arlington, VA: Air Conditioning and Refrigeration Institute.

ARI. 1993. Phone Correspondence with David Martz, Director of Statistics and Administrative Services. Arlington, VA: Air Conditioning and Refrigeration Institute.

ARI. 1994. *ARI Directory of Certified Unitary Air Conditioners, Unitary Air-Source Heat Pumps, and Sound-Rated Outdoor Unitary Equipment.* Arlington, VA: Air Conditioning and Refrigeration Institute.

ARI. 1995. Phone Correspondence with David Godwin. Arlington, VA: Air Conditioning and Refrigeration Institute.

ASHRAE. 1983. *ANSI/ASHRAE Standard 116-1983, Methods of Testing for Seasonal Efficiency of Unitary Air Conditioners and Heat Pumps.* Atlanta, GA: American Society of Heating, Refrigerating, and Air Conditioning Engineers.

ASHRAE. 1988. *ASHRAE Handbook and Product Directory Equipment.* New York, NY: American Society of Heating, Refrigerating, and Air-Conditioning Engineers.

ASHRAE. 1989. *ASHRAE Handbook Fundamentals.* Atlanta, GA: American Society of Heating, Refrigerating, and Air-Conditioning Engineers.

Beseler, F. 1987. Scroll Compressor Technology Comes of Age. *Heating/Piping/Air Conditioning,* Vol. 59, pp. 67-70.

Davis, M. 1993. The Development of a Portable Data Acquisition System for use in Commercial and Industrial Energy Audits. M.S. Thesis. College Station, TX: Texas A&M University.

Energy Conservation Hearing. 1986. Washington, D. C.: United States House Committee on Energy and Commerce.

Farzad, M. 1990. Modeling the Effects of Refrigerant Charging on Air Conditioner Performance Characteristics for Three Expansion Devices. Ph.D. Dissertation. College Station, TX: Texas A&M University.

Farzad, M. and D. L. O'Neal. 1993. Influence of the Expansion Device on Air Conditioner System Performance Characteristics Under a Range of Charging Conditions. *ASHRAE Transactions 99(1).* Atlanta, GA: American Society of Heating, Refrigerating, and Air Conditioning Engineers.

Federal Register. 1995. *Code of Federal Regulations 10(430).* Washington, D. C.: Office of the Federal Register National Archives and Records Administration.

Fischer, S. K., and C. K. Rice. 1985. System Design Optimization and Validation for

Single-Speed Heat Pumps. *ASHRAE Transactions 91(2B).* Atlanta, GA: American Society of Heating, Refrigerating, and Air-Conditioning Engineers.

IEA. 1994. *Electricity Information 1993.* Paris, France: International Energy Agency.

Ikegawa, M., et al. 1984. Scroll Compressor with Self-Adjusting Back-Pressure Mechanism. *ASHRAE Transactions 90(2A).* Atlanta, GA: American Society of Heating, Refrigerating, and Air-Conditioning Engineers.

Knebel, D. E. 1983. *Simplified Energy Analysis Using the Modified Bin Method.* Atlanta, GA: American Society of Heating, Refrigerating, and Air-Conditioning Engineers.

Lennox Industries, Inc. 1993. Lennox Engineering Data, HP19 Series Heat Pump Outdoor Units. Dallas, TX.

Matsubara, K., K. Suefuji, and H. Kuno. 1987. The Latest Compressor Technologies for Heat Pumps in Japan. *Proceedings of the 1987 International Energy Agency Heat Pump Conference Prospects in Heat Pump Technology and Marketing.* Orlando, FL: International Energy Agency.

McQuiston, F. C., and J. D. Parker. 1988. *Heating, Ventilating, and Air Conditioning Analysis and Design.* New York, NY.

Millhone, J. P., and D. B. Pirkey. 1991. Demand-side Management in the United States Building Sector: Successes and New Directions. *Conference on Advanced Technologies for Electric Demand-side Management.* Sorrento, Italy: International Energy Agency.

National Appliance Energy Conservation Act of 1987. 1987. Washington, D. C.: United States Senate Committee on Energy and Natural Resources.

Neal, L., and D. L. O'Neal. 1992. The Impact of Residential Air Conditioner Charging and Sizing on Peak Electrical Demand. *The Eighth Symposium on Improving Building Systems in Hot and Humid Climates.* Dallas, TX: Texas A&M University.

NERC. 1983. *Electric Power Supply & Demand 1983-1992.* Princeton, NJ: North American Electric Reliability Council.

Nguyen, H. V., et al. 1982. Trends of Residential Air-Conditioning Cyclic Tests. *ASHRAE Transactions 88(2).* Atlanta, GA: American Society of Heating, Refrigerating, and Air-Conditioning Engineers.

NRC. 1986. *Electricity in Economic Growth.* Washington, D. C.: National Research Council.

Proctor, J., et al. 1994. Investigation of Peak Electric Load Impacts of High SEER Residential HVAC Units. Report 008.1-94.2. Corte Maderal, CA: Proctor Engineering Group.

Senshu, T., et al. 1985. Annual Energy-Saving Effect of Capacity-Modulated Air Conditioner Equipped with Inverter-Driven Scroll Compressor. *ASHRAE Transactions 91(2B).* Atlanta, GA: American Society of Heating, Refrigerating, and Air-Conditioning Engineers.

Stoecker, W. F., L. D. Smith, III and B. N. Emde. 1981. Influence of the Expansion Device on the Seasonal Energy Requirements of a Residential Air Conditioner. *ASHRAE Transactions 87(1).* Atlanta, GA: American Society of Heating, Refrigerating, and Air Conditioning Engineers.

Subbakrishna, N., J. Solomon, and R. K. Camera. 1991. Environmental Externalities from Power Production: A Comparative Analysis of Demand-side Management and Abatement Strategies. *Conference on Advanced Technologies for Electric Demand-side Management.* Sorrento, Italy: International Energy Agency.

Talukdar, S. and C. W. Gellings. 1987. *Load Management.* New York, NY: Institute of Electrical and Electronics Engineers.

Young, D. J. 1980. Development of a Northern Climate Residential Air-Source Heat Pump. *ASHRAE Transactions 86(1).* Atlanta, GA: American Society of Heating, Refrigerating, and Air-Conditioning Engineers.

APPENDIX A

UNCERTAINTY ANALYSIS

The following uncertainty analysis investigates the bias errors associated with the experimental measurements of capacity and EER. All instrumentation used in the experiment and described in Chapter IV has corresponding measurement uncertainties. To obtain an estimate of these uncertainties, the Kline and McClintock method was used which sums the square of the errors:

$$\omega_A = \left[\sum_{i=1}^{j} \left(\frac{\partial A}{\partial z_i} \omega_z \right)^2 \right]^{1/2} \qquad (A.1)$$

where:

ω_A = total uncertainty associated with the dependent variable A
z_i = independent variable which affects the dependent variable
ω_z = uncertainty for variable z_i

Air-Side Capacity

The air-side capacity was calculated using the mass flowrate of the air across the indoor coil and the evaporator entering and exiting air enthalpies. An uncertainty analysis is discussed below which examines the maximum uncertainty expected for the capacity calculations. Data used in the uncertainty calculations were taken from scan data collected during a steady state wet-coil test at 82°F (27.8°C) outdoor temperature. The following values were used:

Dry bulb temperature of air entering evaporator ($T_{db,i}$):	79.6°F (26.4°C)
Wet bulb temperature of air entering evaporator ($T_{wb,i}$):	66.6°F (19.2°C)
Dry bulb temperature of air exiting evaporator ($T_{db,o}$):	56.9°F (13.8°C)
Wet bulb temperature of air exiting evaporator ($T_{wb,o}$):	56.7°F (13.7°C)
Flow chamber pressure drop (ΔP):	1.81 in H_2O (0.48 kPa)

These data were input into Engineering Equation Solver (EES) software to obtain the following values:

Entering air enthalpy (h_i):	31.2 Btu/lbm (72.7 kJ/kg)
Exiting air enthalpy (h_o):	24.2 Btu/lbm (56.4 kJ/kg)
Air flow rate (Q):	1432 cfm (0.677 m^3/s)
Specific volume of air (v):	13.2 ft^3/lbm (0.821 m^3/kg)

Equation A.2 was used to obtain the air-side capacity.

$$Cap_{air} = \frac{Q*(h_o - h_i)}{v} + q_{fan} \qquad (A.2)$$

where: Cap_{air} = air-side capacity in Btu/h (kW)
q_{fan} = constant heat added to airstream by the indoor fan in Btu/h (kW)

Using the scan data above, the air-side capacity was calculated to be 45,400 Btu/h (13.3 kW).

An expression for the per unit capacity uncertainty was found using the Kline and McClintock method indicated in Equation A.1 and the air-side capacity in Equation A.2. The equation takes the following form:

$$\frac{\omega_{Cap}}{Cap_{air}} = \left[\left(\frac{\omega_Q}{Q}\right)^2 + \left(\frac{\omega_{h_i}}{h_o - h_i}\right)^2 + \left(\frac{\omega_{h_o}}{h_o - h_i}\right)^2 + \left(\frac{\omega_v}{v}\right)^2\right]^{1/2} \qquad (A.3)$$

where: ω_{Cap} = uncertainty in capacity calculation
ω_{hi} = uncertainty in entering air enthalpy calculation
ω_{ho} = uncertainty in exiting air enthalpy calculation
ω_Q = uncertainty in air flow rate calculation
ω_v = uncertainty in specific volume of air calculation

To find the uncertainty associated with the capacity, the uncertainties in Q, h_i, h_o, and v were first found. The air flow rate was measured in a nozzle flow chamber which meets ANSI/AMCA 210-85 specifications. Using recommendations from the standard, the per unit uncertainty in air flow rate was found to be 1.4% of the calculated flow rate. For the enthalpies and specific volume, the Kline and McClintock equation was used to find the corresponding uncertainties. The entering air enthalpy uncertainty is affected by the wet bulb and dry bulb coil entering temperatures and the ambient barometric pressure and can be described as:

$$\omega_{hi} = \left[\left(\frac{\partial hi}{\partial db}\omega_{db}\right)^2 + \left(\frac{\partial hi}{\partial wb}\omega_{wb}\right)^2 + \left(\frac{\partial hi}{\partial P_b}\omega_{wb}\right)^2\right]^{1/2} \qquad (A.4)$$

where: db = dry bulb air temperature entering evaporator in °F (°C)
wb = wet bulb air temperature entering evaporator in °F (°C)
P_b = ambient barometric pressure in in. Hg (kPa)

The uncertainties in these three measurements were taken as half the smallest scale division of the measurement devices and resulted in the following values:

ω_{db} = 0.05 in. Hg (0.17 kPa)
ω_{wb} = 0.5°F (0.28°C)
ω_{Pb} = 0.5°F (0.28°C)

Obtaining the partial derivatives of h_i, h_o, and v was difficult due to the complex steps involved in the process. The values could be approximated, however, using a procedure suggested by Holman. The partial derivatives were approximated by:

$$\frac{\partial h_i}{\partial wb} \cong \frac{f\,(wb+\Delta wb, db, P_b) - f\,(wb, db, P_b)}{\Delta wb} \tag{A.5}$$

$$\frac{\partial h_i}{\partial db} \cong \frac{f\,(wb, db+\Delta db, P_b) - f\,(wb, db, P_b)}{\Delta db} \tag{A.6}$$

$$\frac{\partial h_i}{\partial P_b} \cong \frac{f\,(wb, db, P_b+\Delta P_b) - f\,(wb, db, P_b)}{\Delta P_b} \tag{A.7}$$

The values for equations A.5 through A.7 were found by first increasing each input value by 0.1% and running the EES program to find the new h_i. The original h_i was calculated using the initial inputs. These values were then used to obtain the partial derivatives and the uncertainty in the h_i calculation. A similar procedure was used to determine the uncertainties for h_o and v to obtain the following results:

ω_{hi} = 0.200 Btu/lbm (0.465 kJ/kg)
ω_{ho} = 0.194 Btu/lbm (0.451 kJ/kg)
ω_{v} = 0.0275 ft^3/lbm (0.00167 m^3/kg)

The uncertainties were adjusted by 0.7% to account for the ideal gas approximation. This 0.7% uncertainty was added to the calculated uncertainty to obtain:

ω_{hi} = 0.419 Btu/lbm (0.974 kJ/kg)
ω_{ho} = 0.364 Btu/lbm (0.846 kJ/kg)
ω_{v} = 0.120 ft^3/lbm (0.00749 m^3/kg)

These results, along with the air flow uncertainty, were used with equation A.3 to calculate an uncertainty in the air-side capacity of 8.1%, or:

Cap_{air} = 45,400 ± 3677 Btu/h (13.3 ± 1.08 kW)

This value represents the maximum amount by which the capacity could be expected to be in error for a given measurement. During the same scan, the instantaneous refrigerant-side cooling capacity was calculated as 45,900 Btu/h (13.4 kW). This value is

0.9% higher than the air-side calculation. According to ARI testing standards (ARI 1989), the refrigerant- and air-side capacities must agree within ±6% for a test to be valid. This small difference in the energy balance suggests a probable error less than the 8% found in the uncertainty analysis.

Energy Efficiency Ratio (EER)

The uncertainty in the EER was based on the uncertainty in the air-side capacity and the uncertainty in the power measurements. The EER is calculated as indicated in Equation A.8:

$$EER = \frac{Cap_{air}}{P} \tag{A.8}$$

where: EER = energy efficiency ratio in Btu/kWh
Cap_{air} = air-side capacity (Btu/h)
P = total system power (kW)

The uncertainty of the capacity was found to be 3677 Btu/h (1.08 kW) in prior calculations. The uncertainty of the system power was taken to be 0.5% of the full scale reading of 2872 W at this scan, providing an uncertainty of 14.4 W. These values were used with the Kline and McClintock equation to obtain the following uncertainty for the EER calculation:

EER = 15.8 ± 1.3 Btu/kWh

This results in an uncertainty of 8.1% for the EER measurements at this scan. The uncertainty in the capacity had the greatest affect on the EER uncertainty analysis. Since the capacity directly affects the EER, a high capacity uncertainty results in a high EER uncertainty.